Technische Universität Braunschweig

Institut für Elektrische Messtechnik und Grundlagen der Elektrotechnik

Book of Abstracts

17th German Ferrofluid Workshop

18th-20th July 2018
TU Braunschweig

Program

Wednesday, July 18th

Thursday, July 19th

MPS/MPI

14:00 *S. Draack, N. Lucht, B. Fischer, M. Schilling, T. Viereck, F. Ludwig*
Multiparametric investigations of dynamics in Magnetic Particle Spectroscopy 28

14:20 *K. Weber, N. Löwa, F. Wiekhorst*
Magnetic Particle Spectroscopy of magnetic nanoparticles at different flow rates 30

14:40 *T. Viereck, S. Draack, M. Schilling, F. Ludwig*
Multi-spectral Magnetic Particle Spectroscopy for the investigation of particle mixtures and environment 32

15:00 *L. Wöckel, J. Wells, O. Kosch, K.-H. Herrmann, S. Günther, J.R. Reichenbach, S. Lyer, C. Alexiou, C. Grüttner, F. Wiekhorst, S. Dutz*
Long-term stable solid-state phantoms for multimodal magnetic particle imaging 33

15:30 **Coffee break**

Theory, modelling and simulation

16:00 *G. Pessot, S. Goh, M. Puljiz, H. Löwen, A.M. Menzel*
Magnetically tunable elastic properties and different types of mesoscopic dynamic behavior of magnetic gels and elastomers 35

16:20 *R. Weeber, C. Holm*
Modelling the cross-linking process of a magnetic gel 37

16:40 *P. Gebhart, T. Wallmersperger*
Macroscopic modeling and finite element simulation of fluid-saturated porous ferrogels 38

17:00 *K.A. Kalina, P. Metsch, J. Brummund, M. Kästner*
Microscopic Modeling and Finite-Element-Simulation of Magnetorheological Elastomers 40

17:20 **Award ceremony for the Price of the Ferrofluid Society Germany**
Lecture of the awardee

19:00 **Dinner**

Friday, July 20th

Experimental

9:00 *M. Hermes, E. Roeben, A. Habicht, S. Seiffert, A.M. Schmidt*
Investigation on the local dynamics in supramolecular polymer structures using Magnetic Particle Nanorheology 42

9:20 *J. Landers, S. Salamon, H. Nádasi, R. Stannarius, A. Eremin, S. Aya, F. Araoka, H. Wende*
Probing anisotropic nanoparticle diffusion in soft matter composites exposed to magnetic fields 43

9:40 *M. Gratz, A. Tschöpe*
Scale dependence in Ni nanorod oscillatory rotation microrheometry of poly(ethylene oxide) solutions 45

10:00 *A.O. Ivanov, S.S. Kantorovich, I.M. Arefyev, A.V. Lebedev, A.F. Pshenichnikov*
Weakening of magnetic response experimentally observed for ferrofluids with strongly interacting magnetic nanoparticles 47

10:30 **Coffee break**

Medical and biological applications

11:00 *R. Müller, M. Zhou, N. Kuhl, M. Rabel, P. Warncke, D. Fischer, T. Heinze*
Controlled release and biodegradation of meltable magnetic biocomposites 49

11:20 *D. Zahn, A. Weidner, Z. Nosrati, L. Wöckel, R. Müller, J. Dellith, K. Saatchi, U.O. Häfeli, S. Dutz*
Temperature controlled Camptothecin release from biodegradable magnetic PLGA microspheres 51

11:40 *J. Demut, J.M. Müller, M. Rabel, M. Haist, C. Grüttner, F.A. Müller, R. Quaas, A. Hochhaus, D. Fischer, J.H. Clement*
Cellular cytokine release after magnetic nanoparticle incubation 53

12:00 *R.P. Friedrich, M. Mühlberger, S. Draack, F. Ludwig, D. Eberbeck, F. Wiekhorst, W. Lang, E.I. Wisotzki, S. Mayr, C. Alexiou*
Development of biocompatible Vascular Scaffolds using Magnetic Cell Seeding of SPION-loaded Cells 55

12:30 **Closing**

Posters

Equilibrium properties of a bimodal magnetic suspension: a Langevin dynamics study

A.A. Kuznetsov[1,2]

[1] *Institute of Continuous Media Mechanics UB RAS, Ac. Koroleva 1, Perm, Russia, 614013*
[2] *Perm State University, Bukireva 15, Perm, Russia, 614990*

In this work, a dilute suspension of magnetizable microbeads in a nanodisperse ferrofluid is considered. Langevin dynamics simulations are used to investigate the equilibrium properties of such suspension in a static uniform magnetic field. A microbead is modelled as a rigid dense spherical cluster of single-domain nanoparticles. In simulations, a single microbead is placed in the center of a cubic simulation cell and the ferrofluid nanoparticles are randomly dispersed in the remaining volume. Three-dimensional periodic boundary conditions are imposed on the cell. They implicitly create an infinite cubic lattice of identical microbeads. Orientation and position of the bead remain fixed during the simulation, but the nanoparticles inside the bead retain rotational degrees of freedom. Ferrofluid nanoparticles and nanoparticles inside the bead are the same. Steric, dipole-dipole and Van der Waals interactions between all nanoparticles in the system are taken into account. Initial magnetic susceptibility of the bead is calculated for different values of the sus-

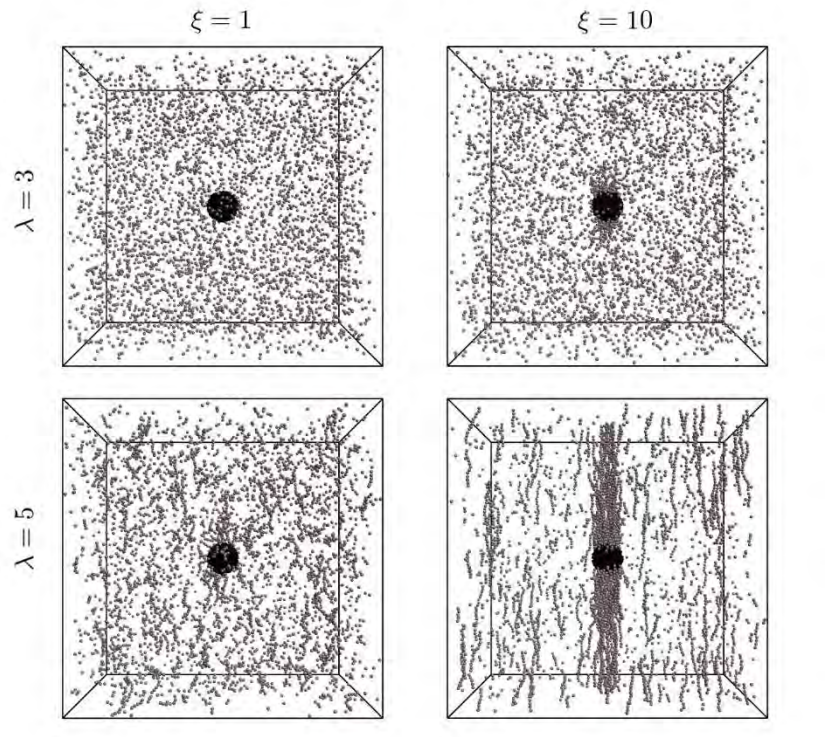

Snapshots of the simulation cell, the volume fraction of nanoparticles in ferrofluid is ≈ 0.3%. Different panels correspond to different values of the Langevin parameter ξ (the ratio of the Zeeman energy of nanoparticles to the thermal energy) and the dipolar coupling parameter λ (the ratio of the dipole-dipole interaction energy of a nanoparticle pair to the thermal energy). ξ = 1 (left column) and 10 (right column), λ = 3 (top row) and 5 (bottom row). The field is directed vertically.

pending ferrofluid concentration. The results are interpreted within the modified mean-field theory [1]. It is shown that at large applied fields nanoparticles concentrate near the magnetic poles of the bead. If dipole-dipole interactions are large enough to induce the formation of nanoparticle chains, these chains form wide columns above and below the bead, which span across the whole simulation cell (see figure). Concentration profiles of nanoparticles near the bead are obtained for a wide range of control parameters. The effect of competition between isotropic Van der Waals and anisotropic dipolar interactions on the nanoparticle distribution is discussed. Simulation results are compared with the data of Ref. [2], where a similar redistribution of nanoparticles in a bimodal suspension was investigated both experimentally and analytically.

Acknowledgments

The work was supported by Russian Science Foundation (Grant № 17-72-10033). Calculations were performed using the "Uran" supercomputer of IMM UB RAS.

References

[1] A.O. Ivanov, O.B. Kuznetsova, "Magnetic properties of dense ferrofluids: an influence of interparticle correlations," Phys. Rev. E 64, 041405 (2001).

[2] C. Magnet, P. Kuzhir, G. Bossis, et al. "Haloing in bimodal magnetic colloids: The role of field-induced phase separation," Phys. Rev. E 86, 011404 (2012).

Static magnetization of an ensemble of interacting superparamagnetic nanoparticles

E.A. Elfimova[1], A.O. Ivanov[1]

[1] *Ural Federal University, Lenin Av. 51, Ekaterinburg 620000, Russian Federation*

We study theoretically the static (equilibrium) magnetic properties of an ensemble of superparamagnetic nanoparticles, the numerical concentration of which is ρ. The macroscopic sample with nanoparticle ensemble has the shape of highly elongated cylinder, along the main axis of which a static uniform magnetic field $\mathbf{H} = H\,\hat{\mathbf{h}}$, $\hat{\mathbf{h}}$=(0;0;1) is applied. This shape allows to neglect the demagnetization effects and to consider an internal macroscopic field inside the sample being equal to an external magnetic field **H**. The directions of *i*-th particle magnetic moment $\mathbf{m}_i$ and its easy magnetization axis are described by the unit vectors $\hat{\mathbf{m}}_i=\mathbf{m}_i/m_i$ and $\hat{\mathbf{n}}_i$.

The ensemble Hamiltonian includes the Neel energy of magnetic anisotropy U_N, the magnetic moment–magnetic field interaction energy U_m, the interparticle hard-sphere repulsion U_{HS} prohibiting the particle interpenetration, and the interparticle magnetic dipole-dipole interaction U_d:

$$U_N(i) = -Kv_m\,(\hat{\mathbf{n}}_i \cdot \hat{\mathbf{m}}_i)^2\,, \qquad (1)$$

$$U_m(i) = -\mu_0(\mathbf{m}_i \cdot \mathbf{H}) = -\mu_0 mH(\hat{\mathbf{m}}_i \cdot \hat{\mathbf{h}}),$$

$$U_d(ij) = \frac{\mu_0 m^2}{4\pi k_B T}\frac{(\hat{\mathbf{m}}_i\cdot\hat{\mathbf{m}}_j)-3(\hat{\mathbf{m}}_i\cdot\hat{\mathbf{r}}_{ij})(\hat{\mathbf{m}}_j\cdot\hat{\mathbf{r}}_{ij})}{r_{ij}^3}\,.$$

Here K is the magnetic crystallographic anisotropy constant; v_m is the particle magnetic core volume; μ_0 stands for the vacuum magnetic permeability; k_BT has a meaning of thermal energy; and vector $\mathbf{r}_{ij}$ connects the centers of *i*-th and *j*-th particles.

To calculate the ensemble magnetization M and the initial magnetic susceptibility χ we used the approach, known as the modified mean-field model of the 1-st order (MMF-1) [1]. The idea is that all magnetic nanoparticles produce the magnetic dipole field, and this averaged dipole field acts on the magnetic moments in addition to an external field. The results are dependent on following dimensionless parameters: the relative height of the intraparticle energy barrier $\sigma = Kv_m/k_BT$; the Langevin parameter (dimensionless magnetic field strength) $\alpha = \mu_0 mH/k_BT$; and the Langevin magnetic susceptibility $\chi_L = \mu_0\rho m^2/3k_BT$ of the system of non-interacting magnetic moments.

For the cases of limiting soft magnetic nanoparticles ($\sigma \to 0$) and the ferrofluids, keeping both the Neel and Brownian rotation degrees of freedom, we got the MMF-1 results [1]:

$$M = M_\infty L(\alpha_e)\,, \qquad \alpha_e = \alpha + \chi_L L(\alpha)\,, \quad (2)$$

$$M_\infty = \rho m\,, \qquad L(\alpha) = \coth\alpha - 1/\alpha\,,$$

$$\chi = \chi_L(1 + \chi_L/3)\,,$$

which are independent on the magnetic anisotropy σ. Here α_e has a meaning of an effective magnetic field, acting on each magnetic moment.

For an ensemble of immobilized nanoparticles, uniformly distributed inside the sample, with parallel texturing of easy axes $\hat{\mathbf{n}}_i||\hat{\mathbf{h}} = (0;0;1)$ we got

$$M_{||} = M_\infty\frac{R_2(\alpha_{||},\sigma)}{R_1(\alpha_{||},\sigma)},\ \alpha_{||} = \alpha + \chi_L\frac{R_2(\alpha,\sigma)}{R_1(\alpha,\sigma)}, \quad (3)$$

$$R_1(\alpha,\sigma) = \tfrac{1}{2}\textstyle\int_{-1}^{1}\exp(\sigma t^2 + \alpha t)\,dt\,,$$

$$R_2(\alpha,\sigma) = \tfrac{1}{2}\textstyle\int_{-1}^{1}\exp(\sigma t^2 + \alpha t)t\,dt =$$

$$\chi_{||} = \chi_L A_{||}(\sigma)[1 + \chi_L A_{||}(\sigma)/3]\,, \quad (4)$$

$$A_{||}(\sigma) = \frac{3}{2\sigma}\left[\frac{\exp(\sigma)}{R(\sigma)} - 1\right],$$

$$R(\sigma) \equiv R(0,\sigma) = \textstyle\int_0^1\exp(\sigma t^2)\,dt\ .$$

Last function was introduced first in Ref. [2] describing the susceptibility of non-interacting immobilized particles.

For an ensemble of immobilized nanoparticles, uniformly distributed inside the sample, with perpendicular texturing of easy axes $\widehat{\mathbf{n}}_i \perp \hat{\mathbf{h}} = (1;0;0)$ we got

$$M_\perp = M_\infty \frac{R_4(\alpha_\perp,\sigma)}{R_3(\alpha_\perp,\sigma)},\ \alpha_\perp = \alpha + \chi_L \frac{R_4(\alpha,\sigma)}{R_3(\alpha,\sigma)}, \quad (5)$$

$$R_3(\alpha,\sigma) = \int_0^1 \exp(\sigma t^2)\, I_0\left(\alpha\sqrt{1-t^2}\right)dt\ ,$$

$$R_4(\alpha,\sigma) = \int_0^1 \exp(\sigma t^2)\, I_1\left(\alpha\sqrt{1-t^2}\right)\sqrt{1-t^2}\,dt\ ,$$

$$\chi_\perp = \chi_L A_\perp(\sigma)[1 + \chi_L A_\perp(\sigma)/3]\ , \quad (6)$$

$$A_\perp(\sigma) = \frac{3 - A_{||}(\sigma)}{2}\ .$$

Behavior of effective fields $\alpha_{||}$ (3) and $\alpha_\perp$ (5) are opposite. In parallel case the dipolar correction term increases the acting magnetic field, but for perpendicular texturing the dipolar interaction reduces the value of acting field.

We also calculated the magnetic properties of interacting immobilized particles with random texturing, when the translational and orientational probabilities are uniform. Magnetization is rather cumbersome, but the initial susceptibility obeys also MMF-1 results

$$\chi = \chi_L(1 + \chi_L/3)\ . \quad (7)$$

Figures 1 and 2 show the magnetization and the initial magnetic susceptibility of the ensemble of interacting immobilized nanoparticles with random, parallel, and perpendicular texturing of easy axes.

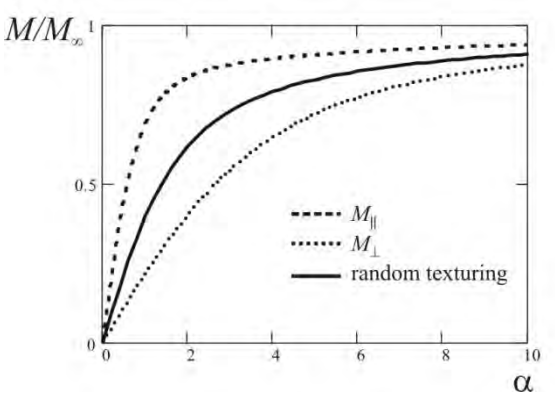

Fig. 1 Dimensionless magnetization of interacting immobilized nanoparticles with random (solid line) parallel (dash line) and perpendicular (dotted line) texturing of easy axes as a function of Langevin parameter α for the $\sigma = 3$ and $\chi_L = 1$.

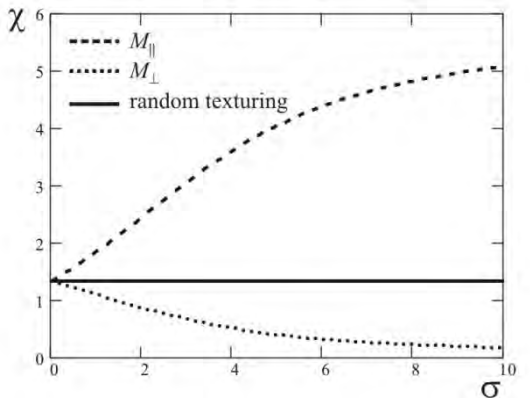

Fig. 2 Initial magnetic susceptibility of interacting immobilized nanoparticles as a function of σ for $\chi_L = 1$. The type of lines denotes the same as in Fig. 1.

Acknowledgments

The research was supported by Russian Science Foundation, (Grant No. 15-12-10003).

References

[1] A.O. Ivanov, O.B. Kuznetsova, *Phys. Rev. E* **64** (2001) 041405.

[2] Yu.L. Raikher, M.I. Shliomis., *Sov. Phys - JETP (Engl. Transl.)* **40** (1974) 526.

Magnetic Properties of Elastomers with Magnetically Hard Particles As Seen in Computer Simulations

P. Sanchez[1,2], E. Minina[1,2], A. Dobroserdova[2], E. Kramarenko[3], S. Kantorovich[1,2]

[1] *University of Vienna, Vienna, Austria*
[2] *Ural Federal Universty, Ekaterinburg, Russia*
[3] *Moscow State University, Moscow, Russia*

Magnetic elastomers are hybrid materials consisting of a soft matrix of polymers with a high volume fraction of embedded magnetic micro- and/or nanoparticles. These materials are elastic enough to experience strong structural changes as a response to external magnetic fields. This makes them promising candidates for a broad range of applications.

In this contribution we discuss three different types of elastomers and study (1) deformation caused by the magnetic field leading to the changes of the elastomer surface hydrophilicity (Fig. 1); (2) influence of the magnetoelastic coupling on the first order reversal curves (FORCs); effects of the interparticle magnetic interactions on the properties of microgels (Fig. 2).

One particularly interesting application of magnetic elastomers is their use as thin coatings that provide a fine control of the hydrophobicity of their free surface, as a consequence of the strong changes in its roughness induced by the application of proper external fields.

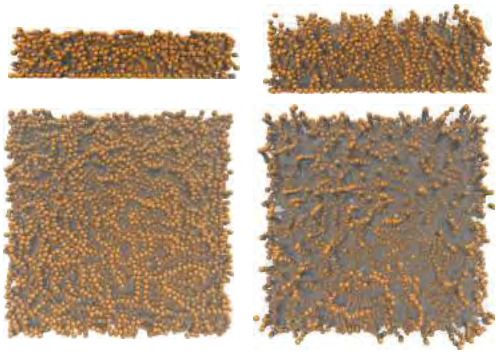

Fig. 1. Layer of magnetic elastome side and top views. Zero field case on the left; applied field is on the right.

Here, we present a minimal computer simulation model of a magnetic elastomer thin coating that captures the dependence of its surface roughness on the elastic properties of the polymer matrix and the magnetic.

The FORC method helps us to study the effect of the matrix on the internal magnetic interactions. We use the classical Pike method [1]. We address both monodisperse (all magnetic particles are of the same size) and bidisperse (large and small magnetic particles) systems. Additionally, we anlyse the influence of the matrix by changing the number of springs attached to each particle.

Finally, we study magnetic microgels - spherical colloidal particles consisting of polymer network with embedded magnetic dipolar particles. Our main focus is concentrated on how the microgels change their shape and size depending on their internal structure and magnetic component. Microgels are initially modelled as bead-spring polymer chains randomly crosslinked into a polymer network. Changing degree of crosslinking allows us to vary microgel's internal structure. This way, we consider weekly crosslinked and highly crosslinked microgels. We show that an appropriate combination of magnetic component and degree of crosslinking may offer an additional way to control such systems.

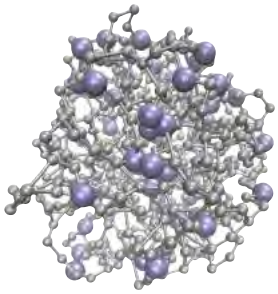

Fig. 2. Microgel with magnetic particles

References

[1] C. R. Pike et al., J. Appl. Phys. 85, 6660 (1999).

Computer modeling of hybrid magnetic elastomers with magnetically hard and soft particles

P. A. Sánchez[1,2], O. V. Stolbov[3], Yu. L. Raikher[3], S. S. Kantorovich[1,2]

[1] *University of Vienna, Vienna, Austria.*
[2] *Ural Federal University, Ekaterinburg, Russia.*
[3] *Institute of Continuous Media Mechanics (RAS Ural div.), Perm, Russia.*

We report our recent progress on the theoretical modeling of a novel type of hybrid magnetic elastomer materials, composed of a mixture of microparticles with different magnetic properties embedded within a polymer matrix. The mixture of microparticles consists of a low fraction of relatively large (5-100μm of diameter) magnetically hard (MH) particles and a high fraction of smaller (<5μm in diameter) magnetically soft (MS) particles [1,2]. The combination of MH and MS particles provides both, active and passive control on the mechanical properties of the elastomer, as its internal structure does not only respond to external magnetic fields but it can also be tuned by inducing an appropriate permanent magnetization on the MH particles.

Our theoretical study is based on a minimal coarse-grained computer model of such type of hybrid elastomer. Specifically, in order to analyze the interplay between MH and MS particles and the field-induced elastic deformations of the microstructure, we focus on the modeling of a fundamental volume of material that includes a single MH particle surrounded by a cloud of smaller, MS particles. The relative positions of the latter with respect to the former are assumed to be constrained by the polymer matrix, represented implicitly as a random network of elastic springs connecting all the particles. As a first approximation to the magnetic properties of the particles, we consider that the MH one carries a permanent magnetic moment, whereas each MS particle has a magnetization that depends on the local field created by the central MH particle and any eventual applied external field. We perform with this model extensive computer simulations in order to analyze the deformations of the fundamental volume depending on the strength and relative orientation of the external field with respect to the magnetic moment of the central particle. Finally, we compare our simulation results to the ones provided by a continuous magneto-mechanical model of this material.

Acknowledgments

Support by DFG, grant Ref. no. OD 18/24-1, is acknowledged.

References

[1] J. M. Linke, D. Y. Borin, S. Odenbach, *RSC Adv.* **6**, 100407 (2016).
[2] M. V. Vaganov, J. M. Linke, S. Odenbach, Yu. L. Raikher, *J. Mag. Mag. Mat.* **431**, 130-133 (2017).

Creating a toolbox of synthetic pathways for the encapsulation of nanoparticles with chemically bound polymer shells

L.S. Fruhner[1], M. Kruteva[1], J. Allgaier[1], W. Pyckhout-Hintzen[1], S. Förster[1], R. Koll[2], H. Heller[2], H. Weller[2]

[1] *Jülich Centre for Neutron Science (JCNS-1&ICS-1), Forschungszentrum Jülich, 52425 Jülich*
[2] *Institut für Physikalische Chemie, Universität Hamburg, Grindelallee 117, 20146 Hamburg*

Functional nanocomposites offer a broad application range from sensors through stretchable electronics to smart coatings for energy conversion and human health. [1] Especially, responsive materials which are able to perform self-assembly in different environments (e.g. in magnetic or electric fields, by mechanical shearing) are in the centre of interest (Fig.1). Further developments in this area would significantly benefit from deeper insights into the interactions between the nanoparticles with each other and their surrounding host matrix. Recently, we developed a synthetic procedure to obtain highly monodisperse nanoparticles consisting of a superparamagnetic iron oxide core (SPION) embedded in a polymeric shell. [2]

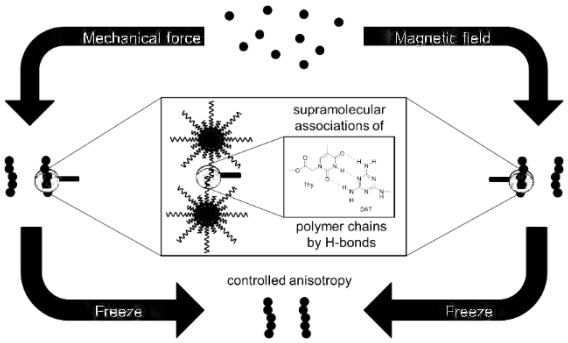

Our strategy aims at synthesising monodisperse superparamagnetic iron oxide nanoparticles (SPIONs) and coating them with α,ω-functionalised elastic polymers like polybutylene oxide (PBO). This allows us to either align the nanoparticles in a magnetic field or by mechanical force (Fig.1). The structure of the nanocomposites as well as their behaviour due to external stimuli are investigated via Small-Angle X-Ray and Neutron Scattering (SAXS/SANS).

Here, we report our recent progress in gaining further knowledge about our encapsulation procedure by varying the polymer chain length, the polymeric ligand as well as the crosslinking procedure to provide a stable inner shell around the nanoparticles. Making use of Small-Angle Neutron Scattering we were able to obtain detailed information about the structure of the polymer shell around our nanoparticles.

Acknowledgments

Financial support is gratefully acknowledged from DFG-SPP 1681 “Feldgesteuerte Partikel-Matrix-Wechselwirkungen”.

References

[1] P. Gómez-Romero, C. Sanchez, *in Functional Hybrid Materials*, Wiley-VCH, Weinheim, 2003.

[2] A. Feld, R. Koll, L. Fruhner, M. Krutyeva et al, *ACS Nano*, **2016**, *11*, 3767–3775.

Hybrid elastomers with tuned particle-matrix interaction

J. Seifert[1], A. M. Schmidt[1]

[1] *Institut für Physikalische Chemie, Universität zu Köln, Luxemburger Str. 116, D-50939 Köln, Germany, email: annette.schmidt@uni-koeln.de*

Hybrid materials consisting of magnetic nanoparticles that are incorporated into complex matrices, such as gels and elastomers, can be manipulated by external magnetic fields. By employing magnetic nanoparticles as multifunctional, inorganic crosslinkers, magnetic node networks with a direct covalent coupling between magnetic and elastic component are obtained. These materials show a novel type of particle-matrix interaction.[1,2] The incorporation of magnetic nanoparticles, showing magnetic as well as geometric anisotropy, leads to direction dependent properties in the magnetic node networks.

Synthetic concept

Here, we present the synthesis of magnetic node networks based on spindle-like α-Fe_2O_3 particles and an elastomeric matrix. Therefore, silica coated nanoparticles are used to crosslink polydimethylsiloxane derivatives via a polycondensation reaction (Figure 1).

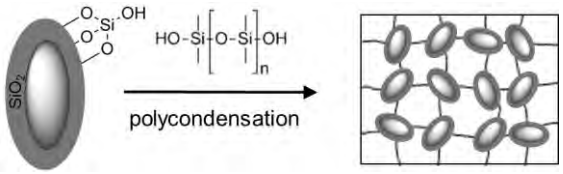

Figure 1. Reaction scheme of the formation of particle crosslinked elastomers.

This new type of magnetically manipulable elastic material is expected to have promising applications for dampers or in robotics, where the mechanic properties need to be reversibly altered. The incorporation of spindle-like hematite particles leads to direction dependent properties in the magnetic node networks, which are a key step for the realization of actuators showing a reversible contraction along one axis.[3,4]

Properties

The prepared magnetic node networks show the typical viscoelastic behavior of particle filled elastomers. Due to the covalent attachment of the magnetic nanoparticles to the elastic matrix, high particle contents of up to 30 m% can be employed without observing particle agglomeration, leading to structures with decent magnetic properties. The occurring magnetic hysteresis in the reversible elastomers is attributed to a reorientation of the magnetic moment within the particle at high fields. In ongoing experiments, we intend to maximize the direction dependent magnetic properties by aligning the magnetic nanoparticles in a magnetic field and conserving the magnetic order through the crosslinking process.

Acknowledgments

Financial support is acknowledged from DFG-SPP 1681 “Feldgesteuerte Partikel-Matrix-Wechselwirkungen”. (SCHM1747/10)

References

[1] N. Frickel, R. Messing, A. M. Schmidt, *J. Mater. Chem.* **2011**, *21*, 8466–8474.

[2] L. Roeder, M. Reckenthäler, L. Belkoura, S. Roitsch, R. Strey, A. M. Schmidt, *Macromolecules* **2014**, *47*, 7200–7207.

[3] L. Roeder, P. Bender, M. Kundt, A. Tschöpe, A. M. Schmidt, *Phys. Chem. Chem. Phys.* **2015**, *17*, 1290–1298.

[4] P. Bender, A. Günther, A. Tschöpe, R. Birringer, *J. Magn. Magn. Mater.* **2011**, *323*, 2055–2063.

Effect of Magnetic Nanoparticle Distribution in PNIPAM Microgels on their Magnetic Response

M.U. Witt[1], S. Hinrichs[2], M. Hermes[3], B. Fischer[2], A. Schmidt[3], R.v. Klitzing[1]

1 Technische Universität Darmstadt, Institut für Festkörperphysik, Alarich-Weiss-Straße 10, 64287 Darmstadt, Germany

2 Universität Hamburg, Institut für Physikalische Chemie, Grindelallee 117, 20146 Hamburg, Germany

3 Universität zu Köln, Institut für Physikalische Chemie, Luxemburger Straße 116, 50939 Köln, Germany

A magnetic field as a trigger allows a fast switching of properties of magnetic materials. Embedding for instance magnetic nanoparticles (MNP) into polymeric microgels (ferrogels) allows fast changes in shape of the ferrogels. This offers future application as sensors and actuators and in drug delivery systems, using the magnetic nanoparticles as guidance and triggers. Here, a thermosensitive poly-N-isopropylacrylamide (PNIPAM) microgel was chosen as matrix for the CoFeO4 nanoparticles [1]. In order to understand and to control the magnetic properties of the ferrogel, the mutual effects of the internal structure of the microgel and the distribution of MNP have to be understood. Therefore it is of high interest to get a deeper insight into the distribution of the cross-linker (BIS) of the microgel and the MNP distribution.

To tailor the structure of the microgels, they were synthesized by two different methods: the batch method [2] which leads to an inhomogeneous distribution of the cross-linker and the feeding method [3] which produces homogeneously cross-linked microgels.

The bare microgels and the magnetic microgels were investigated with dynamic light scattering (DLS), atomic force microscopy (AFM), transmission electron microscopy (TEM) and Zetasizer. Beside the measurement of the microgel characteristics first measurements of the magnetic response of the magnetic microgels will be shown.

The results show that the homogeneity of the crosslinker distribution is the key factor for a homogenous distribution of CoFeO4 nanoparticles inside the microgels. A homogeneous distribution in turn offers a higher response of the magnetic microgel to an externally applied magnetic field as previous experiments have shown [1]. Two systems are compared, one with a heterogeneous structure close to a core/shell structure and one with isotropic distribution of the MNP inside the microgels. As an example a magnetic microgel is shown in figure A detailed analysis of the 2D-TEM images allows a reconstruction of the 3D distribution of MNP.

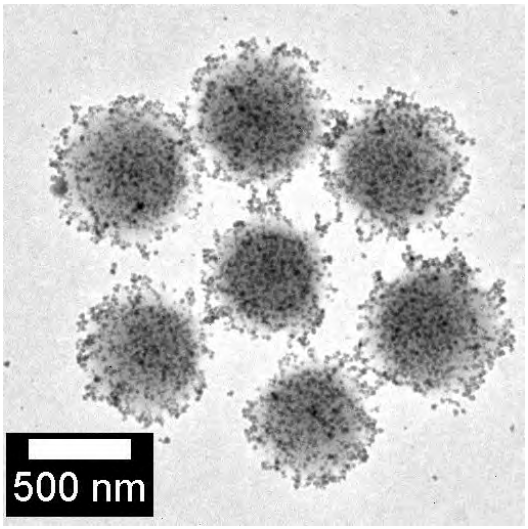

Figure 1. TEM picture of magnetic microgels.

References

[1] S. Backes, M. U. Witt, R. v. Klitzing, J. Phys. Chem. B 2015, 119, 12129-12137

[2] R. Pelton, P. Chibante, Colloids Surf. A, 1986, 20, 247-256

[3] R. Acciaro, Langmuir, 2011, 27, 7917-7925

Efficient ferronematic coupling with polymer brush particles

Karin Koch[1], Matthias Kundt[1], Alexey Eremin[2], Annette M. Schmidt[1]*

[1] *Department Chemie, Institut für Physikalische Chemie, Universität zu Köln, Luxemburger Str. 116, D-50939 Köln, email: Annette.schmidt@uni-koeln.de*
[2] *Otto-von-Guericke-Universität Magdeburg, Institut für Experimentelle Physik, Universitätsplatz 2, D-39016 Magdeburg*

The ability to control nematic phases in thermotropic liquids by external fields is of great importance for their application, e.g. in optical devices. While it is common to use electric voltage in such devices, the employment of magnetic fields is less straight forward due to the low magnetic anisotropy of the mesogens.
However, as already predicted by deGennes and Brochard in 1970, the incorporation of dipolar magnetic particles is expected to result in nematic phases that are readily manipulable at moderate magnetic field strength due to a coupling between nematic and magnetic director.[1] Nonetheless, one of the main challenges for the experimental realization is to overcome the strong tendency of the nanoparticles to agglomerate, as a consequence of the strong molecular interactions of the mesogens and the dipolar interactions between the particles.[2] Thus, up to now, experimental evidence for such coupling is rare.
Our new approach to circumvent this problem, and to achieve ferromagnetically doped liquid crystals with enhanced volume fraction and stability, is based on nanoparticles that are surface-modified with a side-chain LC polymer brush.

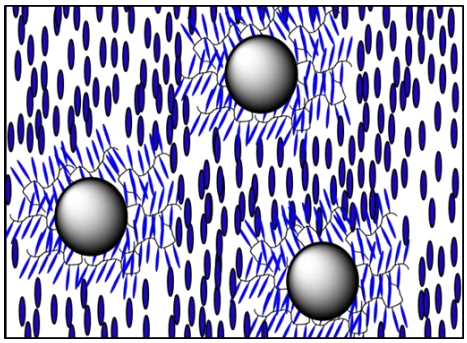

Figure 1: Scheme of LC polymer brush particle.

Thereby we work on two different synthetic pathways with a variation of shell thickness, mesogen density and the spacer length. With this method, a higher compatibility between the particle surface and the mesogenic matrix, and an effective steric stabilization of particles against agglomeration is obtained.
The impact of different doped particles on the phase behavior of 5CB (B_{th} = 250 mT at a layer thickness of d = 25 µm) is investigated with respect to particle concentration. We found that our stabilization approach allows the stabilization of particles up to 0.2 vol% (1 mass-%). Upon addition of 9OCB-PHMS functionalized magnetic particles, the order parameter of the system increases, indicating an effective coupling between the particles and the LC matrix.
The magnetic response of the ferronematic phases is investigated by capacitance measurements in a magnetic field (Figure 2).

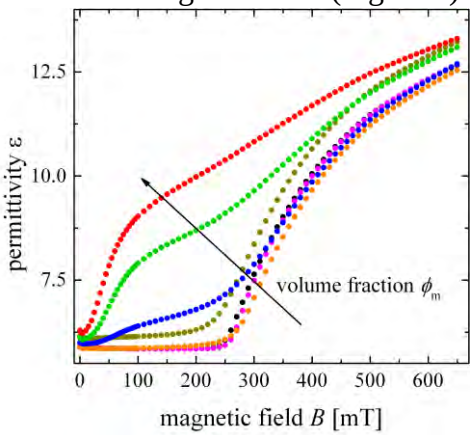

Figure 2: Capacitance measurements with parallel B and E field for pure 5CB(black) and 5CB doped with 9OCB-PHMS@CoFe2O4 and in volume fractions from 0.01 vol% up to 0.1 vol%.

As compared to 5CB, the critical field strength and the shape of the *Fréederickzs* transition is strongly is affected by the particle volume fraction. In fact, at a field as

low as 20 mT, 5CB doped with 0.1 vol% magnetic particles can readily be manipulated.

Acknowledgments

We acknowledge the DFG for financial support in the framework of SPP 1681 “Field controlled particle-matrix interaction”. (Grant No. SCHM 1747/10). Furthermore, Karin Koch acknowledges IHRS BioSoft.

References

[1] F. Brochard, P. P. G. de Gennes, *J. Phys.*, **31**, 691–708, 1970.

[2] O. Buluy, S. Nepijko, V. Reshetnyak, E. Ouskova, V. Zadorozhnii, A. Leonhardt, M. Ritschel, G. Schönhense, Y. Reznikov, *Soft Matter*, **7**, 644–649, 2001

Scope and implications of the new ISO standard for magnetic nanosuspensions

U. Steinhoff, G. Marks, J. Wells, F. Wiekhorst

*Physikalisch-Technische Bundesanstalt, Abbestrasse 2-12, 10587 Berlin, Germany. (*uwe.steinhoff@ptb.de*)*

Magnetic nanoparticles (MNP) are widely used in technical and biomedical applications. Currently, the International Organization for Standardization (ISO) is working on an ISO standard for magnetic nanosuspensions. Here, we review the scope of the new ISO standard and the implications for handling magnetic nanosuspensions in academic and industrial environments.

Introduction

Liquid suspensions of MNP are used in many technical and biomedical areas. Applications range from loudspeakers, mobile phones, vacuum sealings, metal separation and water remediation to in-vitro diagnostics, in-vivo diagnostics and MNP based therapies. The worldwide economic impact of MNP and MNP based products amounts to far more than 2 billion € per year. Obviously, this creates a demand for international standards on the main characteristics of MNP and the respective measurement procedures. ISO currently develops a document standard on magnetic nanosuspensions to provide a more solid base for commercial trade, application development, regulation and science in the MNP sector [1]. In a previous contribution, we had summarized *a priori* considerations on the content of such a standard document [2].
The current draft ISO standard is more application oriented than initially projected, focusing on the necessary definitions of important characteristics of MNP suspensions, and listing relevant measurement procedures in each case.

Scope and content of the new ISO standard on magnetic nanosuspensions

ISO standards are voluntary agreements between stakeholders documenting the state of the art in a technological area for further reference by market participants or regulatory agencies.
In a new field such as nanotechnology, the foremost interest is the definition of terms and characteristics. These terms can then be used by MNP manufacturers for labelling their products and designing technical data sheets, or by scientists exchanging information on MNP [3]. The definitions include general terminology such as “particle”, “nanoparticle” and “fluid nanosuspension” among many others. Physical characteristics of MNP to be measured are also defined, as well as a list of appropriate measurement methods.
While the definitions for chemical composition and mechanical fluid properties could be taken from other existing standard documents, many of the magnetic properties of MNP suspensions needed a new definition. The reason for this was that either they have never been defined before in a standard (e.g. NMR relaxivity), or else their previous definition was targeted at bulk material and impractical for MNP suspensions. Examples for this class of terms are the new expressions for “magnetization” and “saturation magnetization”. They have been explained before in IEC 60050 [4], but for another context than MNP and were found to not be suitable.
A very important part of the new ISO standard is the listing of appropriate measurement methods together with the indication of applicable standards for conducting these measurements, if they exist. Measurement results should be reported along with the applied measurement method, and the main parameters of the measurement.

Another strict requirement is the use of SI units for all physical quantities. Unfortunately, non-SI units for MNP properties are still widely found in the literature, which considerably hampers communication among scientists, and also between scientists and other stakeholders.

Implications of the new ISO standard for scientific, commercial and regulatory activities involving MNP suspensions

First, it must be repeated, that an ISO standard is a voluntary agreement without any binding power. However, since it has been developed by a large group of technical experts, it can be assumed that the content of the standard represents a common view which is based on solid scientific knowledge. Thus, the use of the terms and definitions in the standard is recommended to all scientists to improve their communications, clarify the interpretation of their results and extend the range of possible users. Certainly, the ISO standard will have the most impact for commercial activities involving MNP. It can be used for labelling MNP nanosuspension or describing their properties in technical data sheets. Further, buyers of MNP suspensions have the possibility to ask for the indication of specific MNP properties in clear terms. Companies announcing their product characteristics according to the ISO standard may have a market advantage, due to better understanding and trust of consumers in their product. Also, for manufacturers of measurement systems for magnetic and other properties of magnetic nanosuspensions, the ISO standard can be an indispensable guideline for how to present measurement results.

The further improvement of measurement methods for MNP suspensions requires reference materials for certain (especially magnetic) properties of such suspensions. The ISO standard provides a good basis for the metrological characterization of future reference magnetic nanosuspensions.

Regulatory agencies (whose documents can be binding) focus their considerations on product safety and environmental aspects of magnetic nanosuspensions. For them, the definitions of the main physical parameters in an ISO standard, greatly enhances the work. They can make the use of the ISO standard mandatory in certain application fields, i.e. for labelling MNP suspensions intended for use in humans. They might even issue a rule to make the ISO standard mandatory on a national level to protect the national industry from foreign non-compliant competitors.

Conclusion

An ISO standard for magnetic nanosuspensions is currently under development and is due to be published by the end of 2018. Initially, the standard will serve as a reference document for labelling MNP suspensions. In the further future, other ISO standards, reference materials and even regulatory acts will be based on this document with wide-ranging implications for science and trade of MNP suspensions.

Acknowledgments

This work was supported by the EMPIR program co-financed by the Participating States and from the European Union's Horizon 2020 research and innovation program, grant no. 16NRM04 "MagNaStand".

References

[1] ISO/DTS 19807-1 Nanotechnologies -- Magnetic nanomaterials -- Part 1: Magnetic nanosuspensions -- Characteristics and measurements https://bit.ly/2H22wiM

[2] Steinhoff U, Posth O, Schmidt D: (2015) Aspects of a standardized characterization and description of nanomagnetic suspensions for biomedical applications, Abstracts of the 15th Ferrofluid Workshop, Rostock 2015

[3] Wells, J, et al: (2017). Standardisation of magnetic nanoparticles in liquid suspension. Journal of Physics D: Applied Physics, 50(38), 383003.

[4] Electropedia: The World's Online Electrotechnical Vocabulary. It contains all definitions from IEC 60050. http://www.electropedia.org/

Noninvasive temperature imaging with magnetic nanoparticle spectroscopy

Jing Zhong[1], Meinhard Schilling[1], and Frank Ludwig[1]

[1]*Institut für Elektrische Messtechnik und Grundlagen der Elektrotechnik, Technische Universität Braunschweig*

Introduction

Magnetic nanoparticle (MNP) spectroscopy allows the noninvasive temperature imaging, which is of great significance to biomedical applications, such as magnetic hyperthermia and thermally controlled drug delivery [1]. Generally, two harmonics were used to determine temperature independent of concentration [2-4]. Recently, a scanning magnetic particle spectrometer (SMPS) was designed to measure the spatial distributions of MNP harmonics for noninvasive temperature imaging [5]. In this study, noninvasive temperature imaging with MNP spectroscopy is reported. In addition, the spatial and temperature resolutions are quantitatively characterized and discussed.

Model and methods

In a SMPS system, each measured harmonic is a convolution of the harmonic generated by local MNPs and a point spread function (PSF), defined by the sensitivity profile of a gradiometric pickup coil, as shown in Fig. 1. A reconstruction method is used to independently deconvolute each harmonic to improve the spatial resolution.

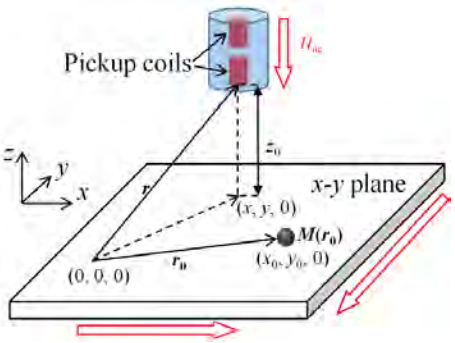

Figure 1. Schematic of the configuration of a spot MNP sample, pickup coil based magnetic sensor and the applied ac magnetic field.

Experimental results and discussion

A phantom E filled with SHP-15 was used for experiments to demonstrate the feasibility of MNP spectroscopy for temperature imaging with the SMPS. Figure 2 shows the photo of the phantom, the measured 1st and 3rd harmonics, and the deconvolved 1st and 3rd harmonics, defining i^{th} harmonic at frequency $i \times f_0$ with fundamental frequency f_0. It shows that the deconvolution improves the spatial resolutions of the 1st and 3rd harmonic images. With either the 1st harmonic image or the 3rd harmonic image, the concentration image can be determined whereas the temperature image can be obtained by combining both the 1st and 3rd harmonic images.

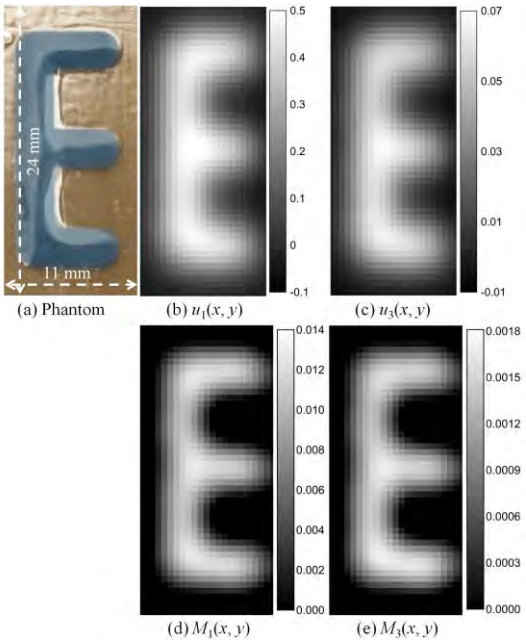

Figure 2. (a) Photo of the phantom. (b) and (c) show the spatial distributions of the measured 1st and 3rd harmonics, respectively. (d) and (e) show the spatial distributions of the deconvolved 1st and 3rd harmonics, respectively.

Figure 3 shows the phantom photo and the temperature image. Temperature-controlled water at 342 K (about 69 °C) passing through a water tube under the phantom was used to change the temperature profile. The temperatures in the upper region, as expected, are higher than in the other region. It demonstrates the feasibility of MNP spectroscopy for temperature imaging with the SMPS.

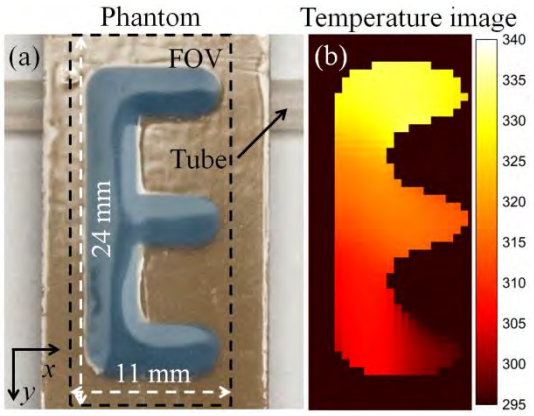

Figure 3. (a) A photo of phantom E and the water tube. (b) Temperature image of the phantom.

In addition, a multi-line phantom with different distances between two adjacent lines is used to study the spatial resolution. Each line has a width of 1 mm and a length of 8 mm. Figure 4 shows the photo of the multi-line phantom and the concentration image. Figure 4b indicates that two adjacent lines with a distance of 1 mm can be resolved whereas adjacent lines with a distance of 0.5 mm cannot be resolved. Taking into account the width of each line, the spatial resolution is about 2 mm.

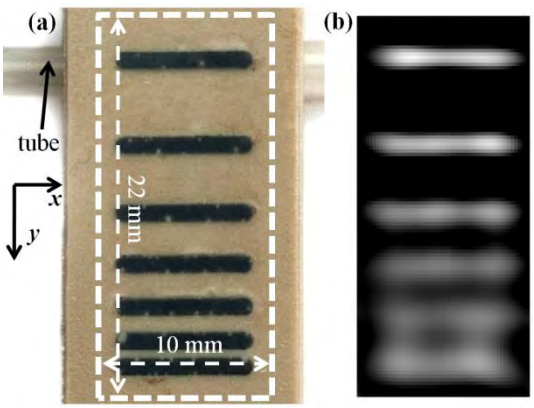

Figure 4. (a) A photo of the multi-line phantom. (b) Concentration image of the phantom.

Conclusion

This study reports on noninvasive temperature imaging with magnetic nanoparticle (MNP) spectroscopy measured with a custom-built scanning magnetic particle spectrometer (SMPS). Experimental results demonstrate the feasibility of MNP spectroscopy for temperature imaging with the SMPS. Experiments on a multi-line phantom show that the spatial resolution is about 2 mm. We envisage that the presented approach is of great significance and interest to biomedicine, such as breast cancer diagnostics and therapy.

Acknowledgments

Financial support from Alexander von Humboldt Foundation is acknowledged.

References

[1] B. Thiesen and A. Jordan, Clinical applications of magnetic nanoparticles for hyperthermia, *Int. J. Hyperthermia*, **24**, 467 (2008).

[2] M. Zhou, J. Zhong, W. Liu, Z. Du, Z. Huang, M. Yang, and P. C. Morais, Study of magnetic nanoparticle spectrum for magnetic nanothermometry, *IEEE Trans. Magn.*, **51**, 6101006 (2015).

[3] J. Zhong, J. Dieckhoff, M. Schilling, and F. Ludwig, Influence of static magnetic field strength on the temperature resolution of a magnetic nanoparticle thermometer, *J. Appl. Phys.*, 120, 143902 (2016).

[4] J. Zhong M. Schilling, and F. Ludwig, Magnetic nanoparticle thermometry independent of Brownian relaxation, *J. Phys. D: Appl. Phys.*, 51, 015001 (2018).

[5] J. Zhong, M. Schilling, and F. Ludwig. Magnetic nanoparticle temperature imaging with a scanning magnetic particle spectrometer. *Measurement Science and Technology*, Submitted.

Magneto-active elastomer as viscoelastic foundation material for artificial tactile sensors with tuneable properties

J. Chavez Vega[1], V. Böhm[2], M. Scharff[3], N. Prem[2], G. Monkman[2], T.I. Becker[1], L. Günther[1], J. Alencastre[3], R. Grieseler[3], K. Zimmermann[1]

[1] *Technische Universität Ilmenau, Technical Mechanics Group, 98693 Ilmenau, Germany*
[2] *Ostbayerische Technische Hochschule Regensburg, Faculty of Mechanical Engineering and Faculty of Electro and Information-Techniques, 93025 Regensburg, Germany*
[3] *Pontificia Universidad Católica del Perú, Faculty of Mechanical Engineering and Academic Department of Science, Lima 32, Peru*

Rodents have tactile hairs on their body. One type of these tactile hairs is the vibrissa. Every vibrissa is supported by its own follicle-sinus complex (FSC). When stimuli are presented the FSC seems to be adjustable by controlling the blood pressure inside the blood vessels. Shape or texture recognition can be done in a wide range by tuning the vibrissa-support properties. Inspired on these biological findings [1], a first approach of a biomimetic sensor system with tuneable properties is built (see Fig. 1). It consists of a magneto-active elastomer (MAE) based support as a viscoelastic representation of the FSC and a steel strip as the vibrissa. The MAE changes its stiffness and damping properties in dependence on the applied magnetic field [2,3].

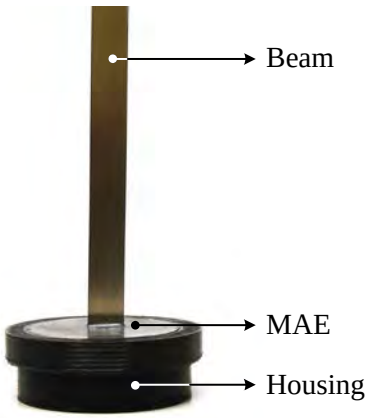

Fig. 1. Sample used for experiments: steel strip embedded on MAE.

Experiments and results

In the experiments, a steel strip (100.15mm x 9.65mm x 0.10mm, ρ=7.850g/cm^3, E=206GPa) is embedded 15mm into a cylindrical MAE-sample (diameter=40mm, height=15mm, partially encased by housings on the circumferential and bottom surfaces). The isotropic MAE [2] consisting of silicone rubber (Alpa-Sil Classic, Alpina Silicone Corp.), silicone oil (Xiameter® PMX-200, 500cSt), and carbonyl iron particles (BASF®, CIP CC, average particle size: 10µm) is used. The composition for the fabrication of the MAE-foundation results from former investigations [2,3] (silicone oil: 29.0vol.%, iron: 40.3vol.%). To characterize the effect of the magnetic field on the first resonance frequency f_1 and damping ratio ξ of the steel strip embedded on the MAE-support, tests are performed to measure its response to the presence of a forced vibration under three conditions of magnetic field (MF) averaged to 0mT, 63mT and 180mT. The MF is considered uniform and its magnitude is controlled by the distance between the MAE-material and two permanent magnets (NdFeB, 40mm x 40mm x 20mm), located at each side of the MAE.
Two kind of test are performed. On tests type I, the system is fixed to a shaker which provides a sinusoidal wave. Constant amplitude of 0.5mm in the frequency range of 2…20Hz is the input. The displacement response of the steel strip is measured. The value of f_1 is approximated to the frequency corresponding to the maximum response amplitude of the steel strip (see Fig. 2). Tests type II are performed to approach the damping ratio ξ.

Additionally, from test type II, f_1 can also be calculated. In this case of test type II, a pulse signal is given by the shaker on the bottom of the MAE; the strip oscillates with amplitude decreasing in time. In this period, the coefficients for the damping ratio can be found (see Fig. 3).

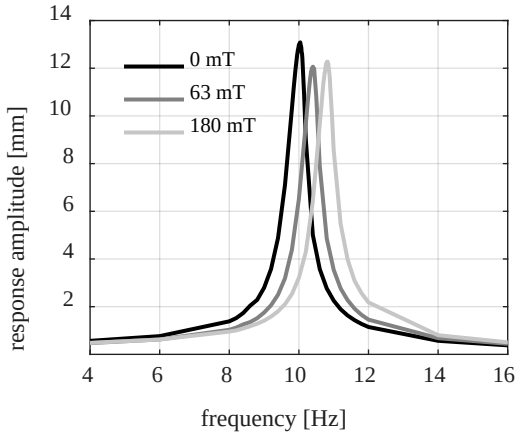

Fig. 2. Response amplitude to a forced stimulus of 0.5mm sinusoidal wave for three conditions of applied MF.

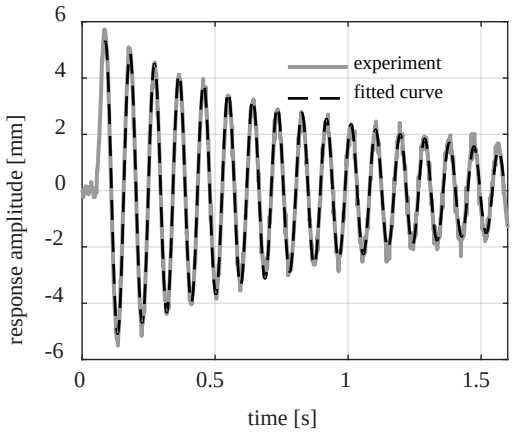

Fig. 3. Response to a pulse on the MAE (applied MF: 180mT).

The average values of f_1 and ξ from five measurements are summarized in Tab. 1. It is noticeable that from both kinds of test, values of f_1 are nearly the same.

Tab. 1. Experimental results of f_1 and ξ for experiments type I and type II.

MF [mT]	Test I	Test II	
	f_1 [Hz]	ξ [-]	f_1 [Hz]
0	10.03	0.00825	10.00
63	10.41	0.00865	10.50
180	10.81	0.01298	10.83

Conclusions and outlook

The resonance frequency and the damping factor can be tuned under the presence of a magnetic field, and the considered effect can be used to realise a vibrissal sensory system which can vary its properties (on its own). Further studies focus on tests with various compositions for the MAE-samples, e.g., diverse levels of visco-elasticity. These considerations include also tests with a wider range for the induced magnetic field as well as more geometries as representation of the vibrissa.

Acknowledgments

This work is supported by the Deutsche Forschungsgemeinschaft (DFG) and the Russian Foundation for Basic Research (RFBR) within PAK 907, projects PO 2013/1-1 and BE 6553/1-1, as well as by the DFG priority programme SPP 1681 under the projects MO 2196/3-1 and ZI 540/17-2.

References

[1] Volkova, T.I.; Hermann, S.; Kaufhold, T.; Böhm, V.; Zeidis, I.; Zimmermann, K.; Naletova, V.A.: Ferrofluid based artificial tactile sensors. 15th German Ferrofluid Workshop, Rostock, 2015, Book of Abstracts, pp. 29-30.

[2] Zimmermann, K.; Böhm, V.; Kaufhold, T.; Chavez Vega, J.; Becker, T.; Odenbach, S.; Gundermann, T.; Schilling M.; Martens, M.: Investigations and simulations on the mechanical behaviour of magneto-sensitive elastomers in context with soft robotic gripper applications. Int. Scient. J. of IFToMM *Problems of Mechanics* **65**, 4 (2016) 13-25.

[3] Chavez Vega, J.; Kaufhold, T.; Böhm, V.; Becker, T.; Zimmermann, K.; Martens, M.; Schilling, M.; Gundermann, T.; Odenbach, S.: Field-induced plasticity of magneto-sensitive elastomers in context with soft robotics gripper applications. Proc. Appl. Math. Mech. **17** (2017), pp. 23-26.

Long-term hybrid phantoms mimicking biological tissue enriched with magnetic nanocomposites for X-Ray and MR imaging

H. Rahn [1,2,3], K. Feindel[2,3], D. Patalawa[2,3], S. Watt[2] S. Dutz [4], S. Odenbach [1], T. StPierre [2,3].

[1] *Institute of Fluid Mechanics, Chair of Magnetofluiddynamics, Measurement and Automation Technology, Technische Universität Dresden, Dresden, Germany*
[2] *School of Physics and Astrophysics, The University of Western Australia, Western Australia*
[3] *Centre for Microscopy, Characterisation and Analysis (CMCA), The University of Western Australia, Australia*
[4] *Institut für Biomedizinische Technik und Informatik, Technische Universität Ilmenau, Germany*

Intruduction

For magnetically assisted local cancer treatments such as e.g. magnetic Drug Targeting (MDT) and magnetic Heating Treatment (MHT) the distribution of the magnetic nanocomposites (MNC) [1] within the target region but also their quantity plays a key role. The quantification of MNC is required e.g. to analyze drug distribution during MDT or study potential heat distribution, and thus to determine, and optimally, regulate the heating power during MHT [2].
MNC distribution in biological tissue can be studied with the help of X-ray computed tomography (XCT) and Magnetic Resonance Imaging (MRI). Clinical XCT represents one of the standard measuring methods in clinical imaging and diagnostics, while microcomputed tomography (XμCT) is gaining increasing relevance in engineering and life sciences [3]. XCT is a powerful tool for the visualization of hard tissues such as bones. Magnetic resonance imaging (MRI) is also one of the mainstays in clinical imaging techniques for visualizing the structure and function of soft tissues as the brain and internal organs, and is particularly sensitive to iron levels within the body [4].
Use of both, XCT and MRI, increases the information attained and enhances the effective impact of the quantitative imaging. This approach can lead to more accurate and timely, reducing the potential for mistakes and costly inefficiencies, which effects beneficially on the patient. The use of a hybrid body tissue and MNC phantom for a cross-calibration of XCT and MRI [5] provides the possibility of data merging, and thus a more precise visualisation of MNC in e.g. tumour sites as well as their 3-dimensional quantification. In this paper we present a promising approach for a hybrid long-term stable phantom which mimics MNC enriched biological tissue as e.g. tumours after magnetically assisted cancer treatments with respect to the imaging modalities of XCT and MRI.

Materials and Methods

For this study two different immobilisation matrices – silicon rubber and gelatin - have been used to create 3 different phantom types loaded with MNC [6]:

a. silicon rubber **E**co**F**lex® (EF) loaded with MNC → EF-MNC
b. **L**ong-**T**erm-**S**table-**G**elatin (LTSG) loaded with MNC → LTSG-MNC
c. **L**ong-**T**erm-**S**table-**G**elatin (LTSG) and raw homogenized **C**hicken **B**reast mixture loaded with MNC → LTSG-CB-MNC.

The phantoms were produced as cylinder disc stacks with alternating layers of blank EF and MNC loaded EF with base diameter of 30 mm (Figure 1a). Furthermore, phantoms with a shape more similar to e.g. a real tumor with MNC enrichments were produced. These cylinder discs have a base diameter of 60 mm and include 3 smaller cylinder discs with 3 MNC concentrations, e.g. LTSG-3-MNC-Phantom as presented in Figure 1b) and c). The MNC concentrations in these phantoms range from 0 mg/ml to

4.95 mg/ml. The phantoms have been analysed with NMR, VSM and visualised with MRI, XµCT.

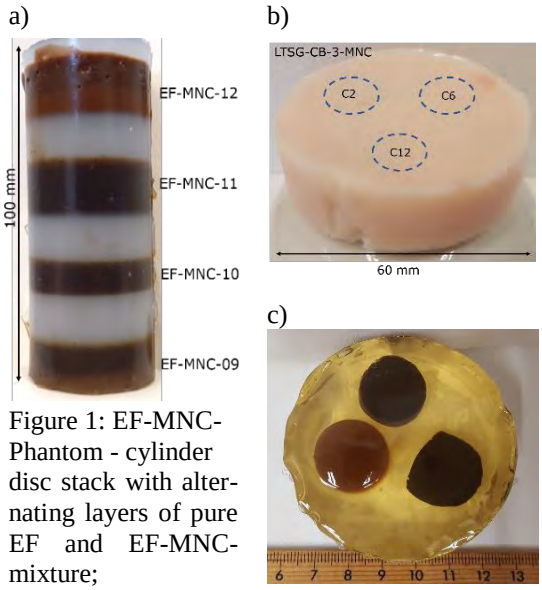

Figure 1: EF-MNC-Phantom - cylinder disc stack with alternating layers of pure EF and EF-MNC-mixture; b) LTSG-CB-3-MNC-Phantoms – cylindrical discs with a base diameter of 60 mm, and included three smaller cylinder discs with variated MNC concentrations – and c) LTSG-3-MNC-Phantom.

Results

The tomographic measurements were performed with a "Bruker SKYSCAN 1176: High-resolution in-vivo Micro CT" [7]. The tomographic data was evaluated with respect to mean grey values for different MNC concentrations. These grey values have been plotted as function of VSM-determined MNC concentrations. This provides a calibration curve and a calibration equation (See Figure 3).

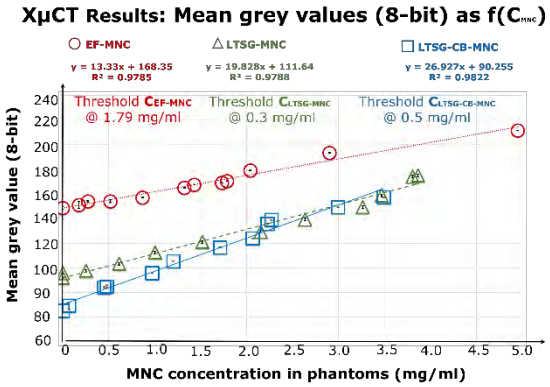

Figure 3: Mean grey values (8-bit) of the three presented phantom systems plotted as functions of VSM-determined MNC concentrations.

MRI measurements were performed with "Bruker BioSpin MRI"which is a small animal and molecular MRI for pre-clinical research. The scanner provides a magnetic field of 9.4 T [7]. The obtained T2 relaxation times have been plotted as a function of the MNC concentrations. This provides a calibration curve and an equation as well.
The cross-calibration of the XµCT and MRI data provides a sensitivity range for each phantom system. An example is given in Figure 4 where the R2 relaxation rates and the mean grey values for the LTSG-MNC-phantoms are merged. The light blue rectangle covers the area where both experimental scanners show an appropriate signal. This sensitivity range for this particular phantom system lies between MNC concentrations from 0.3 mg/ml (minimum detectable MNC concentration with "SKYSCAN 1176") and 2.64 mg/ml (maximum detectable MNC concentration with the "BioSpin MRI").

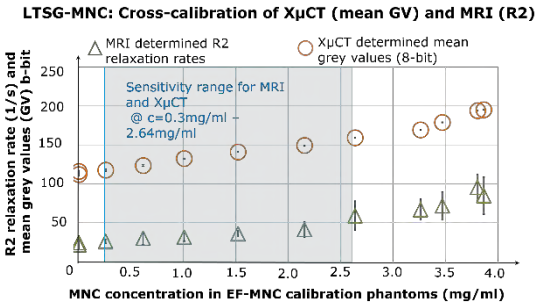

Figure 4: MRI and XµCT results LTSG-MNC-Phantom system. The R2-values and mean grey values are plotted as a function of VSM-detected MNC concentrations.

Acknowledgments

This work was supported by Deutsche Forschungsgemeinschaft (FKZ: RA 2633/2-1; DU 1293/6-1 and TR408/9-1).

References

[1] Q. Pankhurst: J. Phys. D: Appl. Phys., 36, 13; (2003),
[2] S. Laurent: Adv. Colloid Interface Sci.; 166, 1–2, 10, pp.: 8–23; (2011),
[3] H. Rahn: Nanomedicine 4 (8) pp.: 981–990; (2009),
[4] D. Weishaupt: Springer Verlag, ISBN 978-3-642-41616-3; (2014)
[5] H. Rahn: JMMM; 405, , pp.: 78–87; (2016),
[6] S. Dutz et. al: JMMM 321, pp.: 1501 – 1504; (2009),
[7] Bruker: http://www.bruker.com.

Analysis of the interplay between in a PDMS-matrix embedded nickel-particles

H. Schmidt[1], G. K. Auernhammer[1,2]

[1] *Max Planck Institute for Polymer Research, Mainz, 55128, Germany*

[2] *Leibnitz Institute for Polymer Research, Dresden, 01069, Germany*

This work builds on previous investigations of the interaction between magnetic particles with the surrounding matrix in 3D magnetic hybrid materials systems in applied magnetic fields [1-3]. It is divided in two main research topics: the first part is about the progress of buckling magnetic chains consisting of micrometer-sized superparamagnetic particles. The second part focusses on progress of the interplay between larger nickel particles. In both cases, a soft PDMS matrix is used.

Crosslinking the reactive polymer under an external magnetic field leads to chain formation of the suspended superparamagnetic particles. Shilin Huang witnessed a buckling of these particle chains under the influence of a slowly rotating external magnetic field. For this instability to be easily observed, it is essential to adjust the elastic modulus of the matrix below 10 Pa [2]. Since the sample preparation relied on the random self-assembly of particles into chains, the particle chains differ in size and spacing. The distribution of chain lengths and spacings depends mainly on the particle concentration and strength of the magnetic field.

Recent measurements showed an antisymmetric buckling of nearest neighbour chains. To investigate this further, our focus is to move away from the random distribution of the chains in space to a well-defined and controllable spatial arrangement of the particle chains. Various strategies appear promising to this end. Adapting the magnetic field strength influences chain length and spacing. However, the reproducibility must be improved, e.g., by carefully adjusting the magnetic field. An alternative, promising route is the capillary-assisted self-assembling of the particles on structured substrates [4].

By changing to the larger nickel particles, we increase the magnetic moment of the particles. This allows the use of matrices with much higher elastic modulus in the range of 100 to 1000 Pa. Our previous study [3] focused on well-separated particles and their non-pairwise matrix mediated particle interaction. Here, we look at particle pairs distanced by either a particle diameter or even less.

For those systems, when an external magnetic field of 170 mT is rotated respectively to the particle axes, a nicely reproducible jumping apart (gap opening) and closing of nickel-particles (Fig. 1) is observed. These jumps strongly depend on the initial particle distance. The detailed mechanism is yet not completely clarified but evaluated data strongly indicates an interplay between the magnetic dipole-dipole-interaction (perhaps to be supplemented by higher order corrections) and forces due to the elastic deformation of the matrix. Since the exact particle configuration depends on the magnetic field history of the sample, the gap opening and closing is hysteretic, as a function of magnetic field orientation. To clarify this process further, we will extract the deformation field of the matrix around the particles to get an overall picture of the existing influencing forces.

a)

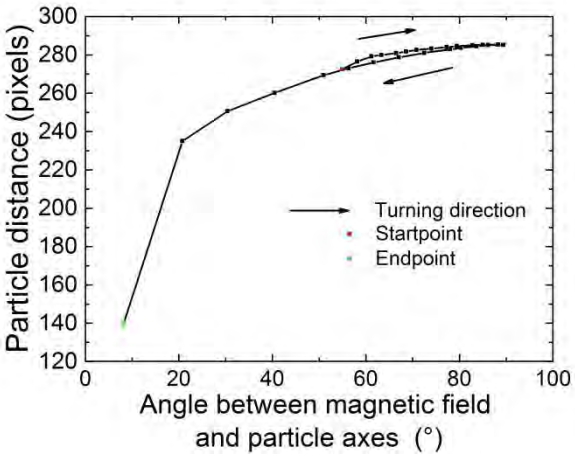

b)

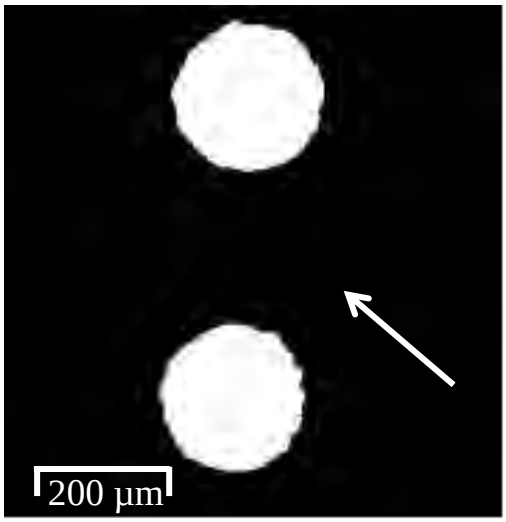

c)

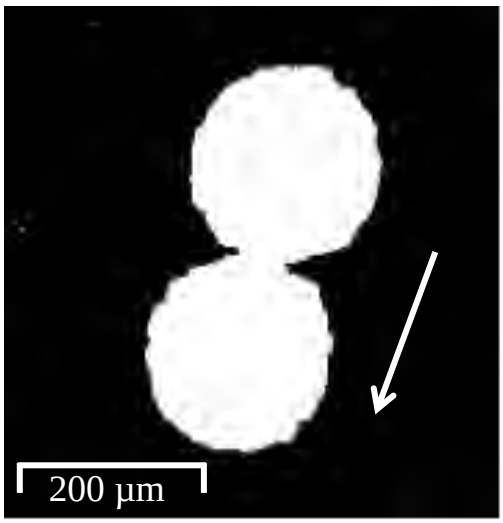

Figure 1. a) Particle distance while rotating the magnetic field. In white the nickel-particles gaped **b)** or closed **c)**. White arrow: The orientation of the external magnetic field.

Acknowledgments

The authors thank for support by the Deutsche Forschungsgemeinschaft (DFG) through the SPP 1681

References

[1] D. Collin, G. K. Auernhammer and O. Gavat, Macromol. Rapid Commun., 2003. 24: p. 737 - 741.

[2] S. Huang, G. Pessot and P. Cremer, Soft Matter, 2016, 12(1): p.228-237.

[3] M. Puljiz, S. Huang and G. K. Auernhammer, Physical Review Letters, 2016, 117(23), 238003.

[4] M. Mayer, M. Tebbe and A. Fery et al., The Royal Society of Chemistry, Faraday Discuss., 2016, 191, 159-176

Magnetically induced movement of NdFeB particles in magnetorheological elastomers

M. Schümann, S. Odenbach

Chair of Magnetofluiddynamics, Measuring and Automation Technology, Technische Universität Dresden

Introduction

Magnetorheological elastomers are a special kind of magnetic field-responsive smart materials developed in the last years, where magnetic micro particles are embedded in a soft elastomer matrix. As a result the magnetoactive effects on the mechanical properties are combined with a soft elastic material. The investigation of the interaction of the particles with the external magnetic fields and the matrix is a subject of ongoing research. X-ray micro tomography proved to be a convenient tool for analysis of the particle micro structure [1-3]. For this investigation a stepwise magnetisation of a magnetically hard magnetorheological elastomer up to 2 T was performed to retrace the chain formation process of the particles. A broad analysis of the change of the magnetic, mechanical and structural properties should provide an understanding in the chain formation process.

Material and methods

40 wt% of Magnequench® MQA were used as magnetic particles. These magnetically hard NdFeB particles are highly anisotropically shaped with a diameter of 100 to 200 µm. PDMS polymer components by Gelest® were used to produce a soft elastomer matrix.

Stress-strain-tests were conducted using a universal testing device with and without the presence of a magnetic field B_{loc} = 250 mT. Subsequently, the sample was tomographed with the TomoTU cone beam tomography setup [2] with and without the presence of B_{loc} = 250 mT as well. The samples were then magnetized externally at B_{ext} = 250 to 2.000 mT in 250 mT steps. After each magnetisation the measurements were repeated. Additionally the material was analysed by XRD to explain the orientation behavior of the particles.

Magnetorheological effect

The results regarding the elastic properties show a signifcant increase of the Young's modulus above a magnetisation of B_{ext} = 1 T, both in presence of B_{loc} = 250 mT and without. A significant magnetorheological effect above B_{ext} = 1 T is present. A slight decrease of the modulus without the field is observed. This can be explained with the fatigue of the sample due to the local destruction of the matrix as a result of the advancing particle displacement. The results are depicted in figure 1.

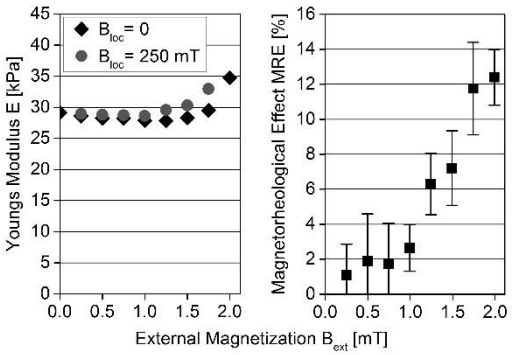

Figure 1: *The measured Young's Modulus for each magnetization step and the calculated magnetorheological effects.*

Particle structure

As external magnetization proceeds, the reconstructed tomography data shows the stepwise rearrangement of the particles from a homogeneous distribution to fully formed chains, as depicted in figure 2. This changing structure leads to the elastic properties observed with the mechanical testing.

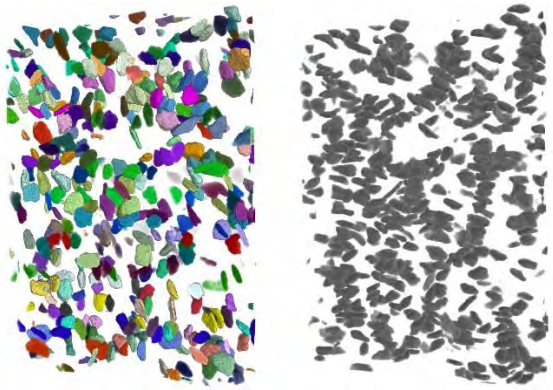

Figure 2: *The particle structure obtained by the reconstructed tomography data. Left: initial state after the particle separation process. Right: final state after magnetization at 2T, before particle separation.*

It's worth noticing, that the particles align perpendicular to the direction of the magnetic field. X-ray diffraction measurements (XRD) show a clear relation between geometrical orientation and crystal orientation of the particles. It can be assumed, that the particles align their magnetic predominant direction of the crystal structure to the magnetic field [3]. This behavior is shown schematically in figure 3.
The tomography data enables an evaluation of position, size, surface, asphericity and angle of the major axis for each of the app. 11.000 particles in the sample.

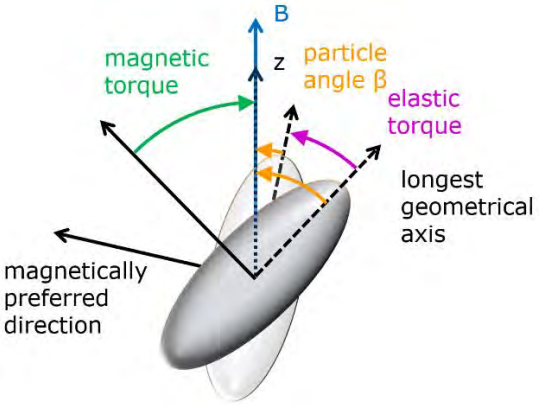

Figure 3: *Rotation of the particle perpendicular to the magnetic field.*

Particle angles

The angle of the first major axis of every particle towards the magnetic field direction was evaluated for each magnetic situation. The density distribution of occurring particle angles is shown in the following figures 4 and 5.

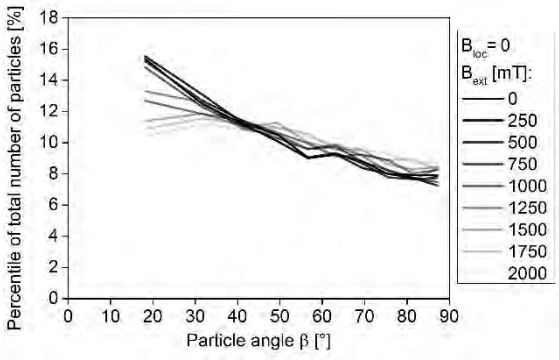

Figure 4: *Density distribution of the particle angles, measured without the local field $B_{loc} = 0$.*

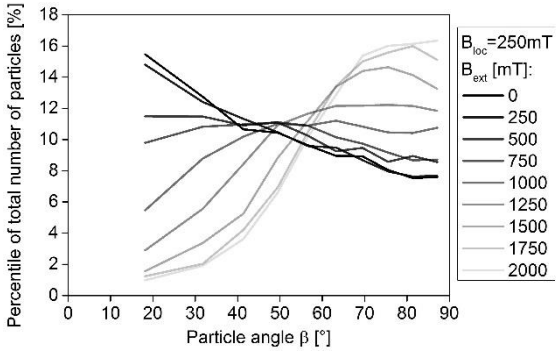

Figure 5: *Density distribution of the particle angles, measured in presence the local field $B_{loc} = 250$ mT.*

The results show a strong and mostly reversible rotation of the particles induced by the local field B_{loc}, which increases for higher magnetizations B_{ext} due to increasing remanence of the particles. Furthermore, increasing B_{ext} leads to a nonreversible rotation of particles with a small initial angle.

Acknowledgments

Financial support by DFG (Grant. No. OD18/21) within SPP1681 is gratefully acknowledged.

References

[1] Borbáth T, Günther S, Borin D Y, Gundermann T, Odenbach S. (2012). Smart Mater. Struct. 21(10), 105018
[2] Günther D, Borin D Y, Günther S, Odenbach S (2012). Smart Mater. Struct. 21(1), 015005
[3] Schümann M, Borin D Y, Huang S, Auernhammer G K, Müller R, Odenbach S (2017) Smart Mater. Struct., 26(9), 095018.

The rotation of high aspect ratio rods in a magnetic field in a thermoresponsive matrix

S. Hinrichs[1], L. Großmann[1], A. Meyer[1], B. Fischer[1]

[1] *University of Hamburg, Department of Physical Chemistry, Grindelallee 117, 20146 Hamburg*

Recently multi-stimuli responsive hydrogels get a lot of attention, because of their broad spectra of application. Here we use a thermoresponsive polymer, namely poly-*N*-isopropylacrylamide (pNIPAM), as a matrix with the ability to undergo a coil-to-globule transition at a critical temperature of about 34°C, the so-called lower critical solution temperature (LCST). Below the LCST pNIPAm chains are hydrophilic and elongated. Once the temperature rises above the LCST the chains collapse and form globules in aqueous solution due to their now hydrophobic character. [1] The second stimulus is provided by anisotropic magnetic particles, goethite rods. Goethite rods can form a lyotropic nematic phase in aqueous solution, similar to liquid crystalline materials.[2] On top of that, goethite rods reorient when a magnetic field is applied. The particle orientation changes from parallel to the magnetic field at low field strengths to perpendicular at high field strengths. Lemaire explains this with the remanent magnetic moments of the rods at weak fields and with their negative anisotropy of magnetic susceptibility at strong fields, respectively.[2]

Goethite particles

Goethite particles were prepared by a hydrothermally facilitated structural phase transition from akaganeite (β-FeOOH) to goethite (α-FeOOH). The particles were characterized by TEM (Fig. 1A) and XRD. The orientational dynamics of the particles in aqueous solution were characterized by small angle X-ray scattering (SAXS) and rheological experiments.
As expected a continuous transition is observed from an isotropic state without an applied field, to a weakly parallel ordered state at low field strengths. At about 150 mT the particles show a slight change in orientation towards a perpendicular alignment. The degree of orientation, measured by a simplified version of Herman's orientation function [3], increased almost linearly with the increasing field strength.

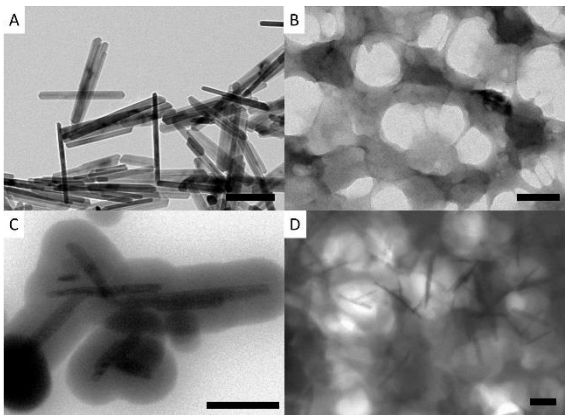

Figure 1: A: Goethite particles directly after the synthesis B: pNIPAm Gel with 0.05 wt% crosslinker density C: goethite particles (10 wt%) in a pNIPAm Gel with 0.05 wt% crosslinker density D: goethite particles (10 wt%) in a pNIPAm Gel with 0.025 wt% crosslinker. The scalebars show 200 nm.

Hydrogel/particle composites

In addition, the particles were embedded into a pNIPAm matrix. Since the collective behavior of the particles is influenced by particle interactions and the particles react only weakly to a magnetic field, large amounts of particles were embedded into the matrix after a method introduced by Nack.[4] In this method pNIPAm is synthesized and crosslinked using glutaraldehyde (GA) (Fig. 1B). Afterwards the particles are introduced into the hydrogel. The number of particles in the system was adjusted to 10 and 30 wt%, respectively.
By varying the ratio of pNIPAm to GA we can create differently sized meshes in the

network (Fig. 1C and 1D) to adjust the mobility of the rods.
The kinetics of the rotation were monitored by SAXS over the course of 20 h, while a field of approximately 1 T was applied. The results were compared to the mechanical properties of the different hydrogel/particle composites measured by rheology.

Acknowledgments

The author thanks the University of Hamburg program for doctoral scholarships for financial support. The authors acknowledge the Deutsche Forschungsgemeinschaft (DFG) via the priority program SPP 1681 "Feldgesteuerte Partikel-Matrix-Wechselwirkungen" Grand Nr. Fi 1235/2-2.

References

[1] Heskins M. et al. *J. Macromol. Sci. A* 2:8 **(1968)**: 1441-1455
[2] B.J. Lemaire, European Physical Journal E 319 **(2004)** 309-319.
[3] T. Yano,Polymer (United Kingdom). 53 **(2012)** 4702-4708.
[4] A. Nack, Dissertation, **(2017)**.

Rheological properties of magnetic biogels

M.T.Lopez-Lopez[1], A.Yu. Zubarev[2]

[1] *Department of Applied Physics, University of Granada, Spain*
[2] *Department of Theoretical and Mathematical Phsyics, Ural Federal University, Ekaterinburg, Russia*

Magnetic polymers (gels and elastomers) are composite materials consisting of nano-sized magnetic particles embedded into a gel matrix. Combination of rich set of physical properties of the polymer and magnetic systems is very perspective for many progressive industrial, bioengineer and biomedical applications. In part, these composites are used as magnetocontrollable dampers, vibration and shock absorbers. Hydrogels with biocompatible magnetic particles are very promising for various biomedical technologies – for drug delivery and biosensors; constriction of soft actuators and artificial muscles; for regenerative medicine and tissue engineering. An overview on the synthesis of magnetic hydrogels and their biomedical applications can be found in [1].

Nonmagnetic biocompatible hydrogels are actively used in bioengineering and clinical medicine as scaffolds for manufacturing, curing and regeneration of biological tissues.

The scaffolds, prepared of magnetic hydrogels, have several advantages in front of their nonmagnetic analogies. First, magnetic particles allow in-vivo visualization of the growing tissue, by using the magnetic resonance imagining. Second, as some experiments demonstrate, the particles stimulate proliferation of the tissue cells [2=6]. Third, in vivo applications, magnetic particles functionalized with the agents of the tissue growth, can be attracted to the magnetic scaffold, providing intensification of this process [2]. Fourth, in-vivo, magnetic hydrogels can be injected into the place of the tissue regeneration in a liquid state, with the help of a syringe, i.e. by the *microinvasive way*. The gel, up to its curing, can be fixed in this place by using magnetic field of necessary configuration. Next, rheological properties and behavior of these magnetic implants can be controlled by the external field [3].

We present review our recent progress on the field of the experimental and theoretical study rheological properties of magnetic biogels. Our experimental systems consist of fibrin networks embedded with magnetite nanoparticles and swelled by water-based solutions. Fibrin is a natural protein involved in the clotting of blood and consequently it has inherent biocompability and biodegradability. As magnetic phase we used commercial magnetite nanoparticles.

Internal structures of the hydrogels, polymerized both without external magnetic field action and under the field are shown in Fig. 1. This Figure shows images taken by scanning electron microscopy (SEM) of nonmagnetic gels (Fig.1a) and magnetic gels (both gelled in absence and presence of applied magnetic field). The nonmagnetic gel (Fig.1a) had fibrin fibers distributed forming a relatively dense porous structure which did not have any junction, except the homogeneously distributed links between couples of fibers. On the other hand, for magnetic gel with 0.2 vol.% of the particles, geleld in the absence of a magnetic field (Fig.1b), we observe a much opener structure, with knots formed presumably by clusters of magnetic nanoparticles and polymer material. For magnetic gel with 0.2 vol.% of the particles, gelled in presence of the field (Fig. 1c and 1d), we can see a heterogeneous structure, consisting of roughly parallel regions with dense concentration of polymer fibers, separated by some regions with low density of fibrin

fibers – this is more evident at lower magnification (Fig. 1d,e)

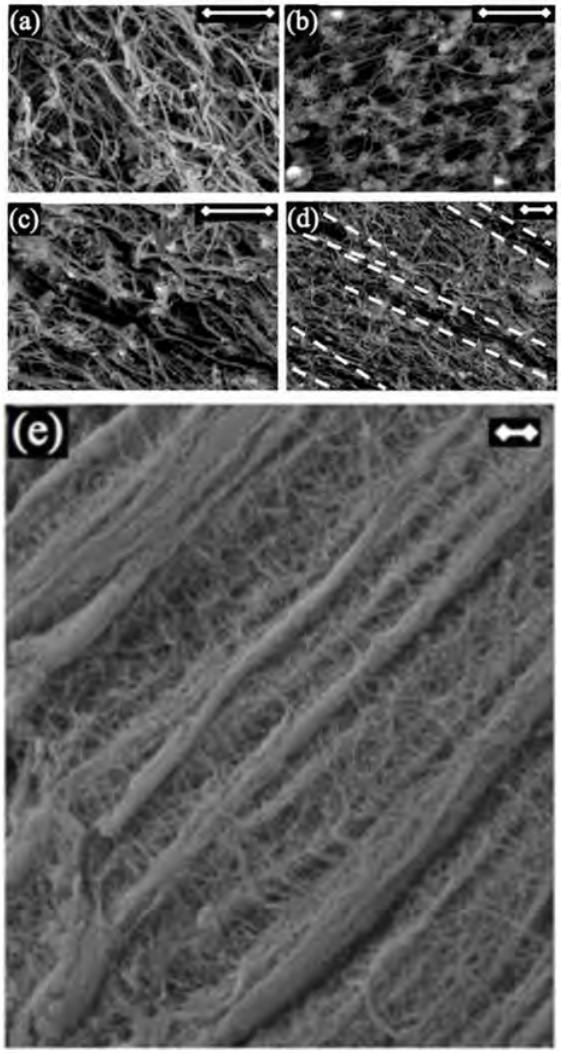

Figure 1. Images of scanning electron microscopy of gels. (a) Fibrin gel; (b) fibrin gel with 0.2 vol.% of magnetic nanoparticles gelled in absence of a magnetic field; (c) and (d) fibrin gel with 0.2 vol.% of magnetic nanoparticles gelled in presence of a 48.6 kA/m magnetic field; (e) fibrin-alginate gel with 3.5 vol.% of magnetic nanoparticles gelled in presence of a 48.6 kA/m magnetic field. Dashed lines in (d) delimit the regions with low concentration of fibrin fibers. Bar length: 5 microns.

Our experiments show that elastic modulus of the biocomposites increase with the particles concentration about three orders of magnitude faster than the classical Einstein theory predicts. Some experimental and theoretical results are presented in Figs.2 and 3.

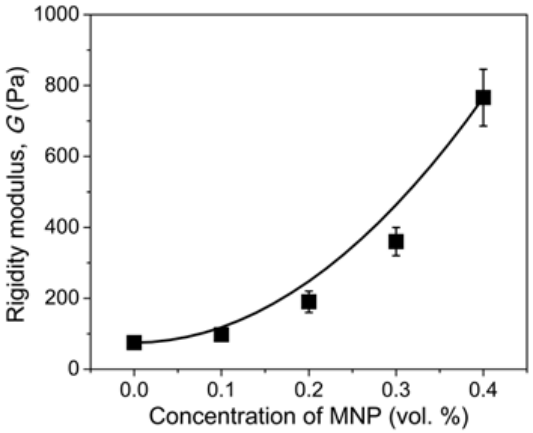

Figure 2. Rigidity modulus of magnetic hydrogels, gelled without magnetic field. Squares represent experimental data, line – theory.

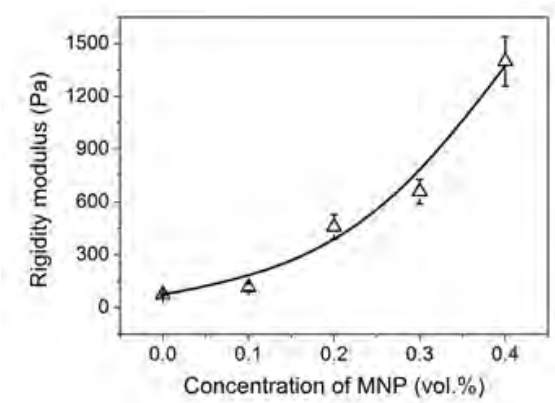

Figure 3. Same as in Fig.2 for the system gelled under the field 48.6kA/m

We present theoretical models of the strong concentration dependence of the rigidity modulus. We suppose that in the composites, gelled without field, the knots, shown in Fig.1b, serve as additional cross-links of the fibrin macromolecules. In the systems, gelled under the field, the dense elongated structures, seen in Fig.1c-e, percolate the sample and resist to the macroscopic shear. Comparison of the theory and experiments are shown in Fig.2,3.

[1] Li Y., Huang G., Zhang X., Li B., Chen Y., Lu T., et al ., Adv Funct Materials **23** (6), 660-672 (2013)
[2] Carmona F., Mouney C., J. Mater. Science, 27(5), 1322–1326 (1992)
[3] Rodriguez-Arco L., et.al., Nanoscale, 8(15), 8138-8150 (2016)

Multiparametric investigations of dynamics in Magnetic Particle Spectroscopy

S. Draack[1], N. Lucht[2], B. Fischer[2], M. Schilling[1], T. Viereck[1], and F. Ludwig[1]

[1] *Institut für Elektrische Messtechnik und Grundlagen der Elektrotechnik, TU Braunschweig, Braunschweig, Germany*
[2] *University of Hamburg, Department of Physical Chemistry, Grindelallee 117, 20146 Hamburg*

The dynamic magnetization characteristics of magnetic nanoparticles (MNP) are influenced by both the Néel and the Brownian relaxation mechanism. Therefore, harmonic spectra in Magnetic Particle Spectroscopy (MPS) experimental data are directly linked to ambient properties as temperature or the dynamic viscosity of the surrounding medium. Investigations of these at least partly nonlinear relationships are of utmost importance for biomedical applications as functional Magnetic Particle Imaging (fMPI) and magnetic hyperthermia. Multiparametric MPS measurements help one to evaluate and validate mathematical models of dynamic particle magnetization. Experimental data will be compared to simulations based on Fokker-Planck equations (FPE).

Materials

The dependence of temperature is studied using various commercially available nanoparticle systems as Ocean NanoTech SHP-25, Ocean NanoTech SHP-30 or Micromod synomag®-D. Additionally, a non-commercial $CoFe_2O_4$ model particle system is used to study Brownian-only relaxation dependence on viscosity. Viscosity effects are investigated on viscosity series whose values are distributed logarithmically equidistant.

Methods

A home-built MPS setup [1] provides selectable excitation frequencies in the range of 100 Hz < f < 25 kHz to investigate different relaxation contributions. The excitation field strength amplitude can be controlled up to 30 mT. Furthermore, the setup allows one to regulate the sample temperature in a control range of -20 °C < T < 120 °C and enables freezing the sample. Hence, direct comparisons of mobile and immobilized states in ice are feasible.

Experimental

Temperature-dependent experimental data were acquired at f_0 = 1 kHz and B = 25 mT for a Brownian and a Néel dominated particle system.

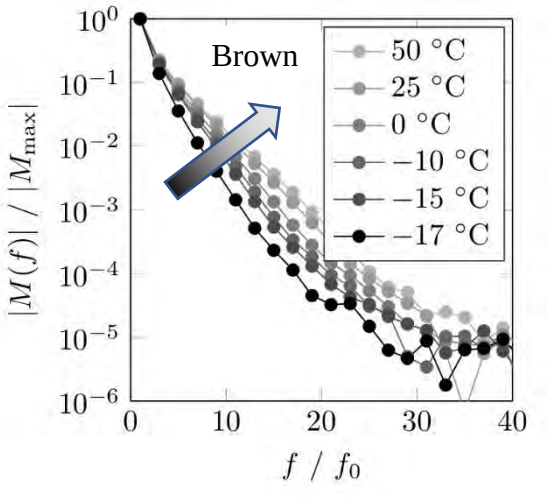

Figure 1: Harmonic spectra of Ocean NanoTech SHP-30 for different temperatures (f_0 = 1 kHz, B = 25 mT).

As can be seen in Fig. 1, the higher harmonics of Ocean NanoTech SHP-30 drop by trend for decreasing temperatures as a result of slowing Brownian relaxation. A non-continuous jump of the harmonic response is observed at -17 °C due to the phase transition of subcooled deionized water to ice. For the same measurements parameters, harmonic spectra of Micromod synomag®-D

are depicted in Fig. 2. The frozen state is reached at -15 °C. Essentially, the temperature dependence of both particle systems is qualitatively inverse due to different relaxation types as can be determined from comparisons with simulations based on Brownian and Néel FPE [2].

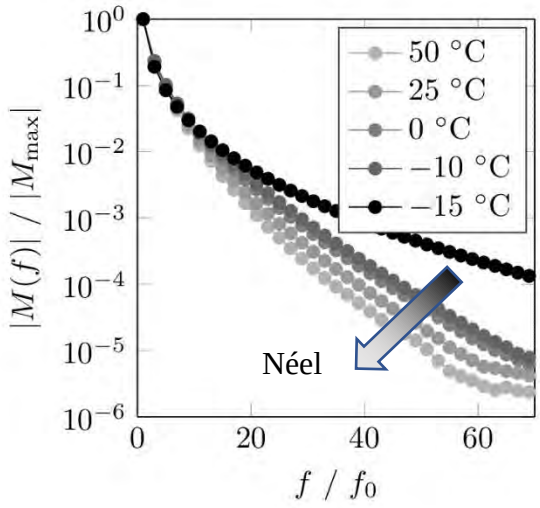

Figure 2: Harmonic spectra of Micromod synomag®-D for different temperatures (f_0 = 1 kHz, B = 25 mT).

For different measurement parameters (f_0 = 5 kHz), Ocean NanoTech SHP-25 shows both Brownian dominated temperature dependence for lower harmonics and Néel dominated temperature dependence for higher harmonics which leads to a crossing of the series of curves in Fig. 3.

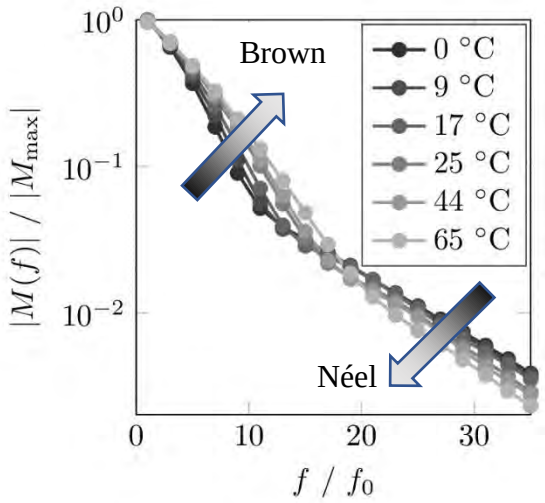

Figure 3: Harmonic spectra of Ocean NanoTech SHP-25 for different temperatures (f_0 = 5 kHz, B = 25 mT).

The particle mobility is investigated for a Brownian dominated $CoFe_2O_4$ particle system. The dependence on dynamic viscosity, excitation frequencies and field amplitudes are discussed based on harmonic spectra and reconstructed dynamic magnetization curves as is exemplarily shown in Fig. 4. Results are compared to FPE simulations.

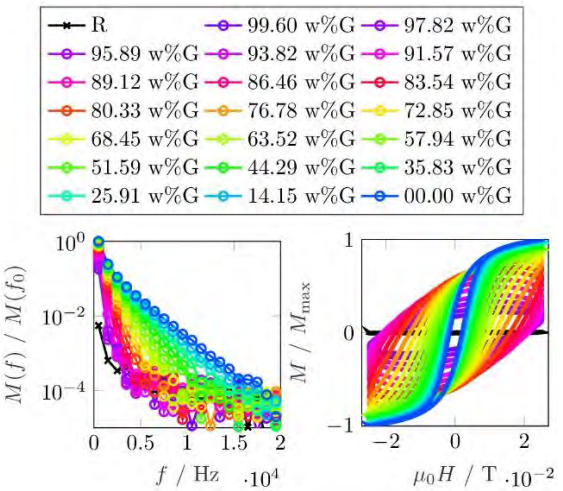

Figure 4: Harmonic spectra (left) and dynamic M(H) curves (right) of a Brownian dominated sample viscosity series.

Acknowledgments

Financial support by the Deutsche Forschungsgemeinschaft DFG via Priority Program SPP1681 (VI 892/1-1, FI 1235/2-2) is gratefully acknowledged.

References

[1] S. Draack et al., “Temperature-dependent MPS measurements”, Int. J. Magn. Part. Imag. 3 (1), 2017

[2] R. J. Deissler et al., “Dependence of Brownian and Néel relaxation times on magnetic field strength”, Med. Phys. 41 (1), 2014

Magnetic Particle Spectroscopy of magnetic nanoparticles at different flow rates

K. Weber, N. Löwa, F. Wiekhorst

Physikalisch-Technische Bundesanstalt, Berlin, Germany

Introduction

Magnetic Particle Spectroscopy (MPS) uses the nonlinear magnetic response of superparamagnetic iron oxide nanoparticles (SPION) to characterize their dynamic magnetic behavior. Originally, MPS was designed for batch mode measurements of small sample volumes to assess the performance of SPION as a tracer for the novel imaging modality Magnetic Particle Imaging. Here, each sample is inserted into the pickup coil of the MPS device and the dynamic response of the magnetization of the SPION exposed to an exciting oscillatory field is recorded. So far, MPS was not applicable for continuous measurements to detect SPIONs in a flow which is highly desirable, e.g. for quality control measurements during continuous SPION production in an industrial installation. Recently, we developed a dedicated flow cell capable for MPS measurements of the dynamic magnetization response while circulating a SPION suspension driven by a peristaltic pump through a closed tube system. In this study we examined the influence of flow velocity on MPS measurements.

Method

For the experiments, we used three particular SPION systems with different hydrodynamic diameters d_{hyd}: Feraheme®/Ferumoxitol (FE) with d_{hyd} = 25 nm, Resovist®/Ferucarbotran (DD) with d_{hyd} = 60 nm and FluidMAG-D with three different hydrodynamic sizes, (FM-50) with d_{hyd} =50 nm, (FM-100) with d_{hyd} = 100 nm, and (FM-300) with d_{hyd} = 300 nm. For all measurements we employed a total suspension volume of 1.5 mL at an iron concentration of c(Fe) = 2.5 mmol/L. The SPION dispersion is filled into a closed tube circuit driven by a peristaltic pump (ISMATEC® IPC-N4, Cole-Parmer GmbH) at selected flow velocities ranging from Q = 0 mL/min up to Q = 2.5 mL/min. The tube system is connected to a flow cell placed into the MPS pickup coil. MPS measurements at a fixed frequency of f_0 = 25 kHz were acquired at different drive field amplitudes ranging from B_p = 5 mT up to 25 mT. To ensure thermal equilibrium we circulated the dispersion ten minutes before starting the MPS measurements.

Results

We observed different flow velocity characteristics for each SPION system as indicated by the ratio between the third harmonic A_3 measured at flow Q and $A_{3,0}$ measured at $\dot{V}$ = 0 (Fig 1 top). Resovist® did not show a significant change of the MPS signal with increasing flow velocity. The other two systems exhibit moderate changes at flow velocities above 0.500 mL/min. While for Feraheme® the MPS amplitude increases with increasing flow velocity, we observe an amplitude decrease for SPION with large hydrodynamic diameter, FluidMAG-D/300, for flow velocities above 0.125 mL/min there is a correlation between MPS amplitude of a particular particle system and flow velocity influenced by hydrodynamic diameter of the SPION system. For smaller (hydrdynamic) particle sizes the dynamic magnetic response increases with flow velocity.

Furthermore this behavior is dependent on the MPS drive field amplitude B_p as shown in Fig. 1 (bottom) for FM-300.

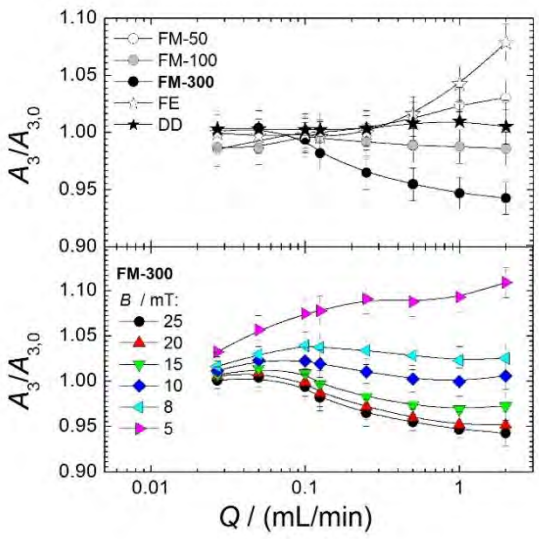

Figure 1. Top ratio between the third harmonic A_3 of the MPS signal measured at flow velocity Q and (harmonic $A_{3,\#}$) at Q = 0 at excitation amplitude B_p = 25 mT. Bottom ratio for FM-300 at different B_p. The uncertainty of 1.5 % was determined from repeating experiments four times. The connecting lines are just guiding the eyes.

We observe at small B_p an increasing flow velocity, which seems to be gradually suppressed at intermediate fields B_p>8 mT and leads to a decrease of amplitude at highest fields B_p>20 mT finally.

Discussion

Flow velocity impacts depending on the hydrodynamic diameter the dynamic magnetization of a SPION system. The increase observed in small particle systems (Feraheme®) may be caused by the effect of stringing these particles together. Since the area of a flowing sphere the velocity of the fluid drops nearly to zero, the formation of chains is energetically favorable [1]. The magnetic interaction effects caused by this chain formation could rise the MPS amplitude.

The MPS amplitude decline observed for SPION with larger diameter (FM-300) with increasing flow velocity could be caused by shear forces which impede the Brownian relaxation process of the SPION, so that the particle moments can less easy follow the excitation field B_p thus reducing the dynamic MPS response.

The unexpected amplitude gain at lower excitation amplitudes B_p needs further investigation. MPS is a versatile technique to analyse the influence of flow velocity on the dynamic magnetic behavior of SPION. Incorporating the understanding of the influence of flow velocity on the dynamic magnetic response of SPION prospects an imaging of perfusion properties by MPI.

References

[1] N. Löwa *Entwicklung neuer Kopplungsverfahren zur Charakterisierung von magnetischen Nanopartikeln besierend auf der Messung der nichtlinearen magnetischen Wechselfeld-Suszeptibilität*, Carl Schünemann Verlag GmbH, p.90, 2017

Multi-spectral Magnetic Particle Spectroscopy for the investigation of particle mixtures and environment

T. Viereck[1], S. Draack[1], M. Schilling[1], F. Ludwig[1]

[1] *Institut für Elektrische Messtechnik und Grundlagen der Elektrotechnik, TU Braunschweig, Germany*

Magnetic Particle Spectroscopy (MPS) records the non-linear response of magnetic nanoparticles (MNP) to large ac magnetic fields. It obtains a harmonic spectrum for the characterization of MNP samples, especially in the context of Magnetic Particle Imaging (MPI). MPS is sensitive to smallest variations in magnetization response, thus different particle types or batches are easily discriminated. Also, since the dynamic magnetization of the particles is driven by both the Néel and the Brownian relaxation mechanisms, the harmonic spectra in MPS scale with ambient factors, such as temperature, viscosity or binding state of the particles. Previous studies mostly observed the dependence of low-frequency harmonic ratios (e.g. 5f0/3f0) to obtain information on temperature or viscosity [1]. Here, we propose a multi-spectral analysis technique, using the full available spectrum, to decompose the collective response of different particles or particles in different states (i.e. temperature, viscosity/binding state, etc.) from an integral measurement on an MNP sample. Potential applications of the new method include the in-vitro analysis of particles in a cell culture, where cell-ingested particles can be distinguished from those still in the culture medium (e.g. cell update study), or the discrimination of different particle types or particle parameters. The proposed method borrows from multi-color MPI [2, 3], where we can spatially resolve different spectral responses to constitute a functional imaging modality. Multi-spectral MPS helps to methodically investigate dependencies of the spectral response on the various particle parameters [4] in a much simpler setting compared to MPI, while still being translatable, and it allows us to study the quantitativeness of proposed method about various factors. In this contribution, we apply the multi-spectral method to analyze binary and ternary mixtures of different particles (e.g. FeraSpin™ XL, perimag®, etc.) and viscosity series of FeraSpin XL regarding parameter estimation, separation quality and quantitativeness. A comparison of multi-spectral MPS to multi-color MPI, both from in-house custom-built measurement and imaging devices, is provided as well.

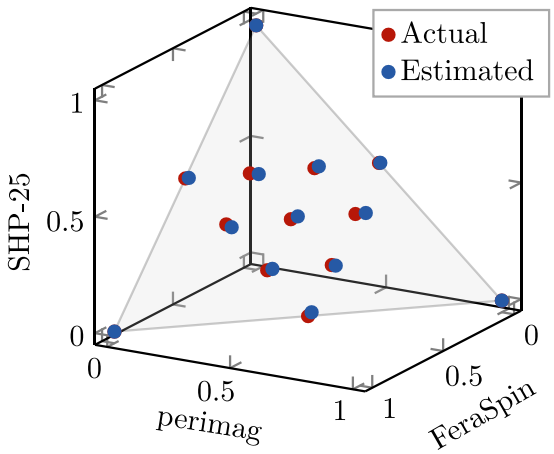

Acknowledgments

Financial support by the German Research Foundation via Priority Program SPP1681 (VI892/1-1) is acknowledged.

References

[1] J. B. Weaver and E. Kuehlert. Med. Phys. 39(5), 2012.
[2] J. Rahmer, A. Halkola, et al.: Phys. Med. Biol. 60(5), 2015.
[3] T. Viereck, C. Kuhlmann, et al: JMMM 427, 156-161, 2017.
[4] S. Draack, T. Viereck, et al.: IJMPI 3(1), 2365-9033, 2017.

Long-term stable solid-state phantoms for multimodal magnetic particle imaging

L. Wöckel[1], J. Wells[2], O. Kosch[2], K.-H. Herrmann[3], S. Günther[4], J.R. Reichenbach[3], S. Lyer[5], C. Alexiou[5], C. Grüttner[6], F. Wiekhorst[2], S. Dutz[1]

[1] *Institut für Biomedizinische Technik und Informatik, Technische Universität Ilmenau, Germany*
[2] *Physikalisch-Technische Bundesanstalt, Berlin, Germany*
[3] *Medical Physics Group, Institut für Diagnostische und Interventionelle Radiologie, Universitätsklinikum Jena, Germany*
[4] *Institute of Fluid Mechanics, Technische Universität Dresden, Germany*
[5] *Department of Otorhinolaryngology, Head and Neck Surgery, Section for Experimental Oncology & Nanomedicine (SEON), University Hospital Erlangen, Germany*
[6] *micromod Partikeltechnologie GmbH, Rostock, Germany*

Introduction

Magnetic Particle Imaging (MPI) is a rapidly developing imaging technique with high potential for clinical applications. This technique detects the response of superparamagnetic nanoparticles (MNP) to an oscillating external magnetic field [1]. With the exception of two commercially available MPI systems (Bruker & magnetic INSIGHT), the MPI systems currently running are prototypes [2]. Due to technical differences between the scanners, they only can be compared with each other regarding their imaging properties by using defined reference objects for imaging studies. Currently, most phantoms for MPI are based on stock or diluted nanoparticle dispersions, which are filled in thin tubes [3]. Liquid phantoms have the disadvantage that they are not long-term stable, which limits their suitability for comparative studies between existing MPI scanners. To address these problems, we focused on development of materials suitable for the preparation of long-term stable solid state phantoms for comparative MPI studies.

Material and Methods

For our studies we used two different magnetic nanoparticle fluids, namely Perimag® (micromod Partikeltechnologie, Rostock) and SEON$^{LA\text{-}BSA}$ (SEON group, Erlangen). For the phantom matrix, a synthetic polymer (ELASTOSIL® RT 604 A/B, Wacker Chemie AG) was used. The influence of embedding the aqueous MNP in a polymer matrix on the MPI performance of the particles was tested by means of Magnetic Particle Spectroscopy (MPS). For the measurements we used a commercial MPS spectrometer (MPS-3, Bruker) operating at 25 kHz drive frequency and a 25 mT excitation field amplitude. We analyzed changes in the amplitudes of the first odd harmonics of the MPS spectrum between the stock MNP fluids and after immobilization of the MNP. The most promising MNP polymer mixture was used for preparing the phantoms for further studies. To this end, we used 3-D printed molds with a structure cross section of 2 x 2 mm^2 which were filled with MNP loaded Elastosil. The resulting phantoms were imaged by means of MPI (MPI 25/20 FF, Bruker, Ettlingen, Germany), MRI (9.4 T small animal scanner – BioSpec 94/20 USR, Bruker, Ettlingen, Germany), and µCT (TomoTU, TU Dresden, Germany).

Results

For phantom preparation, the transfer of the MNP from aqueous suspensions into the synthetic matrix had to be addressed, since aqueous fluids are not soluble in the organic polymer. Therefore, a route of solvent trans-

fer by using ethanol was developed. MPS measurements revealed decreasing higher harmonics after embedding the MNP into the polymer. Repeating the MPS measurements for up to one year after preparation did not reveal major changes of the magnetic properties for both particle types immobilized in the synthetic polymer, thus demonstrating their long-term stable behavior, see figure 1.

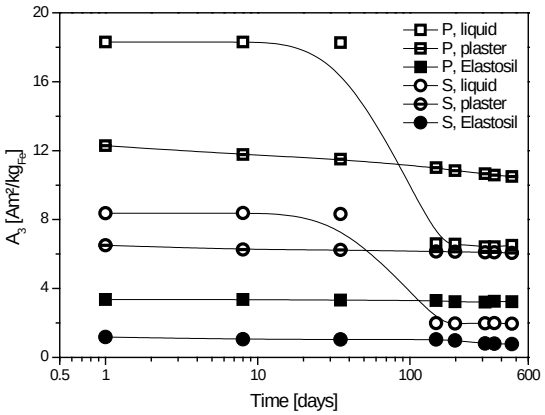

Figure 1: A3 amplitude of Perimag (P) and Seon (S) for liquid and embedded particles as function of storage time for up to 500 days, normalized to the iron amount; lines serve only as a guide to the eye.

Comparing all investigations, the combination Perimag®/ELASTOSIL® was the most promising one regarding long-term stability and signal performance and was used for the preparation of the phantoms. The prepared phantoms were subsequently imaged successfully with MPI, MRI and µCT, see figure 2.

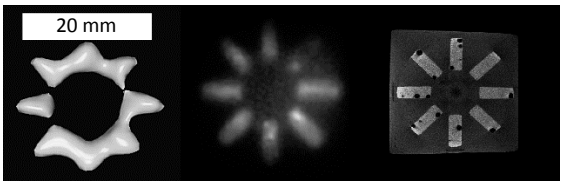

Figure 2: Multimodal imaging of the phantoms (left: MPI, center: MRI, right: µCT).

Conclusions

We present suitable combinations of commercial MNP and a polymer for manufacturing long-term stable MPI phantoms. The presented phantoms show constant magnetic and mechanical properties for more than one year so far and can be used for imaging with MPI, as well as with MRI and µCT for co-registration of the morphological structures. Further work will focus on phantoms having more detailed particle loaded structures, and water based polymers as matrix materials with improved homogeneous particle distributions, to obtain less decreases of higher harmonics after embedding the particles into the matrix.

Acknowledgments

This work was supported by Deutsche Forschungsgemeinschaft (DFG) (FKZ: AL552/8-1, DU 1293/6-1, and TR 408/9-1).

References

[1] Paysen, H., Wells, J., Kosch, O., Steinhoff, U., Trahms, L., Schaeffter, T., & Wiekhorst, F. (2018). Towards quantitative magnetic particle imaging: A comparison with magnetic particle spectroscopy. AIP Advances, 8(5), 056712.

[2] Panagiotopoulos, N., Duschka, R. L., Ahlborg, M., Bringout, G., Debbeler, C., Graeser, M., & Haegele, J. (2015). Magnetic particle imaging: current developments and future directions. Int J Nanomedicine, 10, 3097-311

[3] Ferguson, R. M., Khandhar, A.P., Kemp, S. J., Arami H., Sarias, E. U., Croft, L. R., Konkle, J., Goodwill, P. W., Halkola, A., Rahmer, J., Borgert, J., Conolly, S. M., & Krishnan, K. M. (2015). Magnetic particle imaging with tailored iron oxide nanoparticle tracers. IEEE Trans Med Imaging, 34(5), 1077-1084.

Magnetically tunable elastic properties and different types of mesoscopic dynamic behavior of magnetic gels and elastomers

G. Pessot[1], S. Goh[1], M. Puljiz[1], H. Löwen[1], A. M. Menzel[1]

[1] *Institut für Theoretische Physik II: Weiche Materie, Heinrich-Heine-Universität Düsseldorf, 40225 Düsseldorf, Germany*

Soft elastic rubber-like materials containing magnetic or magnetizable colloidal particles, possibly swollen by a solvent, are called magnetic gels, ferrogels, magnetorheological elastomers, or similar [1].
One of the most interesting properties of these substances is that their overall mechanical properties can be tuned reversibly, from outside, and during operation by applying an external magnetic field [1]. Induced mechanical stiffening by factors of 6 to 7 has recently been achieved experimentally in this way [2]. It has been shown that this large effect is to a big extent due to internal restructuring of the spatial arrangement of the magnetic inclusions [2,3]. Specifically, under sufficiently strong external magnetic fields, the magnetic particles form chain-like aggregates against the restoring forces of the surrounding elastic polymeric matrix [2,3]. Refining our previously established theoretical formalism [4], we can now characterize these features semi-quantitatively, using realistic particle distributions that were obtained from experimental input data [5].
Another subject that has rarely been studied so far on the mesoscopic scale, that is, on the length scale of the individual magnetic particles, are dynamic properties of this type of magnetic composite materials. We address this issue for a finite piece of a one-dimensional dipole-spring model system [6]. Various interesting different types of dynamic behavior are identified upon switching on or off the magnetization of the magnetic particles.

Magnetically tunable dynamical mechanical moduli

In this part, we address how applying an external magnetic field by magnetization of the embedded particles in magnetic elastomers can affect the dynamical mechanical properties in realistic spatial particle configurations. For this purpose, explicit particle arrangements extracted via x-ray micro-computed tomography from real experimental samples of different particle contents [2,3] were used as an input to our calculations. Both, particle positions and their varying volumes were considered, the latter affecting the magnitude of the resulting magnetic moments.
The situation was mapped to a refined version of our previously developed dipole-spring model [4,5], allowing for irregular particle arrangements. A mesh of elastic springs realizes the elasticity of the system, while dipoles include the magnetic interactions. To be able to address the irregular particle arrangements drawn from the experiments, additional interstitial network points need to be introduced. In this way, the changes in the mechanical storage and loss moduli at different frequencies of applied mechanical stress when switching on the magnetic interactions were analyzed.
Interestingly, with increasing magnetic interactions, we observe a non-monotonous behavior of the static Young and shear moduli [5]. While first a small decrease is found for both quantities, a pronounced increase follows afterwards, implying strong me-

chanical stiffening. Our observations indicate that the initial decrease is due to initial smaller internal rearrangements, while the subsequent mechanical stiffening coincides with the formation of chain-like aggregates in the system [2,5].

Mesoscopic dynamical behavior

To analyze on the mesoscopic particle scale the dynamic behavior, we use in this first study a finite piece of a one-dimensional dipole-spring model system [6]. The spatial dynamics of the magnetizable particles is assumed as completely overdamped so that frictional effects dominate. We consider the dynamical behavior upon switching on or off the magnetization.

When switching on magnetic attraction between the particles, the system tends to contract. Depending on the magnitude of the magnetic moments and the initial distance between the particles, qualitatively different types of dynamical behavior are identified [6].

For instance, directly after magnetization, particle pairs can form throughout the system, while the separated pairs can then further contract to larger clusters growing towards the inside from the boundaries. The latter scenario can also be observed without the initial pair formation. Remarkably, and for us also quite unexpectedly, we observed signatures of shock-wave dynamics for magnetic particle clusters growing towards the inside from the boundaries, despite the overdamped nature of the dynamics. Analogous types of behavior were obtained for expansion of the system when turning off the magnetization. We addressed the situation both by particle-scale simulations and by developing an analytical theory [6].

Outlook

Naturally, in the future, we aim at a further refinement of our characterizations. Our investigations on the tunable dynamical mechanical properties shall be extended by including non-spherical shapes of the embedded particles as well as additional rotational couplings between them. Also, more refined models of particles embedded in elastic matrices [7–9] instead of the cruder dipole-spring approaches used so far [4,5,10] shall be employed.

Concerning our dynamical investigations on the mesoscale, the most pertinent task is to extend the description to structures of more than one spatial dimension [11]. A different task is to combine the dynamical framework with statistical approaches, possibly by extending a recent density-functional theory [12] to a corresponding dynamical variant.

Acknowledgments

We thank the DFG for support of our work through the SPP 1681.

References

[1] A. M. Menzel, Phys. Rep. **554**, 1 (2015).
[2] M. Schümann and S. Odenbach, J. Magn. Magn. Mater. **441**, 88 (2017).
[3] T. Gundermann, P. Cremer, H. Löwen, A. M. Menzel, and S. Odenbach, Smart Mater. Struct. **26**, 045012 (2017).
[4] G. Pessot, H. Löwen, and A. M. Menzel, J. Chem. Phys. **145**, 104904 (2016).
[5] G. Pessot, M. Schümann, T. Gundermann, S. Odenbach, H. Löwen, and A. M. Menzel, J. Phys.: Condens. Matter **30**, 125101 (2018).
[6] S. Goh, A. M. Menzel, and H. Löwen, arXiv preprint, arXiv:1803.01225 (2018).
[7] M. Puljiz, S. Huang, G. K. Auernhammer, and A. M. Menzel, Phys. Rev. Lett. **117**, 238003 (2016).
[8] M. Puljiz and A. M. Menzel, Phys. Rev. E **95**, 053002 (2017).
[9] A. M. Menzel, Soft Matter **13**, 3373 (2017).
[10] G. Pessot, P. Cremer, D. Y. Borin, S. Odenbach, H. Löwen, and A. M. Menzel, J. Chem. Phys. **141**, 124904 (2014).
[11] M. Tarama, P. Cremer, D. Y. Borin, S. Odenbach, H. Löwen, and A. M. Menzel, Phys. Rev. E **90**, 042311 (2014).
[12] P. Cremer, M. Heinen, A. M. Menzel, and H. Löwen, J. Phys.: Condens. Matter **29**, 275102 (2017).

Modelling the cross-linking process of a magnetic gel

R. Weeber, C. Holm

Institute for Computational Physics, University of Stuttgart, Allmandring 3, 70569 Stuttgart

It is usually expected that the polymer network architecture of a magnetic gel can have quite a strong influence on the gel's elastic and magnetodeformational properties.
This assumption is supported by simulations that yield qualitatively different elastic behaviour when the network structure is changed. The nature of that relationship is, however, not yet known.
Experimentally it is often not possible to resolve local details of the polymer network. `However, in simulations and theoretical models the network structure is usually an input. Some often used possibilities are regular lattice-based structures, or random structures derived from the location of magnetic particles.
In our contribution, we follow a different route, namely we simulate the cross-linking process of a gel to obtain less artificial structures. We focus on gels in which the magnetic particles act as cross-linkers of the network, as for those, there is a clear picture of the particle-polymer coupling. Our simulations start from an equilibrated suspension of polymers and magnetic nanoparticles. Then, whenever an end of a polymer touches the surface of a magnetic particle, it is attached irreversibly at that point on the surface. That means we model a situation where the synthesis of the polymer is performed separately from the cross-linking of the gel, and in which the ends of the polymers bind covalently to the surface of the magnetic particles.
Based on this simulation protocol, parameters such as the density of magnetic particles and polymers, the ratio of polymers to magnetic particles, and the polymer polydispersity can be linked to the resulting network structures, which may be closer to experiments than the regular structures used previously.
In the long run, the magnetoelastic properties of the resulting gels can be explored. This may lead to a better understanding of the gels' macroscopic properties to parameters chosen during its synthesis.

Acknowledgments

The authors acknowledge funding by the German Science Foundation through SPP 1681 and the Cluster of Excellence EXC 310 SimTech.

References

[1] R. Weeber, M. Hermes, A. M. Schmidt, and C. Holm, Polymer architecture of magnetic gels: a review, *J. Phys.: Cond. Mat.* 30(6) (063002), 2018.

[2] R. Weeber, S. Kantorovich, and C. Holm, Ferrogels cross-linked by magnetic particles: Field-driven deformation and elasticity studied using computer simulations, *J. Chem. Phys.* 143, 2015.

Macroscopic modeling and finite element simulation of fluid-saturated porous ferrogels

P. Gebhart, T. Wallmersperger

Institute of Solid Mechanics, Technische Universität Dresden, 01062 Dresden, Germany

Introduction

In recent times smart materials have received significant attention due to their possibly wide range of applications as sensors and actuators in engineering, medicine and other innovative fields of research. Porous ferrogels are a subclass of these materials, which have the ability to exhibit large deformations and alter their effective material behavior reversibly if subjected to a magnetic field. Within this contribution a framework for the macrosopic modeling of fluid-saturated porous ferrogels at finite strains and its numerical implementation is presented.

Modeling Approach

Porous ferrogels are field-responsive composite materials consisting of a porous polymeric matrix material with embedded micro- or nanosized ferromagnetic particles. The interconnected pore space within the polymeric matrix is filled with a fluid.
The behavior of these materials is a complex phenomenon that spans over multiple length scales. Departing from relevant laws of continuum mechanics of porous media a thermodynamically consistent theory for the modeling of ferrogels at the macroscopic level is derived [1]. Within this modeling approach the ferrogel is treated as the superimposition of a magneto-active solid skeleton and fluid that can move with distinct kinematics. This leads to a continuous description of the porous ferrogel, where the complex microstructure is not resolved explicitly. A prototypical constitutive model for isotropic ferrogels is formulated within an enthalpy-based constitutive setting. The governing equations of the coupled magneto-poro-mechanical problem are solved monolithically by a nonlinear finite element algorithm. Therein, for the discretization in space the skeleton displacement, the magnetic scalar potential and fluid pore pressure are used as primary field variables while an Euler time-integration scheme is applied for the discretization in time. Furthermore a mesh-morphing algorithm is employed to preserve an adequate mesh quality in the space surrounding the material body.

Numerical Simulation

A cylindrical ferrogel specimen with a diameter of 12mm and length of 20mm in X_2-direction surrounded by a truncated free space under magnetic loading is considered. This example is motivated by the experiments conducted in [2, 3].

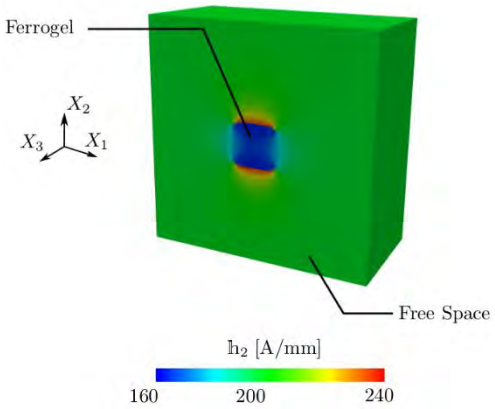

Figure 1: Spatial distribution of the magnetic field strength in X_2-direction within the domain in the X_1-X_2 symmetry plane.

The geometry is spatially discretized by tetrahedral H^1-conforming Lagrange elements. The computed contour plot for the spatial magnetic field strength within the whole domain at maximal loading is shown in Figure 1.

The highest magnetic field strength is located at the top and bottom interface between ferrogel and surrounding due to the continuity requirements of the normal component of the magnetic induction. Furthermore a mean compressive strain of roughly 40% in X_2-direction is reached at maximal loading. The corresponding displacement in X_2-direction is depicted in figure 2.

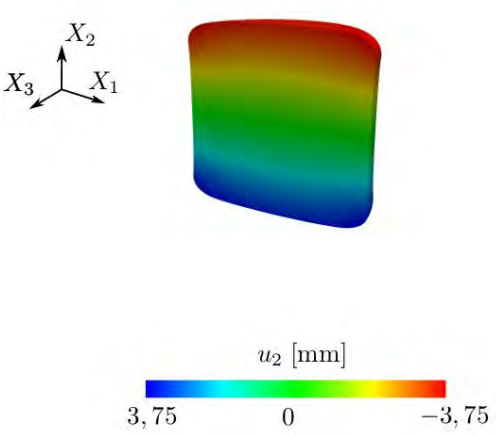

Figure 2: Spatial distribution of the displacement component u_2 within the gel in the X_1-X_2 symmetry plane.

These numerical results are in good agreement with experimental results presented in [2, 3].

Conclusion

In this contribution, a magneto-poro-mechanically coupled constitutive framework for ferrogels that obeys the relevant laws of thermodynamics along with an efficient and stable finite element implementation was presented. The modeling capabilities were demonstrated by a representative numerical example. The presented computational results are qualitatively in good agreement with results available in literature.

Acknowledgments

This research has been financially supported by the Deutsche Forschungsgemeinschaft in the framework of the Priority Programme SPP1681.

References

[1] P. Gebhart, T. Wallmersperger, A general framework for the modeling of porous ferrogels at finite strains, Journal of the Mechanics and Physics of Solids, submitted, 2018.

[2] S. Hong, Y. Jung, R. Yen, H. F. Chan, K. W. Leong, G. A. Truskey, X. Zhao, Magnetoactive sponges for dynamic control of microfluidic flow patterns in microphysiological systems, Lab Chip 14 (2014) 514–521.

[3] X. Zhao, J. Kim, C. A. Cezar, N. Huebsch, K. Lee, K. Bouhadir, D. J. Mooney, Active scaffolds for on-demand drug and cell delivery, Proceedings of the National Academy of-Sciences, vol. 108, no. 1, pp. 67-72, 2011.

Microscopic Modeling and Finite-Element-Simulation of Magnetorheological Elastomers

K. A. Kalina[1], P. Metsch[1], J. Brummund[1], M. Kästner[1,2]

[1] *Chair of Computational and Experimental Solid Mechanics, TU Dresden, 01062 Dresden, Germany*
[2] *Dresden Center for Computational Materials Science (DCMS), TU Dresden, 01062 Dresden, Germany*

Introduction

Magnetorheological elastomers (MREs) are a class of active composites which consist of a polymer matrix filled with micron-sized magnetizable particles. Thus, the effective properties of these materials essentially depend on the constitutive behavior of the individual components as well as their arrangement in the MRE microstructure.
In order to investigate the behavior of MREs, a continuum based computational modeling approach is applied in this contribution.

Microscopic Modeling Approach

The analyzed MREs are described by a microscopic model, where the constitutive models for the particles and the matrix are formulated separately.
In order to connect the macroscopic and the microscopic magnetic and mechanical quantities, a suitable computational homogenization scheme [1-3] is used. The governing equations of the coupled magneto-mechanical boundary value problem are solved within a nonlinear finite element (FE) formulation as presented in [4].
The merit of this modeling strategy is a full resolution of the local fields within the heterogeneous MRE microstructure – it allows to account for systems with high particle-volume fractions and small inter-particle distances.

Comparison of 2D and 3D Simulations

In order to understand basic deformation mechanisms, the differences between simplified 2D and realistic 3D simulations are initially shown for the example of chain-like structures with varying arrangements of the particles. Afterwards different ideal and random microstructures are compared with regard to their effective magneto-mechanical behavior.
The simulation results show that, qualitatively, 2D and 3D approaches are in very good agreement. However, due to differences in the particle-shape and the resulting local magnetic and mechanical fields, considerable discrepancies are revealed in a quantitative comparison, see Figure 1.

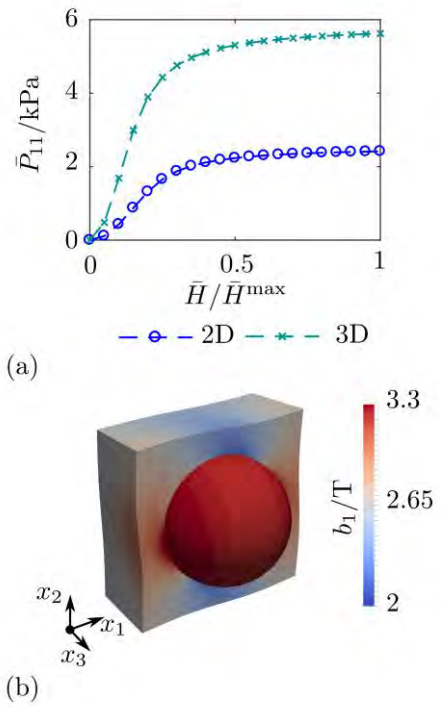

Figure 1: *Cubic RVEs with same particle volume fraction: (a) effective actuation stresses and (b) local induction field for shear loading.*

Fitting macroscopic Models

To allow for the simulation of real MRE structures or samples, macroscopic models provide a computationally efficient possibility. Within these models, the composite is considered to be a homogeneous continuum in which effects of the underlying microstructure are captured via magneto-mechanical coupling terms.

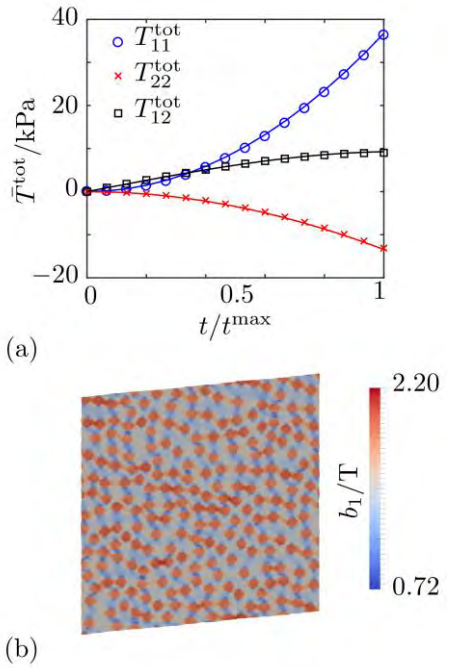

Figure 2: *Parameter identification for shear loading with magnetic field: (a) FE simulation (markers) and macroscopic model (lines) and (b) local induction field.*

A crucial task is to identify the parameters of such a model, which can be done by using the simulation results of a computational homogenization. The parameter identification for an isotropic magnetically linear model is depicted in Figure 2.

Acknowledgments

The present study is funded by the German Research Foundation (DFG), Priority Program 1681, grant KA 3309/2-3.

References

[1] P. Metsch, K. A. Kalina, C. Spieler and M. Kästner, Comput. Mat. Sci., 124, 2016.

[2] K. A. Kalina, J. Brummund, P. Metsch, M. Kästner, D. Yu. Borin, J. M. Linke and S. Odenbach, Smart Mater. Struct., 26, 2017.

[3] K. A. Kalina, J. Brummund, P. Metsch and M. Kästner, Proc. In applied mathematics and mechanics, 17, 2017.

[4] K. A. Kalina, P. Metsch and M. Kästner, Int. J. Solids Struct., 102-103, 2016.

Investigation on the local dynamics in supramolecular polymer structures using Magnetic Particle Nanorheology

M. Hermes[1], E. Roeben[1], A. Habicht[2], S. Seiffert[2], A. M. Schmidt[1]

[1] *Institute of Physical Chemistry, Universität zu Köln, Luxemburger Str. 116, D-50939 Köln, Germany, email:* annette.schmidt@uni-koeln.de
[2] *Institute of Physical Chemistry, Johannes Gutenberg-Universität Mainz, Duesbergweg 10 - 14, D-55128 Mainz, Germany*

Supramolecular polymers consist of (macro-) molecules that exhibit intermolecular non-covalent (dynamic) bonds, typically based on hydrogen bonds, hydrophobic association, π–π–stacking, complex formation, or ionic interactions. If these interactions interlink different chains, macroscopic transient network structures are obtained. In these systems, the self-assembly and the usually rich reversible dynamics of the supramolecular motifs opens access to new functional materials, potentially exhibiting stimuli-responsiveness and adaptability, thereby making them suitable candidates for self-healing materials.

Method

To get an enlightening insight into the structure and dynamics of supramolecular polymer networks, approaches via nanorheology are promising. Here, tracer particles with size of a few nanometers are used to extract local dynamic rheological information on the matrix by analyzing their translational or rotational motion. In our previous works, it was shown that active *Magnetic Particle Nanorheology* (MPN) is successful to extract local dynamic properties of complex matrixes such as the frequency-dependent loss and storage moduli, the viscosity, or characteristic relaxation times.[1,2] In short, by this method, magnetically blocked nanoparticles are excited by an AC magnetic field, and the complex magnetic susceptibility data is evaluated to result in the desired dynamic information of the investigated matrix.

Concept

In this contribution, we report on the application of this method to transient networks of star-shaped polymers with metal-coordinated arm-end groups, with a view to investigate the binding strength and network topology systematically as a function of transition metal ions.

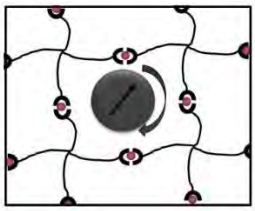

Figure 1. Schematic drawing of the investigated supramolecular polymer system with incorporated probe particle.

For this purpose, star-shaped PEG precursors are end-group functionalized with terpyridine moieties that are then complexed to different metal ions such as Mn^{2+}, Zn^{2+} and Co^{2+} (Figure 1).[3] The strength and connectivity of the polymer networks are characterized by evaluation of bond lifetime, complex formation constant, mesh size, as well as the viscoelastic properties.

Acknowledgments

Financial support is acknowledged from DFG-SPP 1681 (SCHM1747/10). Melissa Hermes acknowledges support by the International Helmholtz Research School of Biophysics and Soft Matter (IHRS BioSoft).

References

[1] E. Roeben, L. Roeder, S. Teusch, M. Effertz, U. Deiters, A. Schmidt, *Colloid Polym. Sci. Sci.* **2014**, *292*, 2013–2023.
[2] M. Hermes, E. Roeben, L. Kibkalo, A. M. Schmidt, *Annu. Trans. Nord. Rheol. Soc.* **2017**, *25*, 97–105.
[3] T. Rossow, S. Seiffert, *Polymer Chem.* **2014**, *5*, 3018–3029.

Probing anisotropic nanoparticle diffusion in soft matter composites exposed to magnetic fields

J. Landers[1], S. Salamon[1], H. Nádasi[2], R. Stannarius[2], A. Eremin[2], Satoshi Aya[3], Fumito Araoka[3], H. Wende[1]

[1] *Faculty of Physics and Center for Nanointegration Duisburg-Essen (CENIDE), University of Duisburg-Essen*
[2] *Department of Nonlinear Phenomena, Institute of Physics, Otto von Guericke University Magdeburg*
[3] *RIKEN Center for Emergent Matter Science, Saitama, Japan*

Motivation

While in ferrofluids the particle response to external magnetic fields – probably its most essential characteristic – can be described by an average particle mobility, in case of anisotropic nanostructures [1], particle chains or non-spherical particles, direction-resolved diffusion coefficients may be required to describe the system correctly. The ability to gain access to diffusion along different directions (in respect to a specific axis of either particle or matrix) shall therefore be demonstrated here for two different scenarios.

Study of chain formation

Ferrofluid samples were prepared by diluting commercial ferrofluid APG1235 with n-dodecane, yielding concentrations of 7 - 13.5 wt% of magnetic material. Mössbauer spectra of these fluids were recorded at 235 – 259 K in magnetic fields of 750 mT parallel- and perpendicular to the γ-ray direction, to study particle mobility and orientation via changes in spectral structure [2-3] and how they are influenced by particle chain formation (see Fig. 1).

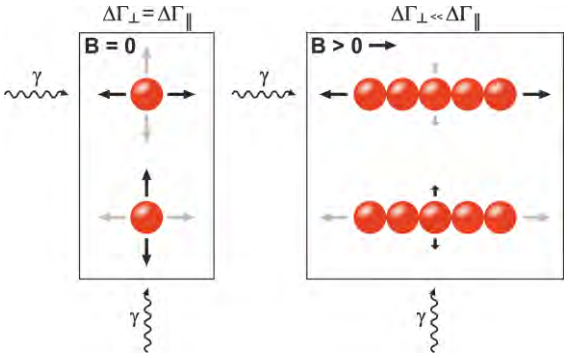

Fig. 1: Schematic illustration which particle motion Mössbauer spectroscopy is sensitive for.

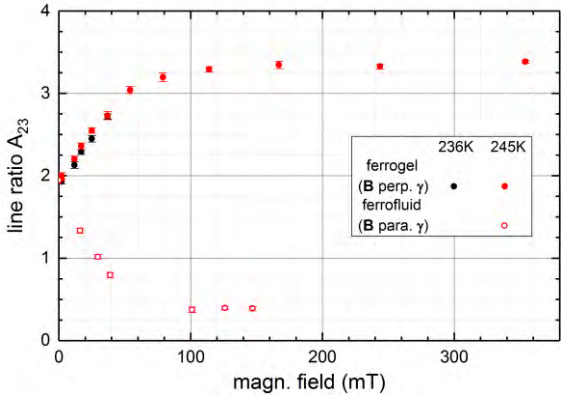

Fig. 2: Line ratio A_{23} vs. external magn. field, indicating the onset of chain formation at ca. 100 mT.

We observed minor deviations from standard Langevin-type alignment behavior, showing saturation in orientation at ca. 100 mT (Fig. 2). Additional information has been inferred from Mössbauer absorption line broadening ΔΓ, being approximately proportional to the diffusion coefficient *along the γ-ray propagation direction*. A clear drop in ΔΓ is observable at higher magnetic fields, indicating chain formation. By comparing ΔΓ measured parallel and perpendicular to the field direction (i.e. chain orientation), different trends for the particle motion along the short and long chain axis were obtained, representing the increase in average chain length and also pointing out the ability of Mössbauer spectroscopy to extract direction-resolved particle mobilities. Preferred particle alignment along field direction by chain formation at about 100 mT could also explain the 'kink' observed in field-dependent magnetic orientation. Spectra recorded before and after maximum field exposure showing the same structure indicate reversible chain formation (Fig. 3).

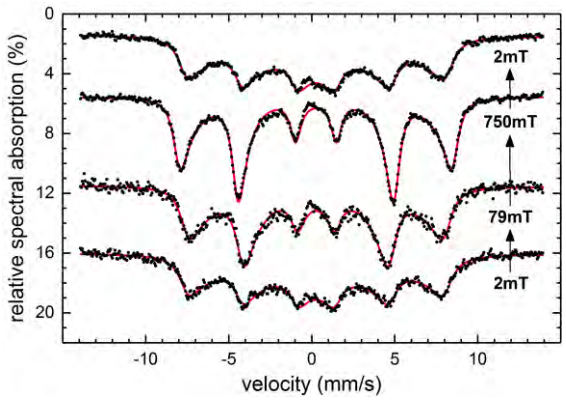

Fig. 3: Mössbauer spectra of a ferrogel at 245K in magnetic fields up to 750mT recorded in perpendicular geometry.

Particle mobility in anisotropic gels

Based on these promising results, we made a first attempt to determine different degrees of particle mobility in anisotropic gel structures. 10 wt% of 12-HOA gelator were added to the original ferrofluid described above. These gels exhibit a fibrilous nanostructure and a magnetically induced birefringence. The typical diameter of the helical nanofibers is about 20 – 30 nm (Fig. 4).

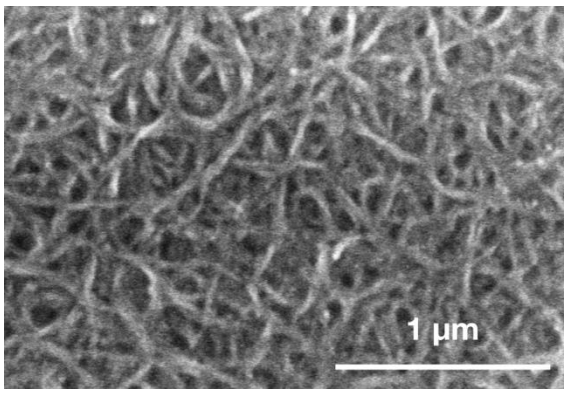

Fig. 4 Scanning electron microscopy images of an isotropic gel with 7 wt% of the MNPs and 10 wt% of the gelator.

Anisotropic ferrogels were prepared by heating these samples above the sol-gel temperature of ca. 345 K, the application of a magnetic field of ca. 750 mT and subsequent cooling to room temperature. While the trend in particle mobility is already noteworthy, reflecting the gel's temperature-dependent viscosity, the difference of ca. 50 % in $\Delta\Gamma$ comparing isotropic- and anisotropic gels is for sure more significant, the latter being measured perpendicular to the gel director (Fig. 5). This could indicate the ability to resolve particle motion along specific particle- (aligned in a field) or matrix directions via Mössbauer spectroscopy.

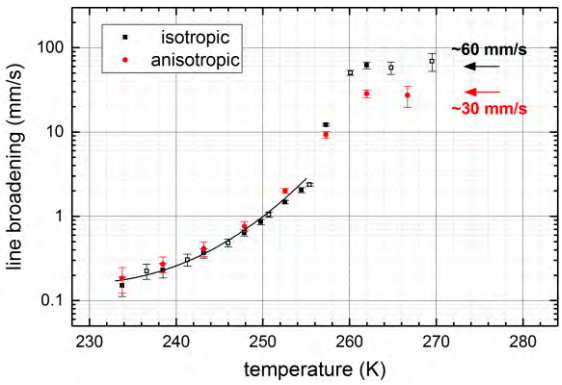

Fig. 5: Line broadening $\Delta\Gamma$ vs. external magnetic field, showing direction-resolved particle mobility in isotropic (black) and anisotropic gels (measured perpendicular to the gel director, red).

Conclusion

In essence, we demonstrated the ability to extract direction-resolved diffusion coefficients via Mössbauer spectroscopy, allowing the observation of chain formation in ferrofluids and also indicating the ability to study the effect of anisotropically nanostructured surroundings on particle mobility in ferrogels.

Acknowledgments

We gratefully acknowledge funding by the DFG through SPP1681 (grant WE-2623/7-3 and STA 425/36-3).

References

[1] H. Nádasi et al., *in preparation*
[2] J. Landers, S. Salamon, H. Remmer, F. Ludwig, H. Wende *Nano Lett.* **16** 1150 (2016)
[3] J. Landers, S. Salamon, H. Remmer, F. Ludwig, H. Wende *in preparation*

Scale dependence in Ni nanorod oscillatory rotation microrheometry of poly(ethylene oxide) solutions

M. Gratz, A. Tschöpe

Universität des Saarlandes, Experimentalphysik, Campus D2 2, 66123 Saarbrücken

Introduction

In microrheometry, the motion of colloidal particles is analyzed in order to retrieve the viscoelastic properties of the medium in which they are dispersed. When applied to complex soft matter, the size of the tracer particle is an important issue. Sufficiently large colloidal probes sense their environment as a homogeneous continuum with the macroscopic viscoelastic properties. Below a critical size, however, structural inhomogeneities are resolved and the particle motion reflects local properties, e.g. the bare solvent viscosity in polymer solutions as an extreme example.
The present study focused on the size scale effect in the rotational dynamics of Ni nanorods dispersed in poly(ethylene oxide) (PEO) solutions. The molecular weight and concentration of the macromolecules provide two control parameters which enable access to a wide spectrum of length and time scales. Variation of the probe size was achieved by using colloids of Ni nanorods with different rod length. The dynamic modulus, derived from optical transmission measurements of nanorod rotation in oscillating magnetic field was compared with results from macroscopic shear rheometry of the polymer solutions.

Methods

Four Ni nanorod colloids with different mean rod length were synthesized by the AAO-template method. The basic physical properties of the nanorods were obtained from transmission electron microscopy (TEM) and static field-dependent optical transmission [1]. Oscillating field optical transmission (OFOT) [2] measurements in Newtonian reference fluids were used for calibration (see below) and to estimate the mean hydrodynamic diameter $\langle D_h \rangle$ and length $\langle L_h \rangle$ of the nanorods.
Three PEO standards with different molar mass (50k, 220k, 1M [g/mol]) were purchased from PSS GmbH (Mainz), dissolved in distilled water at ≈pH 8 and gently mixed in a rotator for at least 48 h. Nanorod colloid was added to a total volume fraction $\phi_v \approx 10^{-6}$ and mixed for up to 24 h.
The rotational dynamics of the nanorods in the polymer solutions was characterized by OFOT measurements. The equation of motion for a magnetic dipole in a linear viscoelastic material exposed to an oscillating field at large Langevin parameter ($\xi > 30$) is directly related to the dynamic modulus $G^*(\omega)$ of the matrix. The frequency dependent complex OFOT response function $X^*(\omega) = \int P(K)\left(1 + KG^*(\omega)\right)^{-1} dK$ was solved numerically for G* at each frequency. The profile function $P(K)$, characterizing the distribution of hydrodynamic size and magnetic moment within each nanorod colloid, was obtained from the calibration measurements by numerical inversion.
Macroscopic reference measurements were performed using an Anton-Paar DAM4100 M rolling ball viscosimeter and an Anton Paar MCR702 dual drive rheometer (CP2° geometry, small amplitude oscillatory shear (SAOS) and steady shear viscosimetry).

Results

The zero-shear rate viscosities of the PEO solutions are shown in Figure 1 as function of the polymer concentration. Measurements of the intrinsic viscosities for each polymer size and the analysis of the power

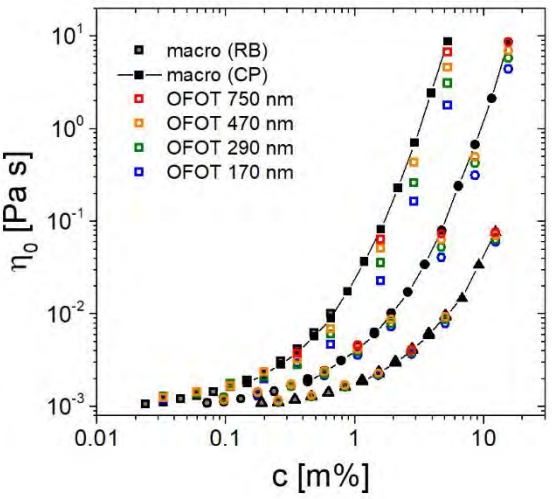

Figure 1: Zero shear rate viscosity of PEO-50k (▲), -220k (●) and -1M (■) solutions as function of concentration, obtained by rolling ball (RB) and cone-plate (CP) shear viscosimetry and from OFOT measurements using Ni nanorods of given hydrodynamic length

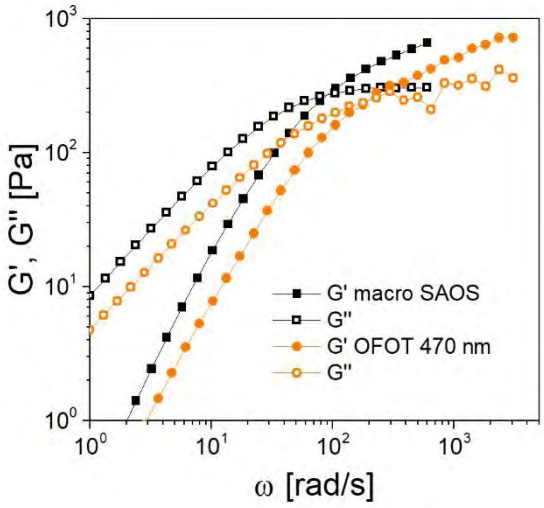

Figure 2: Angular frequency dependent dynamic modulus of a $5.29\ g/cm^3$ PEO-1M solution, measured by small amplitude oscillatory shear (SAOS) and results obtained from OFOT using Ni nanorods with $L_h = 470\ nm$.

law scaling revealed the viscosity of $\eta_0 \approx 0.03\ Pa \cdot s$ as the lower boundary of the semi-dilute entanglement regime. At selected concentrations, OFOT measurements were performed using Ni nanorods with similar hydrodynamic diameter $\langle D_h \rangle = 115 \pm 30\ nm$ but different length $\langle L_h \rangle$ in the range of 170 – 750 nm. The derived local viscosities were systematically reduced as compared to the macroscopic values. The reduction was larger for smaller rod length and large PEO molecule size. From the detailed analysis, the relevant length scales could be identified and simple empirical relationships derived.

In addition to the zero-shear rate viscosity, the dynamic behavior in the viscoelastic regime was investigated. In the SAOS dynamic modulus of a $5.29\ g/cm^3$ PEO-1M solution, the crossing of the storage modulus G' and loss modulus G'' at $\omega = 90\ rad/s$ characterizes the longest time constant of stress relaxation, Figure 2. The results obtained from the nanorod OFOT measurements were shifted to higher frequencies and lower modulus values, which is attributed to the localized deformation of the polymer network.

The Cox-Merz rule for the SAOS dynamic modulus and the steady share rate-dependent viscosity was validated for the PEO solution. This enabled the comparison of macroscopic shear thinning with the results obtained by Ni nanorod OFOT measurements.

Acknowledgments

We acknowledge access to the rheometry equipment by C. Wagner (Saarland University) and financial support by the DFG, priority program 1681 (TS62/4-3).

References

[1] F. Krämer, M. Gratz, and A. Tschöpe, *J. Appl. Phys.* **120** (2016) 044301.

[2] A. Tschöpe, K. Birster, B. Trapp, P. Bender, and R. Birringer, *J. Appl. Phys.* **116** (2014) 134305.

Weakening of magnetic response experimentally observed for ferrofluids with strongly interacting magnetic nanoparticles

A.O. Ivanov[1], S.S. Kantorovich[12], I.M. Arefyev[3], A.V. Lebedev[4], A.F. Pshenichnikov[4]

[1] *Ural Federal University, Lenin Av. 51, Ekaterinburg 620000, Russian Federation*
[2] *University of Vienna, Boltzmanngasse 5, 1090 Vienna, Austria*
[3] *Ivanovo State Power University, Rabfakovskaya Str. 34, 153003, Ivanovo, Russian Federation*
[4] *Institute of Continuous Media Mechanics, Korolev Str. 1, 614013 Perm, Russian Federation*

We present experimentally measured magnetic response of specially obtained four ferrofluid samples S1– S4, different in magnetic material concentration (grows from S1 to S4), but identical in granulometry and rich with large, strongly magnetically interacting particles. Both static (χ_s) and dynamic ($\chi_d = \chi' - i\,\chi''$) initial magnetic susceptibilities were measured in a broad range of temperatures (T).

In the static regime, on cooling, S1-S4 exhibit unusually low values of χ_s. It is the first time, to the best of our knowledge, that a clear maximum of the χ_s on cooling was experimentally obtained (Fig. 1).

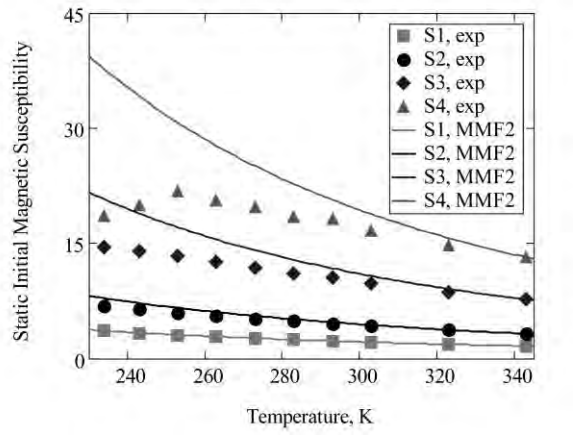

Fig. 1. Static magnetic susceptibility, symbols – experiment, curves – predictions of mean-field approach [1].

Nonmonotonic behaviour of χ_s with decreasing T indicates the presence of structural transformations leading, first, to an enhancement of the response due to the magnetic correlations, and then to the decay of this response caused by the closure of magnetic flux within the clusters [2]. The fraction of particles in such clusters was estimated to reach 50 percent for S4 at the lowest T.

In order to verify the stability of these clusters, a weak probing AC field was applied in a broad range of frequencies. Debye-like spectra were only obtained for the highest T.

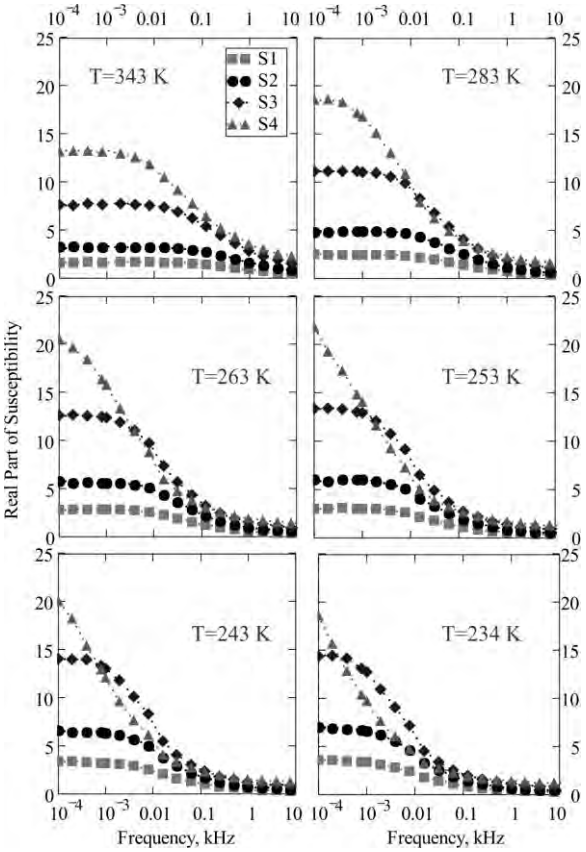

Fig. 2. Real part of the magnetic dynamic susceptibility vs AC field frequency, kHz, for samples S1–S4. From top to bottom, and from left to right, T decreases, the values are provided in each plot. The symbols are explained in the legend. Lines are guides for the eye.

The frequency dependences of χ' and their evolution on cooling are presented in Fig. 2. Here, one can also distinguish between various characteristic regimes. For the temperature range T ~ 280 K, as expected a Debye-like plateau of χ' is observed at low frequency for all four samples. For the measured range of frequencies, this plateau is not reached by sample S4 for temperatures T ~ 260 K. For the rest of our samples, plateau can be detected for all temperatures, albeit it shifts towards lower frequencies.

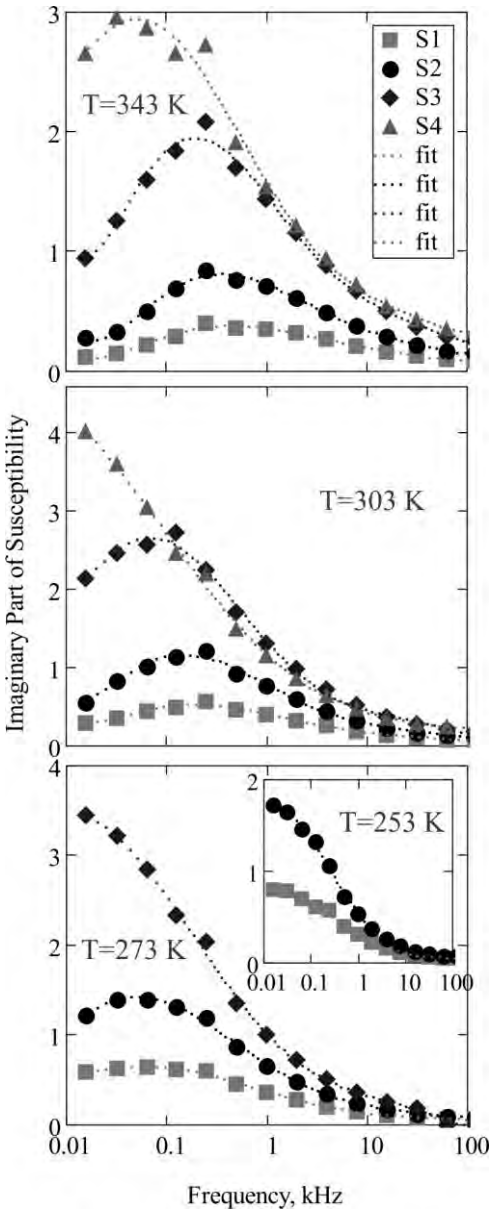

Fig. 3. Imaginary part of the magnetic dynamic susceptibility vs AC field frequency, kHz, for samples S1–S4. From top to bottom T decreases, the values are provided in each plot. The symbols are explained in the legend. Lines are guides for the eye. The inset of the lowest plot corresponds to the lowest experimentally accessible temperature specific to these measurements.

On cooling, the maximum of χ'' of the samples rapidly shifts to the region of ultra-low frequencies (Fig. 3), unveiling the presence of highly correlated magnetically passive clusters, whose relaxations are very slow. Moreover, the signs of vast expansion of such magnetically inert clusters were discovered for the most concentrated sample, making the percolation in the systems of dipolar hard spheres [3] a possible explanation of the dramatic slowing of the magnetic response.

Acknowledgments

The research was supported by Russian Science Foundation, (Grant No. 15-12-10003).

References

[1] A.O. Ivanov, O.B. Kuznetsova, Phys. Rev. E 64 (2001) 041405.
[2] S. Kantorovich et al., Phys. Rev. Lett. 110 (2013) 148306.
[3] L. Rovigatti, J. Russo, F. Sciortino, Phys. Rev. Lett. 107 (2011) 237801.

Controlled release and biodegradation of meltable magnetic biocomposites

Robert Müller[1], Mengbo Zhou[2], Natascha Kuhl[2], Martin Rabel[3], Paul Warncke[3], Dagmar Fischer[3], Thomas Heinze[2]

1 Leibniz-Institute of Photonic Technology. (IPHT), P.O.B. 100239, D-07702 Jena, Germany.
2 Institute of Organic Chemistry and Macromolecular Chemistry, Friedrich Schiller University of Jena, Humboldtstraße 10, D-07743 Jena, , Germany.
3 *Department of Pharmaceutical Technology and Biopharmacy, Friedrich -Schiller -University of Jena, Lessingstr. 8, D-07745 Jena, Germany*

The proof of principle using meltable polysaccharide based biocomposites containing magnetic nanoparticles (MNPs) as a magnetically remote controlled matrix for drug release was already shown in a previous work [1]. Thereby the release of a model substance (green fluorescent protein (GFP) nad Rhodamine B (RhB)) by softening the material through an induced alternating magnetic field (AMF) was demonstrated. Thus, it could be a suitable alternative path compared to hydrogel-MNP composites as remote controlled material [2]. The present work extends the investigations with respect to long term RhB release behavior and biodegradation of the composite (up to 60 and 28 days, respectively).

For the fabrication of biocompatible composites, fatty acid esters of dextran with adjustable melting points between 30 and 140 °C were synthesized [3]. The magnetically responsive composites were prepared by combined dissolution/suspension of the dextran ester and oleic acid hydrophobized magnetite MNPs in an organic solvent followed by ultrasonication, casting the solution, drying, and melting of the composite for shaping. The process leads to a uniform MNP distribution in the composite [4].

The biodegradability of the biocomposites was tested in simulated body fluid (SBF, pH=7.4) and artificial lysosomal fluid (ALF, pH=4.5) to simulate the plasma or lysosomal compartment, respectively. The iron release from the incorporated MNPs was assessed as a measure for the stability of the composites (Fig. 1). For degradation testing the composites (1% m/m MNP) were incubated in ALF or SBF each for 28 days at 37 °C and 110 rpm in an incubation shaker. After certain times 1 mL supernatant was collected and replaced with fresh fluid. The released iron was measured by bathophenantroline disulfonic acid complexation and spectroscopic quantification using a multiwell-plate reader [5]. The degradation of iron oxide nanoparticles in lysosomes after systemic application is known. Biocomposites stored in SBF release only 0.31% (dextran palmitate) or 0.19% (dextran myristate) of the total iron content indicating the stability of the MNPs in the composites. The iron release from biocomposites in ALF was higher; a cumulative amount of 5.4% (dextran palmitate) or 2.2% (dextran myristate) was mobilized after 28 d at 37 °C.

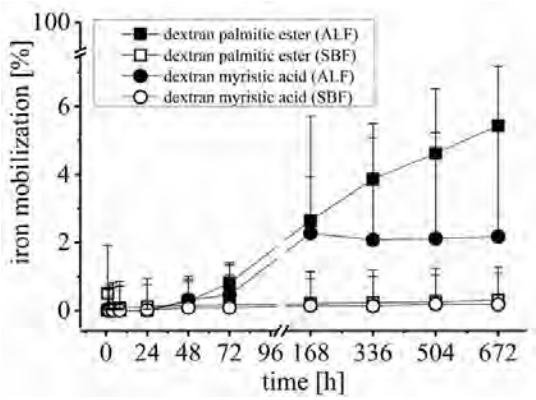

Fig. 1: Stability behavior of MNP loaded composites in artificial body fluids. Iron release from MNPs [%] as measured for degradation (n=3).

GFP and RhB were loaded separately as model drugs into the composite, GFP in a container-like sample geometry and RhB homogeneously dissolved in the composite

material. The application of an AMF heated the MNPs and resulted in a temperature increase above the melting range that leads to an increased diffusion of model drugs. GFP can be blocked in the composite, when no external stimulus was applied, because it cannot penetrate the polymer layer (thickness≈1mm) in the solid state [1]. The AMF cycles of 12 min induce a release of a stepwise accelerating behavior.
In short term experiments with RhB, three 12 min-cycles of AMF heating (after 1, 4 and 6 hours) have doubled the amount of RhB released compared to control samples [1]. There is a quite continuous release over time (not only during the heating).
In long term tests, measurements of the RhB concentration were carried out after a 12 min heating cycle (after 1, 2, 3, 7, 14, 30 and 60 days each). The amount of released RhB is comparable for samples stimulated by AMF and external heating (42 °C, water bath), considering the same heating cycles in both cases: however in the case of AFM heating the time above melting temperature was much shorter (Fig.2A). The cumulative released RhB is almost twice the amount compared to that of control samples treated at 25 °C after 60 days.
The release rate of AMF in Fig. 2B is calculated as the difference of released mass between the AMF or external heated sample, respectively, and the control sample over the cumulative heating time (12 min cycles). The release rates of the heated samples are higher than that of the control sample which means that the heating increased the diffusion rate. Interestingly the rates differ for shorter release times, i.e. surface effects might be dominant. This is maybe due to the internal heating by AMF, which can help the diffusion of RhB outwards.

Conclusion

The release behavior and degradation of meltable and biocompatible nanocomposites loaded with model drugs under alternating magnetic field was studied. The novel composite can be potentially applied as drug carrier in the field of controlled release applications.

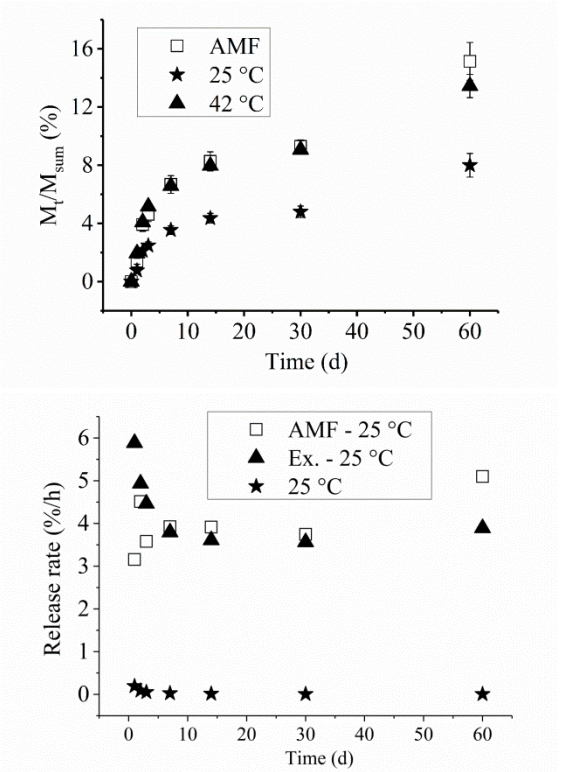

Fig. 2. A: Cumulative released mass of RhB from composites (square: heating by AMF, triangle: externally heated) and (circle: control sample at 25 °C) in phosphate buffered saline (pH 7.4). M_t: cumulative mass released at time *t*. M_{sum}: total mass loaded. **B:** release rates of heated samples calculated from difference to the control sample over the cumulative heating time, control sample over the total time

Acknowledgments

The financial support of the German Science Foundation (DFG, priority program SPP 1681, contracts HE2054/14-2 and MU2382/5-1) is acknowledged.

References

[1] R. Müller, et al., J. Magn. Magn. Mater. 431, 289-293, 2017
[2] N. S. Satarka, et al., Acta Biomater. 4, 11-16, 2008.
[3] T. Liebert, et al., Biomacromolecules 12, 3107-3113, 2011.
[4] M. Zhou, et al., Biomacromolecules 16, 2308- 2015
[5] A.S. Arbab, et al., NMR in Biomedicine, 2005. 18(6): p. 383-389.

Temperature controlled camptothecin release from biodegradable magnetic PLGA microspheres

D. Zahn[1], A. Weidner[1], Z. Nosrati[2], L. Wöckel[1], R. Müller[3], J. Dellith[3], K. Saatchi[2], U.O. Häfeli[2], S. Dutz[1]

[1] *Institut für Biomedizinische Technik und Informatik, Technische Universität Ilmenau, Germany*
[2] *Faculty of Pharmaceutical Sciences, University of British Columbia, Vancouver, Canada*
[3] *Leibniz Institute of Photonic Technology, Jena, Germany*

Introduction

Magnetic microspheres (MMS) are essential for magnetic drug targeting and typically consist of a polymeric matrix material loaded with magnetic nanoparticles (MNP) and a drug [1]. MMS can be magnetically guided to a target area where the drug is released either by degradation of the matrix or diffusion. Both release mechanisms can be accelerated by increasing the temperature of the MMS [2]. The needed temperature increase can be achieved by magnetic hyperthermia due resulting magnetization reversal losses when an alternating magnetic field is applied to the MMS [3]. In order to guarantee optimal magnetic targeting and defined drug release, MMS with uniform and controllable particle sizes, high specific heating rate and known degradation and release kinetics are necessary. To investigate the aspects listed above, poly(lactide-co-glycolide) microspheres (PLGA MS), loaded with the drug camptothecin and magnetic nanoparticles, were prepared and characterized concerning degradation behavior, drug release kinetics, and magnetic properties.

Methods

PLGA MS were prepared by an oil/water (o/w) emulsion evaporation method. For that, PLGA, camptothecin, and bisphosphonate coated MNP were dissolved/suspended in an organic solvent (o-phase) and emulsified by using a mechanical homogenizer in an aqueous PVA solution (w-phase). The obtained micro droplets were allowed to harden by evaporation of the solvent and collected using centrifugation or magnetic separation. Homogenization velocity was altered and its impact on the MS size was measured via DLS and SEM investigation. Degradation behavior of pure PLGA MS was studied using three types of PLGA with different monomer contents at 20 and 37 °C for 12 weeks. Drug release kinetics of camptothecin was investigated for the same three PLGA types at 20, 37 and 43 °C in water bath to evaluate the influence of different temperatures. Therefore, MS were suspended in phosphate buffered saline and remaining drug concentration in the MS was determined at defined intervals. From these values the released amount of drug was calculated. Drug concentrations were measured by UV/VIS spectroscopy using a standard calibration curve for camptothecin. MMS containing magnetic nanoparticles where investigated by VSM, SAR measurements and SEM.

Results

MS with perfect spherical shape and tunable mean diameters between 1 and 2 µm were prepared, with an inversely proportional correlation between homogenization velocity and diameter. Degradation experiments showed significant decomposition of the MS after 5 to 7 weeks at 37 °C, with proportional correlation between glycolide content and degradation velocity. Camptothecin was loaded into the MS with concentrations up to 0.5 wt% (1 wt% intended) and was released in a burst type release profile at 37 and 43 °C within few hours. The release

rates increased with increasing temperature (Figure 1).

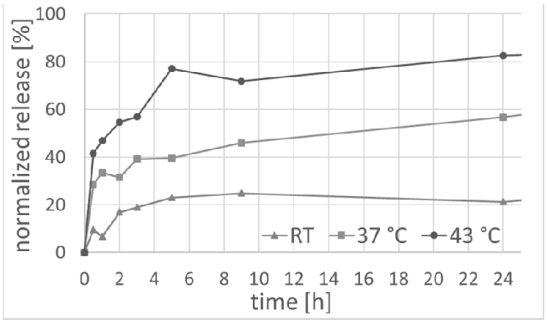

Figure 1: Drug release profiles of 65:35 PLGA MS as function of temperature; RT: room temperature

During drug release studies no significant differences between the different PLGA types in drug release were measured, which suggests a mainly diffusion-controlled drug release, in which the degradation behavior of the PLGA has only weak influence.
Magnetic microspheres show MNP concentrations of about 16 wt% (20 wt% intended) with a saturation magnetization of 12 emu/g, a coercivity of 7 Oe, and a specific heating power suitable for magnetic heating for enforced drug release from the PLGA at a MMS in tissue concentration of 2 % by mass. SEM images confirm that MNP are mainly located in the outer layer of the microspheres (Figure 2).

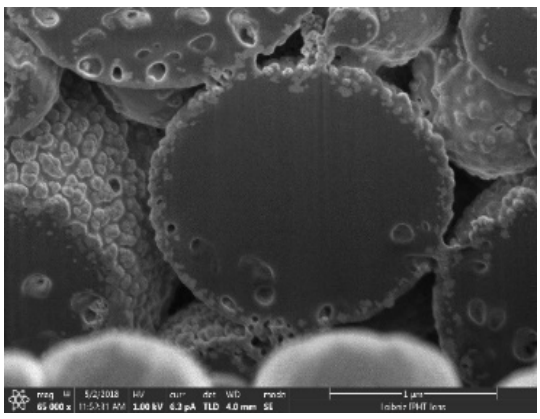

Figure 2: SEM imaging after FIB cut through the MMS reveals that MNP are located on the surface of the MMS.

Conclusion

Drug loaded magnetic microspheres were prepared by the o/w emulsion evaporation method, whereby the introduction of the drug camptothecin and magnetic nanoparticles did not hinder the generation of spherical shaped particles. Increasing drug release with increasing temperature confirms the approach of loading MNP into the MS to control the drug release by means of magnetic heating. In ongoing studies, the drug concentrations have to be increased and MNP should be distributed more homogenously in the MS. Drug release studies have to be realized by magnetic heating instead of incubating the MS in a heated water bath.

Acknowledgments

This work was supported by German Academic Exchange Service (DAAD) in the frame of an Alumni Project of Research Mobility (PPP) and in the frame of DFG Priority Program (SPP) 1681 (FKZ: MU2382/4-2).

References

[1] Fang, Kun et al. (2015): *Magnetic field activated drug release system based on magnetic PLGA microspheres for chemo-thermal therapy*. Colloids and surfaces. B, Biointerfaces 136: 712–720.

[2] Xu, Yihan et al. (2017): *Polymer degradation and drug delivery in PLGA-based drug–polymer applications. A review of experiments and theories.* Journal of Biomedical Materials Research Part B: Applied Biomaterials 105/6: 1692–1716.

[3] Dutz, Silvio and Hergt, Rudolf (2014): *Magnetic Particle Hyperthermia – A promising tumour therapy?* Nanotechnology 25: 452001.

Cellular cytokine release after magnetic nanoparticle incubation

J. Demut[1], J.M. Müller[1], M. Rabel[2], M. Haist[1], C. Grüttner[3], F.A. Müller[4], R. Quaas[5], A. Hochhaus[1], D. Fischer[2], J. H. Clement[1]

[1] *Klinik für Innere Medizin II, Abt. Hämatologie & Internistische Onkologie, Universitätsklinikum Jena, Am Klinikum 1, D-07747 Jena, Germany; mail to: johanna.demut@med.uni-jena.de*
[2] *Institut für Pharmazie, Abt. Pharmazeutische Technologie, Friedrich-Schiller-Universität Jena, Lessingstraße 8, D-07743 Jena, Germany*
[3] *Micromod Partikeltechnologie GmbH, Friedrich-Barnewitz-Straße 4, D-18119 Rostock, Germany*
[4] *Otto-Schott-Institut für Materialforschung, Professur für Oberflächen- und Grenzflächentechnologie, Löbdergraben 32, D-07743 Jena, Germany*
[5] *Chemicell GmbH, Eresburgstraße 22-23, D-12103 Berlin, Germany*

Introduction

Superparamagnetic iron-oxide nanoparticles (SPIONs) are of specific interest for biomedical applications, such as contrast agents in magnetic resonance imaging or for therapeutical interventions [1,2]. Their long-term effects have to be considered since SPIONs may remain at distinct sites in the human body. Thus, potential inflammatory responses, e.g. cytokine release should be evaluated to assure biocompatibility and to make precautions to avoid adverse effects.
The aim of the present study is to examine the effects of SPION incubation on the secretion of pro- and anti-inflammatory cytokines on the long run. Furthermore the production of reactive oxygen species (ROS) upon SPION incubation is investigated.

Materials & Methods

FaDu (hypopharyngeal squamous cell carcinoma) were cultivated in a conventional 2-dimensional manner as well as in 3-dimensional multicellular spheroids (MCS). The cells were incubated with different SPIONs (starch-coated fluidMAG-D, glucuronic acid-coated fluidMAG-ARA, polyethylenimine-coated PEI-M, PEG-5kDa coated BNF-Dextran, silica-iron oxide composite SiliFe41) as well as with fluorescence labelled variants of these particles (except for SiliFe41). Vitality of the cells in the presence of the nanoparticles was determined with the PrestoBlue assay. The internalisation of the particles into the cells was analysed via laser scanning microscopy (LSM). For this purpose the cells were counterstained with phalloidin-AF633 and DAPI. For determination of the interaction of the particles with the MCS, they were embedded in 1% agarose, formalin-fixed, dehydrated and then embedded into paraffin. 4 µm FFPE-sections were prepared which were stained with Prussian blue and counterstained with Nuclear Fast Red.
Different pro- and anti-inflammatory cytokines and chemokines were analysed from cell culture supernatant via LEGENDplex human inflammation panel (BioLegend, San Diego) and a Proteome Profiler Array – Human Cytokine Array (bio-techne, Wiesbaden-Nordenstadt).
Finally the concentration of ROS in these cell culture supernatants was determined via Oxiselect *in vitro* ROS/RNS Assay Kit (Cell Biolabs Inc., San Diego).

Results

The SPIONs used in this study were selected out of a panel of more than 20 nanoparticle formulations with regard to their chemical composition and their charge. All SPIONs were biocompatible up to a concentration of 100 µg/cm^2 with the exception of PEI-M. An intense interaction and uptake of PEI-M particles was observed via LSM for 2D-cell cultures of FaDu and histologic analysis of MCS. FluidMAG-D and SiliFe41 exhibited a moderate interaction whereas only a few fluidMAG-ARA and PEG-5kDa nanoparticles could be detected in both cell culture models.

An important concern regarding nanoparticle-cell interaction is an alteration of cytokine release, which can lead to an inflammatory response. Therefore 2D-cell cultures were analysed for 13 cytokines / chemokines with an ELISA-based assay. The investigated SPIONs showed a pronounced effect on the secretion of IL-6 and IL-23 after 24 h. In detail, fluidMAG-ARA, PEG-5kDa and SiliFe41 increased the amount of secreted pro-inflammatory IL-6. PEG-5kDa-coated particles do also elevate the release of pro-inflammatory IL-23.

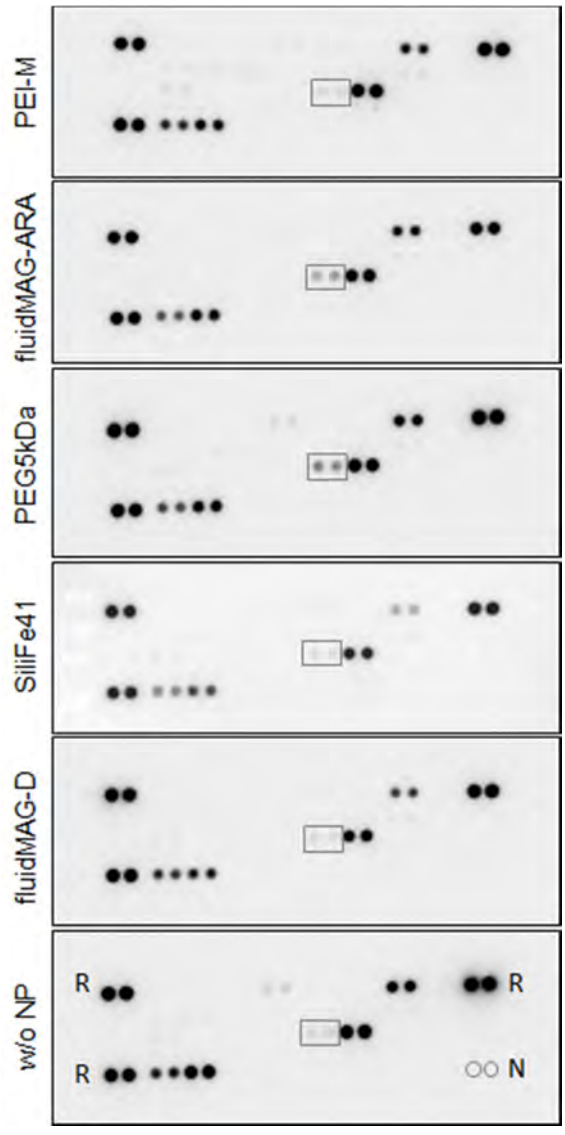

Figure 1: SPIONs modulate cytokine release. FaDu 2D-cell cultures were incubated with 25 µg/cm^2 SPIONs as indicated for 24h. Supernatant was collected, lysed and applied onto the Proteome Profiler Arrays. Immunoreactivity was measured by LAS4000. Data were analysed by ImageJ. Box labels the IL-6-specific spots. R = reference spots (positive control); N = negative control

A more extended study with a Proteome Profiler Array covering 36 proteins showed a complex time- and nanoparticle-dependant release of cytokines / chemokines (Figure 1). In total, 24 cytokines exhibited clearly detectable alterations of total amount. The previously described increase of IL-6 secretion could be confirmed (fluidMAG-ARA (3.5-fold), SiliFe41 (1.3-fold) and PEG-5kDa (3.2-fold).
Concerning oxidative stress fluidMAG-ARA seems to elevate the amount of ROS present in the cell culture supernatant.

Conclusion

We could show that differentially charged SPIONs interact with FaDu cells in 2D-cell culture and in multicellular spheroids. The latter allow studying SPION effects in a more complex cellular context including cell orientation and extracellular matrix. SPIONs activate a multi-facetted cascade of cytokines and chemokines.
Future work will focus on the long-term changes in cytokine release (up to 14 days) with the help of the MCS model and elucidation of the down-stream targets and their activities.

Acknowledgements

We thank the Federal Ministry of Education and Research (BMBF), Germany, as well as the PTJ Jülich, Germany, for funding the research project NanoBEL (03XP0003). This work was supported in part by Europäische Fonds für regionale Entwicklung – Europa für Thüringen (EFRE) (FKZ 2016 FGI 0006)

References

[1] Dutz, S., Clement, J.H., Eberbeck, D. et al., *J Magn Magn Mater*. **2009**, *321*, *1501*
[2] Pankhurst, Q.A., Connolly, J., Jones, S.K. et al., *J. Phys. D: Appl. Phys.* **2003**, *36*, R167

Development of biocompatible Vascular Scaffolds using Magnetic Cell Seeding of SPION-loaded Cells

R. P. Friedrich[1] , M. Mühlberger[1], S. Draack[2], F. Ludwig[2], D. Eberbeck[3], F. Wiekhorst[3], W. Lang[4], E. I. Wisotzki[5], S. Mayr[5], C. Alexiou[1]

[1] *Department of Otorhinolaryngology, Head and Neck Surgery, Section for Experimental Oncology and Nanomedicine (SEON), Else Kröner-Fresenius-Stiftung-Professorship University Hospital Erlangen, Germany*
[2] *Institut für Elektrische Messtechnik und Grundlagen der Elektrotechnik, TU Braunschweig, Braunschweig, Germany;*
[3] *Department of Vascular Surgery, University Hospital, Erlangen, Germany*
[4] *Physikalisch-Technische Bundesanstalt Braunschweig und Berlin, Berlin, Germany*
[5] *Leibniz Institute of Surface Modification (IOM), Leipzig, Germany*

Background / Purpose

Progress in the production of hybrid materials for tissue engineering is mandatory in the field of regenerative medicine. Nanotechnology provides us with therapeutic possibilities to cure a wide range of different diseases or harmful conditions like atherosclerosis and thrombosis [1,2]. In these diseases, lack of adequate venous material for transplantation constitutes a common problem in cardiovascular surgery, resulting in a strong need for biocompatible vascular grafts. Tissue-engineered hybrid materials combining a biocompatible scaffold and a cell-coated lumen may reduce the risk of thrombosis, intimal hyperplasia and calcification of currently available grafts.

Methods

At SEON, we design and produce a variety of superparamagnetic nanoparticles (SPIONs) for biomedical applications [3-5]. Some of those particles were especially designed for the production of tubular endothelialized scaffolds. The cell-coating of tubular scaffolds is achieved by magnetic cell seeding of SPION-loaded endothelial cells using a 3-dimensional magnetic technique [6] (Fig. 1a,b). This technique is based on a machine producing a radial magnetic field (VascuZell Endothelizer) resulting in the directed movement of cells, with sufficient amounts of SPIONs, towards the inner lumen of the vascular graft.

Results

In a proof of concept study using tubular scaffolds based on polyethylene, endothelial cells preloaded with non-toxic polyacrylate-co-maleate coated SPIONs (SPION-PAM) showed stable and homogeneous adhesion and colonization of the inner surface, without a noticeable change in cell viability. Increased cultivation periods caused a more dense coverage and proved the proliferation potential of magnetically seeded cells. Currently, we are investigating the cellular colonization efficacy on different biocompatible vascular prostheses with one and two different cell-layers (fibroblasts and endothelial cells) (Fig 1c).

Conclusions

We have successfully shown the feasibility of 3-dimensional magnetic cell seeding of vascular scaffolds. The method had no adverse effect on cell viability and proliferation (Fig 1d). Future preclinical in vivo studies will analyze the applicability and potential advantages of these transplants.

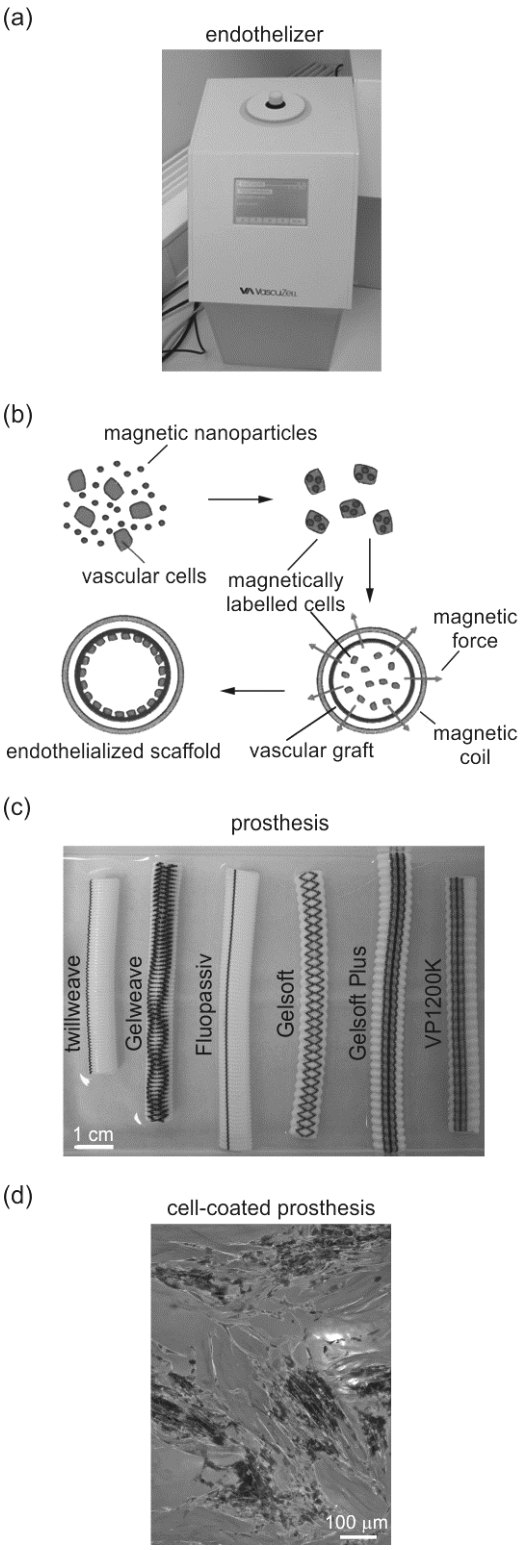

Figure 1: 3D Magnetic cell seeding (a) Endothelizer. (b) Principle of endothelialization with magnetic nanoparticles. (c) Different commercial vascular grafts from Terumo. (d) Cell-coated inner surface of a prosthesis after fluorescent staining and microscopic imaging.

Acknowledgments

DFG SPP 1681 (AL552/5-3)

References

[1] Cicha I, Singh R, Garlichs CD, Alexiou C: Nano-biomaterials for cardiovascular applications: Clinical perspective. J Control Release, 229: 23-36, 2016

[2] Cicha I: Thrombosis: Novel nanomedical concepts of diagnosis and treatment. World J Cardiol, 7: 434-441, 2015

[3] Friedrich RP, Zaloga J, Schreiber E, Toth IY, Tombacz E, Lyer S, Alexiou C: Tissue plasminogen activator binding to superparamagnetic iron oxide nanoparticle-covalent versus adsorptive approach. Nanoscale Res Lett, 11: 297, 2016

[4] Heid S, Unterweger H, Tietze R, Friedrich RP, Weigel B, Cicha I, Eberbeck D, Boccaccini AR, Alexiou C, Lyer S: Synthesis and characterization of tissue plasminogen activator-functionalized superparamagnetic iron oxide nanoparticles for targeted fibrin clot dissolution. Int J Mol Sci, 18: 2017

[5] Zaloga J, Janko C, Nowak J, Matuszak J, Knaup S, Eberbeck D, Tietze R, Unterweger H, Friedrich RP, Duerr S, Heimke-Brinck R, Baum E, Cicha I, Dorje F, Odenbach S, Lyer S, Lee G, Alexiou C: Development of a lauric acid/albumin hybrid iron oxide nanoparticle system with improved biocompatibility. Int J Nanomedicine, 9: 4847-4866, 2014

[6] Perea H, Aigner J, Hopfner U, Wintermantel E: Direct magnetic tubular cell seeding: A novel approach for vascular tissue engineering. Cells Tissues Organs, 183: 156-165, 2006

Initial susceptibility of microgels in computer simulations

E.S. Minina[1,2], P.A. Sanchez[1,2], C.N. Likos[1], S.S. Kantorovich[1,2]

[1] *University of Vienna, Boltzmanngasse 5, 1090, Vienna, Austria*
[2] *Ural Federal University, Lenin av. 51, 624000, Ekaterinburg, Russia*

Microgels are spherical colloidal particles consisting of polymer network. Due to their nature, microgels are able to swell and shrink as a response to their external environment [1]. This ability makes them promising materials for many applications including drug delivery and design of artificial muscles. The desire to control microgels therefore has drawn the attention of researches to studying their properties.

However, the spectrum of application of microgels can be broadened by embedding magnetic particles into microgel's polymer network. The presence of magnetic particles dramatically changes the behavior of microgels and also offers an additional mechanism to control their properties. For example, elastic and magnetic response of soft materials to the surrounding environment can change as it has been demonstrated in the resent works on the novel magnetic dipolar materials like magnetic gels and filaments [2-4].

In this work, we study magnetic microgels in molecular dynamics computer simulations. Microgels are initially modelled as bead-spring polymer chains randomly crosslinked into a polymer network. To make the microgels magnetic, we incorporate magnetic particles into the polymer network. The fraction of magnetic particles is in the range between 0.5 to 10 per cent of the total fraction of particles comprising the polymer network. Changing degree of crosslinking and the fraction of magnetic particles allows us to vary microgel's internal structure. This way, we consider weekly crosslinked and highly crosslinked microgels and observe how the microgels change their shape and size depending on the internal structure and magnetic component. Studying such systems at different strength of dipole-dipole interactions, we estimate the change of magnetic microgel in size, self-assembly of magnetic particles and the initial magnetic susceptibility[5]. We show that an appropriate combination of magnetic component and degree of crosslinking may offer an additional way to control.

References

[1] A. Fernandez-Nieves, H. M. Wyss, J. Mattsson, and D. A. Weitz. Microgel Suspensions: Fundamentals and Applications. 2011.

[2] R. Weeber, S. Kantorovich, and C. Holm, J. Chem. Phys. 143 (15) (2016).

[3] P.A. Sanchez, E.S. Pyanzina, E.V. Novak, J.J. Cerda, T. Sintes and S.S. Kantorovich, Faraday Discuss. 186, 241 (2016).

[4] P.A. Sanchez, E.S. Pyanzina, E.V. Novak, J.J. Cerda, T. Sintes and S.S. Kantorovich, Macromolecules 48 (20), 7658 (2015).

[5] E.S. Minina, P.A. Sanchez, C.N. Likos and S.S. Kantorovich, JMMM 459, 226 (2018)

Non equilibrium long-living structures in magnetic gels and suspensions

L.Yu.Iskakova, A.Yu. Zubarev

Department of Theoretical and Mathematical Phsyics, Ural Federal University, Ekaterinburg, Russia

Numerous experiments show that magnetic field, applied to a flat gap filled by a magnetic fluid (suspension), induces appearance of dense cylindrically shaped aggregates, elongated along the field and percolating the gap. Theoretical models of this phenomenon have been suggested in refs.[1,2]. These models treat the aggregates as a consequence of the field induced condensation phase transitions in ensembles of the magnetic particles. The discrete morphology of the domains of dense phase is explained by the competition between the effect of the interphase tension on the domains surfaces, which tends to amalgamate the domains into one massive sphere, and effect of the demagnetizing field, which tends create highly elongated needle-shaped domains. In [1,2] these domains have been considered as cylinders, fully stocked by the particles; this morphology corresponds to thermodynamically equilibrium state of the fluid (suspension) in the external field.

Experiments [3] have demonstrated appearance of stable (long-living) tube-like aggregates with empty central part in a flat gap, filled by magnetic suspensions. These tubes present a new, unstudied type of structures in MR suspensions. They do not correspond to the thermodynamically equilibrium state of the suspensions, and must be considered as some "frozen" non-equilibrium structures in these systems.

We present results of theoretical study of these stable non equilibrium "tubes". In the frame of this model, a system of the dense tubes, elongated along the applied field, is considered; the length of the tube is restricted by the size of the container with the suspension. We determine energy U of the system, consisting of the energy of the magnetized aggregates in the applied field as well as the surface tension energy.

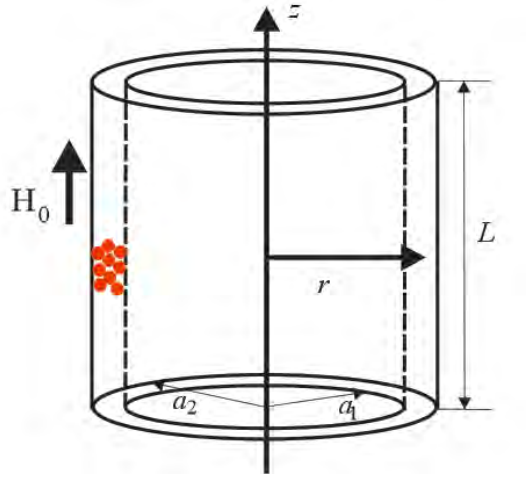

Sketch of the tube-shaped aggregate. Red circles illustrate some of the particles, the tube consists of.

If the volume V of the tube is changeable (because of the particles exchange between the aggregates), the equilibrium morphology of the suspension corresponds to the systems of dense elongated cylinders (tubes with zero internal radius). However, if the volume V is fixed (the intertube exchange does not take place), minimum of the energy U corresponds to the systems of the tubes, with some finite internal a_1 and external a_2 radiuses. Note that the exchange of the particles between the tubes can take place due to intensive Brownian motion of the particles. If this motion is "supressed" by the large size (micron and more) of the particles and/or high viscosity of the host liquid, the volume of the tube is not being changed for long time and the system is stacked in the transition non-ergodic state with the tube-shaped aggregates.

References

[1] Zubarev and Iskakova, *Physica A* **367**, 55 (2006).

[2] Gutillas et al., *Phys.Rev.E.* **57**, 804 (1998).

[3] Gunter et al., *Smart Mater. Struct*. **21** 015005(2012).

Coarsening dynamics of ferromagnetic granular networks – experiment and simulation

P. A. Sanchez[1,2], A. Kögel[3], R. Maretzki[3], T. Dumont[3], E. S. Pyanzina[2], S. S. Kantorovich[1,2], R. Richter[3]

[1] *University of Vienna, Vienna, Austria*
[2] *Ural Federal University, Ekaterinburg, Russia*
[3] *University of Bayreuth, Bayreuth, Germany*

We investigate the phase separation of a shaken mixture of glass and magnetised steel spheres after a sudden quench of the shaker amplitude (Fig. 1). Then transient networks of steel spheres emerge in the experiment. For the developing network we observe an initial regime, where the network incubates, followed by a regime where network structures are elongated and broken, and finally a regime where the structures have relaxed to compact clusters of rounded shapes. This phaenomenology resembles the initial, elastic and hydrodynamic regimes observed by [1] during the viscoelastic phase separation for dynamically asymmetric mixtures of polymers.

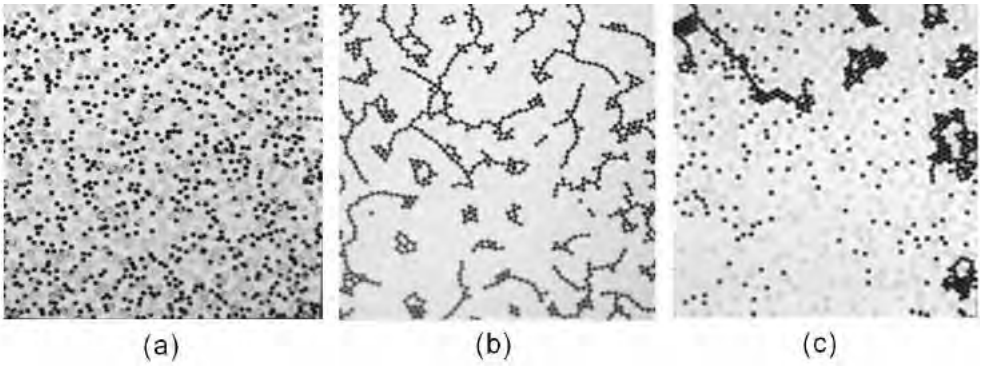

Fig. 1.Snapshots of the coarsening dynamics after a quench of the vibration amplitude from 3g to 1.93g recorded at a vibration frequency of 60 Hz. Gas phase (a), transient networks (b), and compact crystallites with only a few loops (c).

In order to unveil the three regimes, we measure order parameters like the mean number of neighbors and the efficiency. To elucidate the origin for a viscoelastic phase separation, we use a simple simulation approach to define the key interactions in the experimental system. This way, we discover that along with dipolar and steric interactions, a central attraction between the magnetised spheres is decisive for the coarsening dynamics. Our simulations (Fig.2) show three regimes in the evolution of characteristic order parameters.

Fig. 2. Mixtures of magnetic (dark) and non magnetic (light grey) particles. Simulation snapshots are obtained for dimensionless magnetic coupling parameter 5, temperature 0.5, and attraction parameter 0.5, at different integration steps after quenching: 2500 (a), 10^5(b) and $2.5 \cdot 10^5$ (c). Taken from [2].

References

[1] H. Tanaka, J. Phys.: Cond. Mat. 12, R207 (2000).
[2] A. Kögel et al., Soft Matter, 14, 1001-1015, 2018

Self-assembly of magnetic filament solutions under the influence of additional interactions

E. Novak[1], E. Pyanzina[1], D. Rozhkov[1], P. A. Sánchez[1,2], S. Kantorovich[1,2]

[1] *Ural Federal University, Ekaterinburg, Russia*
[2] *Computational Physics: Faculty of Physics, University of Vienna, Vienna, Austria*

Latest technologies have made it possible to create magnetic or supracolloidal magnetic polymers (SMPs). SMPs are semiflexible polymer-like chains of magnetic nanoparticles permanently crosslinked with polymers. Here we present the study of low-concentrated solutions of filaments using Langevin dynamics simulations. We analysed their self-assembly under the influence of various internal parameters: dipole-dipole interaction, additional attraction potentials, particle sizes, conformations and lengths of chains. Self-assembly of simple open chains, closed rings and branched structures with "X" and "Y" junctions were investigated with help of extensive cluster analysis based on graph theory. We calculated cluster size distribution, amount of additional connections, their distribution and compared the structures formed by filament solutions to those observed in conventional magnetic fluids containing non-crosslinked nanoparticles. For example, cluster size distribution has totally different behavior for ferrofluid and filament's solution. We have shown that permanent links in the system of magnetic particles and their conformation can drastically change microstructure of dispersion. On the next step we considered the behavior of such a system under the influence of additional attractive potential to explore the difference in the existent scenario of self-assembly. Also, we were interested in the impact of polydispersity in the self-assembly of filament solutions. Following the seminal theoretical work [1] on the effects of polydispersity on the properties of ferrofluids we consider a bidisperse model as a first approximation to a polydisperse system. We studied four types of individual magnetic polymer chains: consisting of only large particles (0); with all large, but one small particle located at one chain end (1); with two small particles at the chain ends (2); with three small particles, two of them at the chain ends and one in the middle (3). We examined the radius of gyration and magnetic moment of a single linear SMP in a wide range of temperatures. We observe that the presence of even a little fraction of small particles in the chains significantly affects their structural behaviour. For example, the existence of a small particle in the central part of the chain tends to decrease the radius of gyration with respect to the same reference system. All these results will form the basis for developing theoretical models and provide recommendations for the design of novel magnetoresponsive systems.

Acknowledgments

This research has been supported by the Russian Science Foundation Grant No.17-72-10145. P.A.S and S.S.K acknowledge support from the Austrian Research Fund (FWF), START-Projekt Y 627-N27. The computational results presented here have been achieved using the Ural Federal University Cluster.

References

[1] A. O. Ivanov and S. S. Kantorovich, Phys. Rev. E 70, (2004).

Magnetic polymer brush-like coatings: the impact of filament inhomogeneities on the equilibrium structure

D. Mostarac[1], P. A. Sánchez[1,2], S. S. Kantorovich[1,2]

[1] *University of Vienna, Vienna, Austria.*
[2] *Ural Federal University, Ekaterinburg, Russia.*

Magnetic gels and elastomers, consisting of a polymer matrix with embedded magnetic colloidal particles, can be attached as thin layers to the surface of solid substrates in order to create responsive coatings whose structure and rheological properties can be controlled by means of external magnetic fields. Simple conventional synthesis approaches, however, provide a limited control on the structure of the polymer matrix.

Recently, we proposed the build up of a magnetoresponsive coating with a well defined microstructure, analogous to the one corresponding to a polymer brush but at a supracolloidal scale, based on the use as building blocks of magnetic micro- or nanoparticles precrosslinked into polymer-like linear chains. Such magnetic filaments could be tethered to the substrate in a brush-like arrangement [1]. In this way, one could obtain a thin film coating that could extend the broad set of applications of 'smart' polymer brushes to highly magnetoresponsive systems. This has interesting potential applications as, for example, the creation of magnetically controlled filtering and flow control elements in microfluidic devices. By means of computer simulations, we analyzed the equilibrium structure and scattering properties of such an interesting magnetic brush system [1-3].

In our preliminary studies, we assumed the ideal case of a perfectly homogeneous system, formed by identical filaments. Here we extend our previous work by considering the existence of inhomogeneities in the properties of the filaments, analyzing their impact on the brush equilibrium properties. In particular, in this contribution we focus on the effects of the presence of non magnetic particles along the filament's backbone.

Acknowledgments

Research funded by the FWF Start Projekt Y 627-N27.

References

[1] P. A. Sánchez; E. S. Pyanzina, E. V. Novak, J. J. Cerdà, T. Sintes, S. S. Kantorovich, *Macromolecules* **48**, 7658-7669, (2015).
[2] P. A. Sánchez, E. S. Pyanzina; E. V. Novak, J. J. Cerdà, T. Sintes, S. S. Kantorovich, *Faraday Discuss.* **186**, 241-263 (2016).
[3] E. S. Pyanzina, P. A. Sánchez, J. J. Cerdà, T. Sintes, S. S. Kantorovich, *Soft Matter* **13**, 2590-2602 (2017).

Influence of dipolar interactions on the characteristic times of ferrofluids subjected to oscillating field

V.S. Zverev[1], E.A. Elfimova[1], A.O. Ivanov[1]

[1] *Ural Federal University, Lenin Av. 51, Ekaterinburg 620000, Russian Federation*

A conventional way to describe the dynamic properties of magnetic fluid is based on the study of the timescales of the nanoparticle rotations [1]. Transient processes are associated with their characteristic times, which determine properties of ferrofluids. This work is devoted to the analysis of the influence of dipole interactions on the characteristic relaxation times. Ferrofluid is modeled as a monodisperse system of uniformly magnetized spherical particles suspended in a cylindrical container. An external linear polarised, harmonic probing magnetic field is applied along the symmetry axis of the container. It is assumed that the direction of a magnetic moment can change due to the rotation of the nanoparticle as a rigid body (Brownian mechanism). One of possible characteristic timescale is connected with returning to equilibrium state after some perturbation. The formula for the relaxation time in such sense was derived using effective-field method in the form [2]

$$\tau = \tau_B \frac{d \ln L(\alpha)}{d \ln \alpha},$$

where τ_B is zero-field Brownian relaxation time, L is Langevin function and α is has a meaning of the Langevin parameter (relation magnetic enegry to the thermal).

Previously suggested approach for describing dynamic magnetic response of interacting ferroparticles in magnetic fluids allows us to obtain correction this formula for the case moderately concentrated ferrofluids [3]. Applying the effective field method, it can be shown that when dipole-dipole interaction is taken into account the the formula for the relaxation time has the same form, but the correction for the Langevin parameter is required.

Another characteristic times are connecting with features of the susceptibility spectrum. These features are the low-frequency behaviors of the real and imaginary parts of the spectrum, and the maximum value of the imaginary part. It yields three characteristic times of the magnetic response process. In current work dynamic spectrum is obtained via solution of the Fokker-Plank-Brown equation [3]. Two methods of solution, namely finite-difference numerical method and effective field approximation [2], are used and results are compared. For the case of noninteracting particles, dynamic susceptibility is described by the Debye-like relations and all kinds of characteristic times coincide with each other. However, it was found that when dipole-dipole interaction is taken in consideration the characteristic times noticeably differ from the ideal case.

Acknowledgments

This research was supported by Russian Science Foundation, Grant No. 15-1210003.

References

[1] J. Dieckhoff et al. J. Appl. Phys. 119, no. 4 (2016).
[2] Y. L. Raikher and V. I. Stepanov, Adv. Chem. Phys. 129, pp. 419–588 (2004).
[3] A. O. Ivanov et al. J. Magn. Magn. Mater. 431, pp. 141-144 (2017).

Preparation of DNA-flagellated $CoFe_2O_4$@Pt nanostructures and study of their electrophoretically induced motion

Y. Martinez, M. Raphael, A. M. Schmidt*

Institute of Physical Chemistry, Department of Chemistry, University of Cologne, Luxemburger Str. 116, D-50939 Cologne, Germany, email: annette.schmidt@uni-koeln.de

Introduction

Developing nanomotors capable of executing non-random motion represents one of the main challenges confronting nanotechnology.[1] Beyond keeping a low complexity design, such systems should also overcome the influence of Brownian motion, viscous drag and various surface phenomena in environments dominated by a low Reynolds number. Hence, these implications suggest a clear necessity to develop enhanced swimming strategies for the inertialess limit, oriented towards nonreciprocal motion and a symmetry-breaking architecture.

Some successful approaches in this direction have thus resulted in synthetic motors, which simulate the navigation patterns displayed by biological swimmers.[2] Mimicking this natural design, we present here the preparation of DNA-flagellated nanostructures based on the general structure of flagellated bacteria and sperm cells. Within this approach, the nanohead is built with heterofunctional $CoFe_2O_4$@Pt nanostructures, whereas the flagella is assembled by the selective attachment of DNA strands to the platinum counterpart. Moreover, the electrophoretically induced motion is evaluated in a confined media (agarose gel), pointing out the role of the surface charge of the DNA-flagellated nanostructures.

Synthesis of heterofunctional $CoFe_2O_4$@Pt nanostructures

The preparation of heterofunctional $CoFe_2O_4$@Pt nanostructures entails a stable interface linkage between the $CoFe_2O_4$ and platinum domain *via* a two-step process developed in our research group.[3] Initially, platinum nanocubes in a size range of (6.4 ± 0.8) nm are prepared by a modified thermal decomposition route.[4] The seed-mediated growth of a $CoFe_2O_4$ domain is induced in organic phase nucleated from the platinum counterpart. Next, the capping surface of these obtained nanostructures is further modified using a ligand exchange treatment.[5] In this way, it is possible to obtain poly(acrylic acid) capped nanostructures with an edge length of (29.6 ± 3.7) nm as shown in Figure 1. These nanostructures are well-dispersible and stable in aqueous media as well as in diluted buffer solutions at physiological pH.

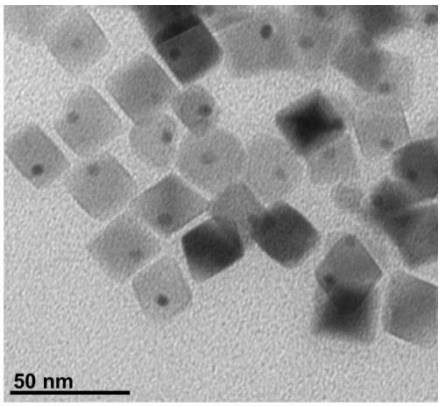

Figure 1. Transmission electron microscopy of heterofunctional CoFe2O4@Pt nanostructures.

Preparation of DNA-flagellated $CoFe_2O_4$@Pt nanostructures

The platinum counterpart of the heterofunctional nanostructures is further functionalized with 60 bp and 90 bp DNA strands *via* chemisorption. To this end, thiolated single-stranded DNA is attached and then hybrid-

ized to yield double-stranded DNA. A methodical investigation including four conjugation procedures (*i.e.* salt aging, SDS-assisted salt aging, pH-assisted and freezing-thawing)[5] is conducted.
It is found that the SDS- assisted salt aging process enables stable flagellated-like nanostructures with a lifetime of three weeks when preserved in HEPES buffer at 4 °C and physiological pH. After characterization *via* elemental analysis and UV-vis spectrophotometry, it is also possible to estimate that depending on the experimental conditions 2-12 double strands of DNA are attached to each nanostructure. Furthermore, atomic force microscopy (AFM) confirms the presence of organic material (DNA) around the nanostructure as shown in Figure 2.

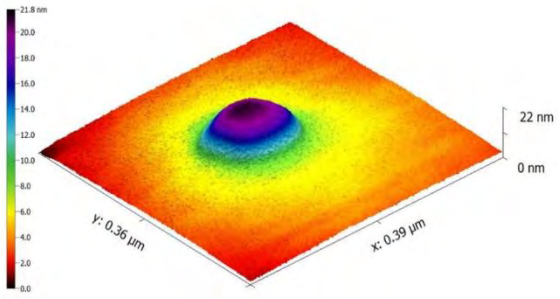

Figure 2. Atomic force microscopy topography imaging of heterofunctional $CoFe_2O_4$@Pt functionalized with DNA.

Electrophoretically induced motion of DNA-flagellated $CoFe_2O_4$@Pt nanostructures

The mobility of the DNA-flagellated nanostructures confined inside agarose gel (0.6 % m/v) is evaluated under an electric field. In a general way, the most interesting feature of these systems is that the DNA-flagellated nanostructures migrate more slowly than the nanostructures alone as a consequence of hydrodynamic and charge effects. This significant shift allows the possibility to finely tune their electrophoretic migration through agarose gel.

Acknowledgment

Financial support is acknowledged from Deutsche Forschungsgemeinschaft (DFG, Grant SPP1681) and NanoSciE+. YM also gratefully acknowledges a Doctoral Scholarship granted by the Deutscher Akademischer Austauschdienst (DAAD).

References

[1] Wang, J. Nanomachines: fundamentals and applications. John Wiley & Sons, **2013**.
[2] Ceylan, H., Giltinan, J., Kozielski, K., Sitti, M., *Lab on Chip* **2017**, 1705-1724.
[3] Effertz, M., Dissertation, Universität zu Köln, **2017**.
[4] Zhang, H. T., Ding, J., Chow, G. M., Langmuir **2008**, 24(2), 375-378.
[5] Rapahel, M., Bachelor Thesis, Universität zu Köln, **2018**.

Stable Suspensions of Magnetic Nanoparticles in Thermotropic Liquid Crystals

M. Hähsler[1], A. Eremin[2], R. Stannarius[2], S. Behrens[1]

[1] *Institute of Catalysis Research and Technology, Karlsruhe Institute of Technology (KIT), post office box 3640, 76021 Karlsruhe*
[2] *Abteilung Nichtlineare Phänomene, Otto-von-Guericke-Universität Magdeburg, Universitätsplatz 2, 39106 Magdeburg*

Liquid crystals (LCs) combine properties of both the liquid and crystalline state. The magnetic susceptibility of low-molecular-weight organic LCs is relatively small. Therefore, alignment of such LCs in thin cells requires high magnetic fields. Integration of magnetic nanoparticles (MNPs) in LCs can increase the magnetic susceptibility and thereby the response to an applied magnetic field [1]. Mertelj et al. realized the integration of magnetic NPs in LCs with interesting static and dynamic magneto-optical properties [2, 3, 4]. However, a long-term stabilization of magnetic NPs in LCs is still a challenging task.

The properties of the MNPs (size, shape and magnetic properties), LC anchoring at MNP surfaces, as well as interparticulate interactions are the crucial parameters that determine the behaviour of ferronematics. In order to modulate the LC-MNP interactions and MNP stability in the LC, a series of (pro)mesogenic ligands (Lig) were prepared by systematically varying the chemical nature of the functional ligand entities. $CoFe_2O_4$@Lig MNPs (size 2.5 nm) yielded stable colloidal suspensions in 5CB and E7, respectively. As compared to pure 5CB, the $CoFe_2O_4$@Lig-5CB hybrids showed an increased sensitivity to the magnetic field, affecting the Fréedericksz transition. The coupling of the small, spherical MNPs with the LC director in the magnetic field suggests the formation of LC-induced, anisometric MNP clusters [5]. The interaction of the MNPs with the 5CB host and cluster formation was monitored by SAXS, SANS and by SQUID magnetometer measurements [6].

The understanding of this process supports the preparation of stable colloidal systems with well dispersed MNPs. In view of bigger MNPs, dendritic ligands equipped with mesogenic units may minimize the distortion of the ligand sphere and thus aggregation effects, and offer a promising approach for MNP-LC hybrids, in particular if the dendritic ligand itself exhibits liquid crystalline properties [7, 8].

Acknowledgments

The financial support by the DFG via SPP1681 (BE 2243/2 and BE 2243/3) are gratefully acknowledged.

References

[1] F. Brochard et al., Journal de Physique 1970, 31 (7), 691-708.
[2] A. Mertelj et al., Nature 2013, 504 7479, 237-241.
[3] T. Potisk et al., Phys. Rev. Lett. 2017, 119, 09780.
[4] T. Potisk et al., Phys. Rev. Lett. 2018, 97, 1, 0127.
[5] I. Appel et al., Chemical Phys. Chem. Chem. Phys., 2017, 19, 12127-12135.
[6] V. Gdovinova et al., Soft Matter 2017, 13, 7890-7896.
[7] M. Draper et al., Adv. Funct. Mater. 2011, 21, 1260–1278.
[8] M. F. Prodanov et al., Soft Matter 2016, 12, 6601-6609.

Capillary rheometer for magnetorheological fluids

S.M. Allebrandi[1], S.G.E. Lampaert[1], R.A.J. van Ostayen[1]

[1]*Delft University of Technology, Mekelweg 2, 2628 CD Delft, The Netherlands*

Introduction

The viscous behaviour of magnetic fluids at low shear rates ($<10^5 s^{-1}$) has been extensively discussed in literature. However, little is known about the behaviour at high shear rates($>10^5 s^{-1}$), [1]. The behaviour at these shear rates is crucial for improving the performance of industrial applications such as bearings and viscous dampers, [2].
Parallel plate or cone plate rheometers are often used to measure the magnetorheological effect. These concepts have a theoretical shear rate limit of about 10^5 s^{-1}. For example, bearing applications easily reach shear rates above 10^6 s^{-1}, which means that these measurement systems are not suitable to predict the behaviour at the operational range. Therefore, other concept, such as capillary or concentric cylinder rheometers, should be considered as solutions to reach the high shear rates. This paper presents the design of a capillary magnetorheometer capable of measuring magnetic fluids at shear rate over 10^6 s^{-1} under the influence of a homogeneous magnetic field.

Method

The analysed concepts for achieving high shear rates are: concentric cylinder, parallel plate, cone plate, slit capillary and round capillary. The physical limitations of these concepts identify their maximum performance. The best candidate, taking into account the feasibility of applying a magnetic field, determines the principle used in the design. The concepts are limited by radial migration, secondary flows, turbulence and viscous heating. Figure 1 presents the calculated maximum shear rates of the analysed concepts for a kerosene carrier fluid at a common characteristic gap height of 50µm.

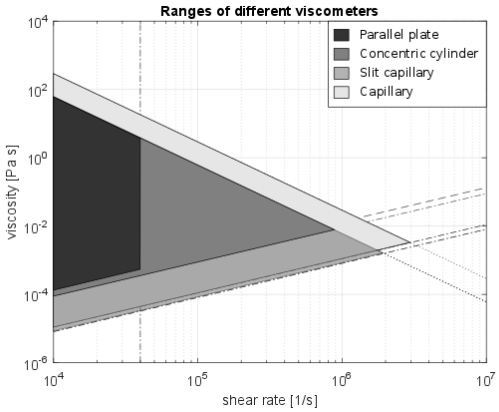

Figure 1: Theoretical performance of different measuring principles at a characteristic gap height of 50µm for kerosene.

Setup

The best performing concepts are capillary devices as they reach high shear rates with a reasonable gap height. Furthermore, their linear design simplifies the application of homogeneous magnetic fields. In addition, the continuous flow of new fluid minimizes the heat developed by viscous heating. A slit capillary prototype is used as rectangular microchannels are relatively simple to manufacture.

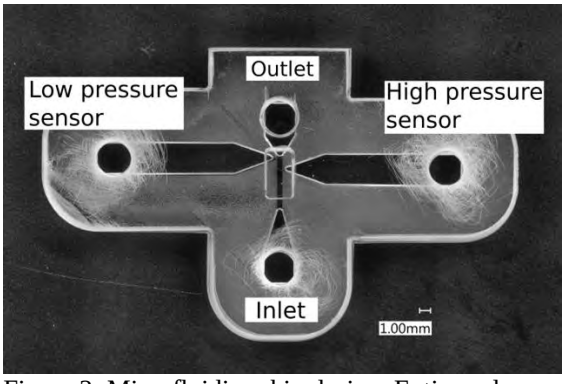

Figure 2: Microfluidics chip design. Entire volume is filled with the measured medium. The fluid is forced from inlet to outlet. The pressure drop between high and low pressure channels is measured.

A produced prototype demonstrates the potential of the designed device. The fluid flows through a 4 mm long microchannel

with a gap height of 30 µm. Figures 2 and 6 presents the prototype which measures the pressure drop over a 1mm length. Measurements with deionised water, Shell Tellus VX15 oil and EFH1 ferrofluid validate respectively the maximum shear rate, the accuracy and the ability to measure magnetic fluids.

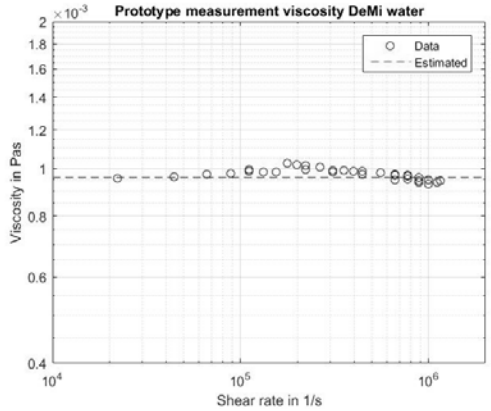

Figure 3: Viscosity vs. shear rate plot of the deionized water measurement.

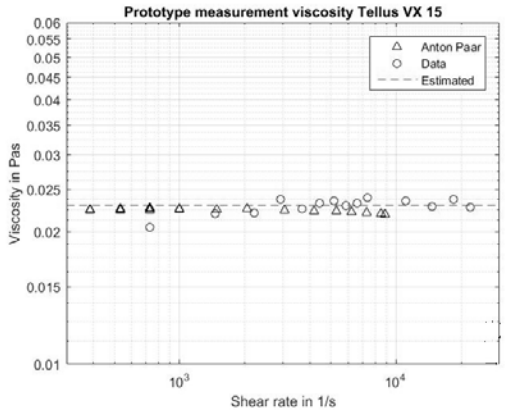

Figure 4: Viscosity vs. shear rate plot of the Tellus VX15 measurement.

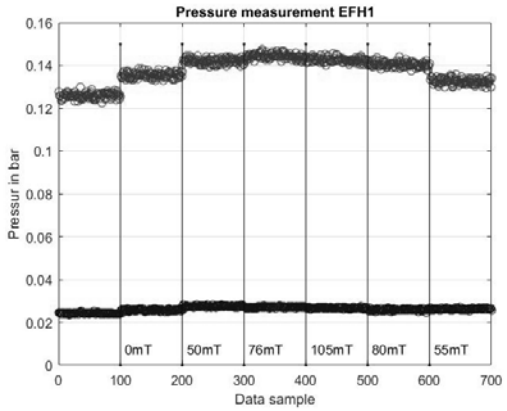

Figure 5: Pressure steps caused by magnetorheological effect of EFH1 due to external magnetic field.

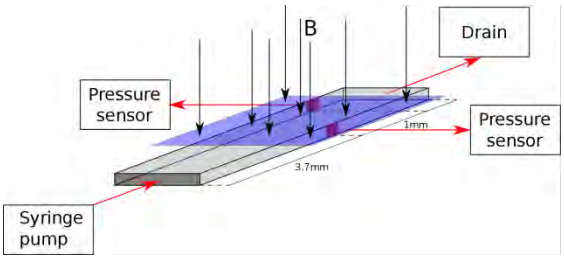

Figure 6: Sketch of measurement setup.

Results

The deionised water test reached a shear rate of 1.16e6 s^{-1} with an accuracy of <8% to the estimated viscosity of deionised water (figure 3). The measurement could not reach higher shear rates due to the stalling of the syringe pump used.
Figure 4 presents the measurement with Shell Tellus VX 15 oil. The viscosity is validated using an Anton Paar MCR2 rheometer. The resulting accuracy of the prototype for the oil is <8%.
Figure 5 presents the measurement with the magnetorheological behaviour using the ferrofluid EFH1. The graph shows small increases in pressure, thus increases in viscosity, due to the magnetic field.

Conclusions

A high shear rheometer capable of measuring magnetorheological fluids is designed, built and demonstrated. The device measures the viscosity with an accuracy of 8% over a range of 10^4 s^{-1} to 10^6 s^{-1}.

References

[1] Wang, Xiaojie & Gordaninejad, Faramarz. (2006). Study of magnetorheological fluids at high shear rates. Rheologica Acta. 45. 899-908.

[2] Baranwal, D & Deshmukh, T.S. (2012). MR-Fluid Technology and its application- A Review. International Journal of Emerging Technology and Advanced Engineering 2. 563-569.

Field-Induced Deformation of Nanorod/Hydrogel composites

K. Birster, R. Schweitzer, C. Schopphoven, A. Tschöpe

Universität des Saarlandes, Experimentalphysik, Campus D2.2, 66123 Saarbrücken

Introduction

Shape-changing smart materials are able to reversibly deform in response to an external stimulus such as temperature, pressure, an electric or magnetic field [1,2]. An evident application is their use as active components in soft microactuators.
In the present study, we used ferromagnetic single domain nanorods as magnetic phase in soft polyacrylamide (PAM) hydrogels. We investigated the deformation of two macroscopic composite cylinders that are distinguished by their spatial distribution of the anisotropy axes. Magnetic fields with different geometries were applied during the crosslinking process of the hydrogel to imprint homogeneous or spatially modulated magnetic anisotropies. The field-induced torsion or bending deformation of the composite filaments was measured by video microscopy.

Methods

Nickel nanorods were synthesised by pulsed electrodeposition of nickel into a nanoporous AAO template [3]. After dissolution of the oxide layer, the colloidal suspension was electrostatically (pH8) and sterically stabilised using polyvinylpyrrolidon and polyacrylic acid as surfactant.
Basic physical properties of the nanorods were obtained by transmission electron microscopy, magnetization measurements, static [4] and oscillating field [5] optical transmission measurements.
Composite cylinders of Ni nanorods in a polyacrylamide hydrogel matrix were prepared by filling the nanorod/PAM precursor mixture into a PTFE tube of 1-2 mm inner diameter. During the polymerisation process, the nanrods were aligned in a static magnetic field of predefined geometry. In particular, a spatially modulated field with nearly constant magnitude and periodically changing direction into one half-space perpendicular to the cylinder axis was generated by a specific arrangement of permanent magnets. The field profile was measured using Hall probes which were mounted on motorized translation stages.
The composite cylinders were fixed at the upper face and either encapsulated to prevent evaporation of water from the hydrogel or completely suspended into water to profit from the hydrostatic uplift. The composite cylinder was placed between the pole pieces of an electromagnet. The deformation as function of the magnetic flux density was recorded by a video camera and evaluated using LabVIEW image analysis.

Results

Preceding characterization of the nanorods by TEM imaging revealed a mean length L=250 nm and a mean diameter D=22 nm.
From the mean magnetic moment $m = 3.7 \cdot 10^{-17}$ Am² and the magnetic anisotropy constant $K_a = 65$ kJ/m³ a maximum torque of $\approx 5 \cdot 10^{-18}$ Nm per nanorod can be estimated. A significant macroscopic deformation required an adjustment of the hydrogel shear modulus G≈1–5 kPa to the total torque at the volume fraction $\varphi = 4.3 \cdot 10^{-5}$ of nanorods. The distribution of the local torque within the composite, which is determined by the

local magnetic anisotropy, controls the specific deformation pattern.
Homogeneous alignment of the nanorods perpendicular to the cylinder axis results in a field dependent torsion in a transversal field, Figure 1. The macroscopic torsion angle Ω showed a nonlinear behaviour and was larger at increased deflection of the texture axis. Both the field- and orientation dependent torsion could be modelled quantitatively using a continuum model with volume-distributed torques calculated using the Stoner-Wohlfarth model. The finite magnetic anisotropy of the nanorods implies a maximum in the field-dependent torsion, which was confirmed experimentally.

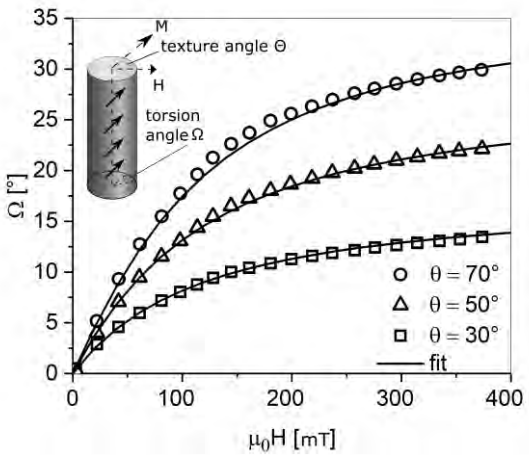

Fig. 1) Torsion angle Ω as function of the magnetic flux density and varying initial texture angles θ.

A more complex spatially modulated alignment of the anisotropy axis into one half-space (see arrows in Figure 2a) caused a sinusoidal bending of the composite filament, Figure 2. This example demonstrates the potential of tuning the field induced deformation of magnetic composites which will be extended to 2D multilayers.

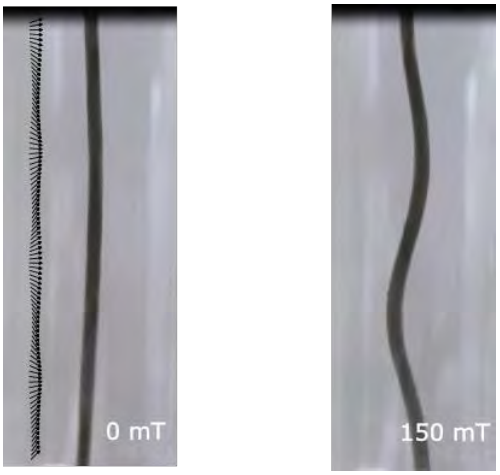

Fig. 2: a) PAM/nanorod composite cylinder in zero field and profile of the magnetic field during polymerization, b) bending deformation induced by a homogeneous transversal magnetic field.

Acknowledgments

We acknowledge financial support by the DFG Priority Program 1681 (grant TS62/4-3).

References

[1] M. Zrinyi, L. Barsi and A. Buki; J. Chem. Phys. 104 (21) (1996), 8750.
[2] J. Kim, S. Chung. S.E. Choi, H. Lee, J. Kim and S. Kwon, S; Nature Mat. 10 (2011), 747.
[3] P. Bender, A. Günther, A. Tschöpe and R. Birringer; JMMM 323 (2011), 2055.
[4] F. Krämer, M. Gratz and A. Tschöpe; J. Appl. Phys. 120 (2016), 044301.
[5] A. Tschöpe, K. Birster, B. Trapp, P. Bender and R. Birringer; J. Appl. Phys. 116 (2014), 184305.
[6] C. Schopphoven and A. Tschöpe, J. Appl. Phys. D 51 (2018), 115005

Influence of the structural anisotropy on the magnetization of magnetorheological elastomers

D. Borin, E. Dohmen, B. Kraus, S. Odenbach

TU Dresden, Institute of Fluid Mechanics, Dresden 01062

Magnetorheological (MR) materials are composites of magnetically soft microparticles dispersed in a carrier medium, which typically is a liquid (MR fluid) or a solid elastic matrix (MR elastomer) [1]. Conventionally, the powder suspended in the matrix of a MR material is carbonyl iron which is a material without magnetic hysteresis. However, magnetically hard powder can be as well used in order to provide a passive tuning of MR elastomers [2]. Under applied external magnetic field, the particles of a MR composite become magnetized and can form aggregates elongated in the direction of the field. The aggregation of particles results in a change of the physical properties of the material. Moreover, it is possible to tune an anisotropy of MR elastomers orienting the particles with an external magnetic field applied during the matrix cross-linking process.

In the current work we experimentally analyze magnetic properties of the anisotropic MR elastomers. The primary goal of the investigation is an evaluation the field-angle dependency of the composites magnetization. The samples considered in this study are highly filled with magnetically soft carbonyl iron powder (ϕ~40 vol. %, diameter of particles ~5 μm). In the experiments we use the Lake Shore 7407-S Vibrating Sample Magnetometer. Anisotropic elastomer samples during the measurements are positioned between electromagnetic coils of the magnetometer with structures oriented at various angles to an externally applied magnetic field. Figure 1 shows normalized magnetization curves of the differently oriented anisotropic sample as well as a magnetization curve of the isotropic composite manufactured of identical components. Influence of the structural anisotropy on the magnetization of the composite is obviously demonstrated. Detailed results and corresponding discussion will be presented during the workshop.

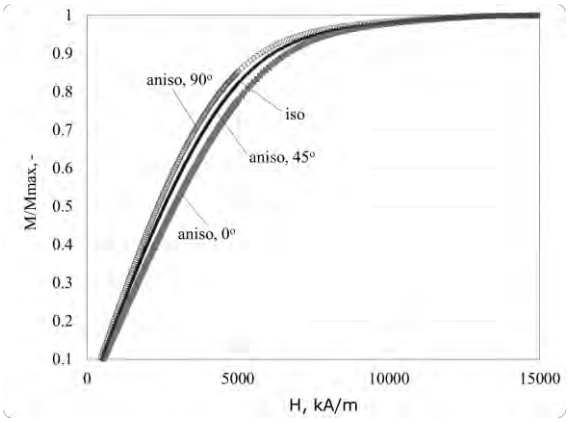

Figure 1. Normalized magnetization curves of the anisotropic sample with structures oriented at various angles (0°, 45 °, 90 °) to an external field H and of the isotropic composite (iso).

Acknowledgments

Financial support by DFG (Deutsche Forschungsgemeinschaft) under Grant Bo 3343/2-1 within SPP 1681 providing the basis for our investigations is gratefully acknowledged.

References

[1] Norman M Wereley, editor. Magnetorheology. RSC Smart Materials. The Royal Society of Chemistry, 2014.

[2] Borin D Yu, Stepanov G V, Odenbach S (2013) J Phys Conf Ser 412(1):012040.

Jump-like behavior of magnetically doped polymer solution in temperature dependent magnetization measurements

S. Webers[1], M. Hermes[2], J. Landers[1], A. M. Schmidt[2] and H. Wende[2]

[1] *Fakultät für Physik, Center für Nanointegration Duisburg-Essen (CENIDE), Universität Duisburg-Essen, Lotharstraße 1, D-47057 Duisburg*
[2] *Department Chemie, Institut für Physikalische Chemie, Universität zu Köln, Luxemburger Str. 116, D-50939 Köln*

Introduction

Temperature dependent magnetization measurements can reveal information on phase transitions and characteristic jump temperatures of polymer solution doped with magnetic nanoparticles.
Here we investigate the characteristic temperatures of a polymer water solution, in which polyethylene glycol (PEG) with various polymer lengths and concentrations were used to tailor the complexity of the system by entanglement formation [1].

Method

Therefore, a SQUID magnetometer was used to record the temperature dependent magnetization from 5-350 K at different applied magnetic fields of 0.4 up to 10 mT following a zero field cooled-field cooled (ZFC-FC) protocol.

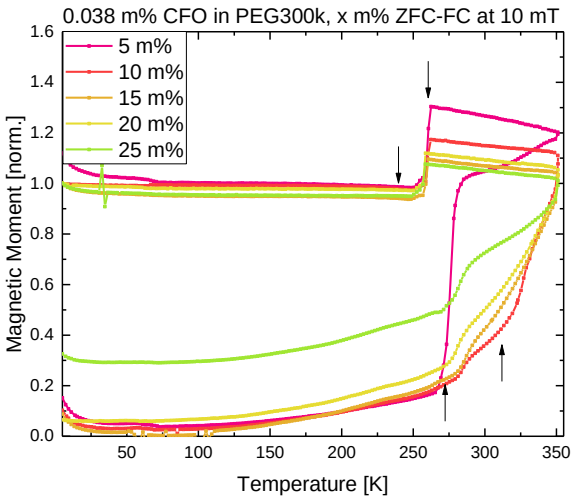

Figure 1: The ZFC-FC curves for 0.038 m% CFO particles in the polymer solution of PEG300k with polymer concentrations from 5-25 m%. A double-step like jump is observed in ZFC and FC branch.

Magnetic Nanoparticles in polymer solution

Monodisperse cobalt ferrite nanoparticles with a magnetic core diameter of 17.3 nm were used as tracer particles. As a reference sample, cobalt ferrite particles were dispersed in pure water solution and measured under the same ZFC-FC conditions. Since the degree of the PEG complexity plays an important role for the particle mobility in such solutions [2], the polymer concentration was tuned from low to high content to influence the sample's viscosity. Further the polymer length was changed from 4k $gmol^{-1}$ to 300k $gmol^{-1}$ resulting in different ratios of polymer lengths to the particle size. A third parameter which was modified is the particle concentration. We suggest a structure formation of particles which also influences the diffusive mobility of the particles in solution. The possibility of particle chain formation is increased by a higher particles content.
This can be observed either in the PEG concentration dependent (see. Fig. 1) or in the field dependent (see Fig. 2) ZFC-FC measurements. Up to 200 K the ZFC and FC branch is constantly splitted. Between 200 K and 350 K the melting and freezing temperature shows a double step like behavior which is more pronounced for highly doped polymer solutions. The difference of the melting and freezing temperature reveals a supercooling of the solution.

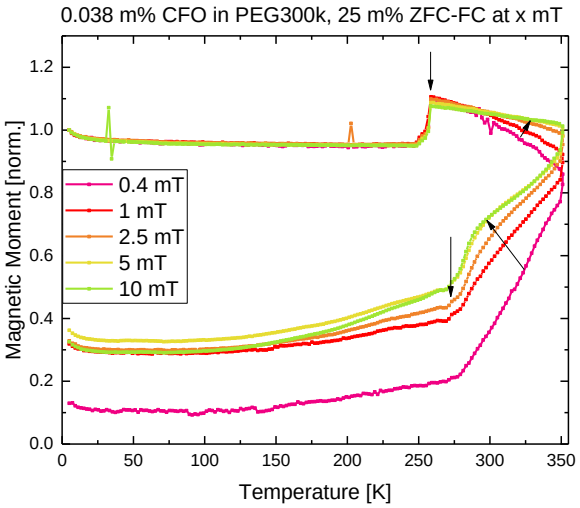

Figure 2: The field dependent zero field cooled-field cooled curves for 0.038 m% CFO particles in the polymer solution of PEG300k, 25 m%.

Acknowledgments

This work was supported by the DFG priority programme SPP1681 (WE2623/7-3) and by the research unit FOR1509.

References

[1] E. Roeben et al., Colloid Polym Sci (2014) 292, 2013-2023.

[2] P.-G. de Gennes, Scaling Concepts in Polymer Physics, Cornell University Press (1979).

Dynamics of magnetic nanoparticles in Newtonian and viscoelastic media

H. Remmer[1], M. Hermes[2], T. Kahmann[1], A. M. Schmidt[2], M. Schilling[1], and F. Ludwig[1]

[1]*Institut für Elektrische Messtechnik und Grundlagen der Elektrotechnik, TU Braunschweig, Hans-Sommer-Str. 66, D-38106 Braunschweig*
[2] *Institute of Physical Chemistry, Universität zu Köln, Köln*

The dynamics of magnetic nanoparticles (MNP) play an important role for many applications, such as magnetic hyperthermia and homogeneous MNP-based bioassays. In addition, the measurement of the dynamic magnetic properties of the MNP provides information on their embedding in and interaction with the matrix, proposed that the MNP are thermally blocked.
To study the MNP dynamics in various matrices, we apply ac susceptometry (ACS) as well as measurements in a rotating magnetic field (RMF). As matrix systems we exemplarily investigate Newtonian fluids like water and glycerol as well as more complex viscoelastic media such as gelatin. The utilized ACS setup, which was originally designed for RMF measurements involves two Helmholtz coil pairs, allowing one e.g. to use the second coil for the application of an additional dc field perpendicular to the ac field.

The imaginary parts of ACS spectra for a suspension of FeraSpin XL multi-core particles (nanoPET pharma GmbH) in different water-glycerol mixtures are shown in Fig. 1. Despite the rather complex changes of the ACS spectrum with increasing viscosity, the generalized Debye model allows one to extract the dynamic viscosity in very good agreement with the theoretical expectation.

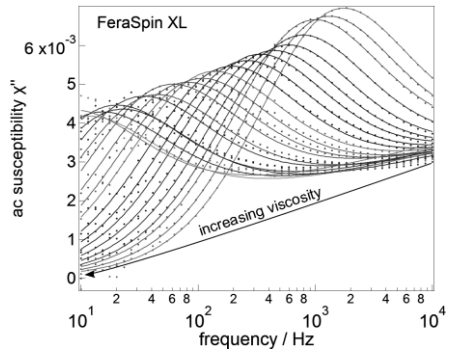

Figure 1: Imaginary parts of ACS spectra for samples with FeraSpin XL particles in different water-glycerol mixtures. Brown peaks shift to lower frequencies with increasing viscosity.

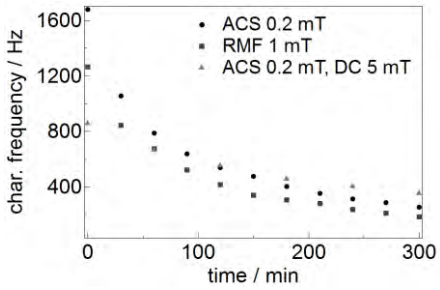

Figure 2: Characteristic frequencies of ACS spectra in different modes for sample with $CoFe_2O_4$ particles dispersed in aqueous gelatin solution (2.5 w%) over time.

ACS measurements of the gelation process of aqueous gelatin solutions of $CoFe_2O_4$ single-core particles – after rapidly cooling the sample down from 313 K to 296 K – indicate a complex behavior. Qualitatively similar progress in the variation of the characteristic frequency (maximum of the imaginary part of ACS spectrum) was observed when applying an ac, oscillating or rotating magnetic field (Fig. 2).
Viscoelastic parameters such as viscosity and shear module can be extracted applying the Voigt-Kelvin model.

Acknowledgments

Funding by the Deutsche Forschungsgemeinschaft, DFG Priority Program 1681 is gratefully acknowledged (LU800/4-3, SCHM1747/10-3).

A magnetorelaxometry setup for measurements at high excitation fields in the presence of a transverse DC bias field

M. Liebl, R. Körber, P. Hömmen, D. Eberbeck and F. Wiekhorst

Physikalisch-Technische Bundesanstalt, Abbestrasse 2-12, D-10587 Berlin, Germany

Introduction

Magnetorelaxometry (MRX) has been proven a valuable tool to characterize, quantify and image magnetic nanoparticles (MNP) for several biomedical applications in therapy and diagnosis. Besides basic magnetic characterization of MNP, the probing of a biological or physiological environment by changes of the magnetic behavior of MNP is of growing interest. MRX measures the magnetization decay of the MNP moments after their (partial) alignment by an external magnetic field of an amplitude below 5 mT. Higher magnetic excitation fields would increase the sensitivity for detecting MNP. Furthermore, as recently demonstrated in a theoretical work [1] MRX could benefit by using an additional DC bias field to gain information about the MNP's viscoelastic corona. Here, we experimentally explore the applicability of high excitation fields (up to 60 mT) and an additional static offset field (>1 mT) in MRX. In contrast to the excitation field, the static field is applied during the detection of the relaxation of the MNP by a highly sensitive Superconducting Quantum Interference Device (SQUID). Since the bias field amplitude (mT) is several orders of magnitude larger than the tiny MRX signals (nT), special care has to be taken to stabilize and gradiometrically compensate their coupling into the SQUID sensor.

Material and Methods

The setup for MRX measurements in additional DC bias fields is depicted in figure 1. It comprises of an excitation coil of d=20 mm inner diameter having a flux-to-current ratio of 3.3 mT/A connected to a current source providing up to I=20 A. A fast switch-off circuit allows to detect the MNP relaxation after a dead time of a few 100 µs. Additionally, a Helmholtz coil arrangement generates the DC bias field up to 1.25 mT aligned perpendicular to the magnetizing field coil and the SQUID. Therefore, the DC bias field at the SQUID sensor is suppressed by several orders of magnitude. We used a MNP sample containing 1.72 ml of MNP (Berlin Heart GmbH, Germany, c(Fe)=3.6 mg/ml) immobilized in a gypsum matrix. The sample was magnetized for t_{mag}=1 s at different magnetizing fields B_{mag} up to 66 mT in the presence of a constant DC bias field B_{trans} ranging from 0 to 1.5 mT and subsequently, the MNP relaxation was detected for t_{meas}=1 s after a dead

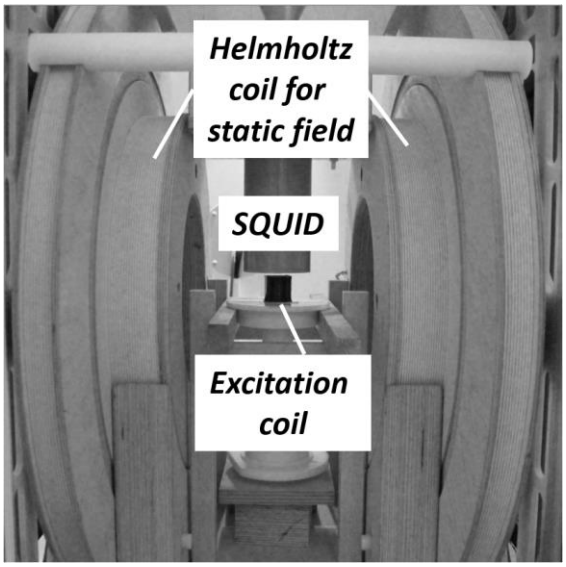

Figure 1: Photograph of the setup for field dependent MRX measurements. The MNP sample is placed inside an excitation coil underneath a SQUID sensor. A Helmholtz coil arrangement provides an additional static offset field parallel to the SQUID sensing area.

time of 200 µs (recovery time of the SQUID electronics). The resulting MRX curves were parametrized using a stretched exponential to determine the characteristic relaxation time $t_{1/e}$, i.e. the time interval after which the MRX amplitude has dropped to 36.7% of its starting value.

Results

We first varied the MRX excitation field B_{mag} in the absence of a DC bias field. The effective relaxation time $t_{1/e}$ exponentially decreases with increasing B_{mag} as depicted in figure 1. A saturation of $t_{1/e}$ at 55% of the initial relaxation time is reached for excitation fields above 20 mT.

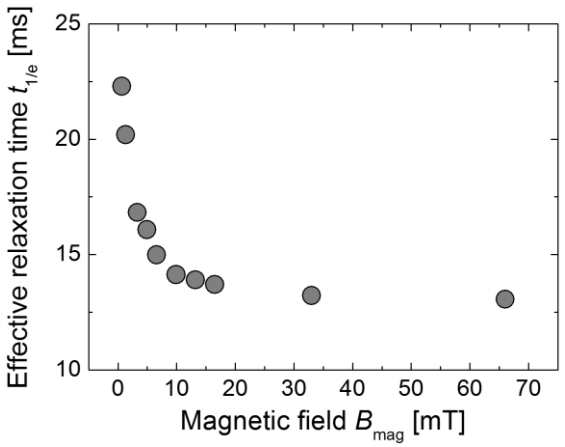

Figure 2: Relaxation time $t_{1/e}$ as a function of the magnetic excitation field B_{mag}.

Then, we considered the relaxation of the sample at B_{mag}=3.3 mT and different DC bias field amplitudes B_{trans} between 0.01-1.25 mT. The effective relaxation time $t_{1/e}$ decreases with increasing B_{trans} as shown in figure 3. Since technically the available range of B_{trans} was much smaller than for B_{mag}, no saturation of $t_{1/e}$ was observed.

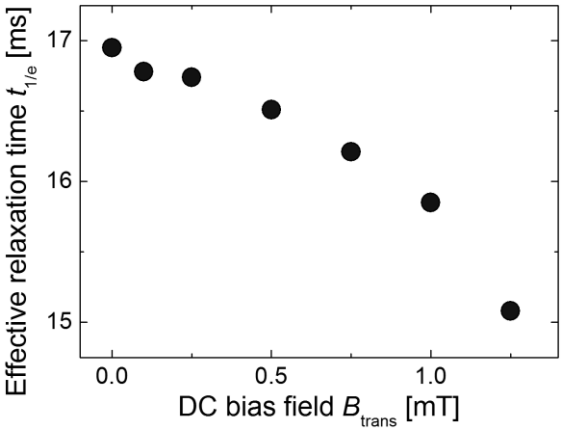

Figure 3: Relaxation time $t_{1/e}$ as a function of the DC bias field B_{trans} and magnetizing field B_{mag}=3.3 mT.

Discussion and Conclusion

A clear decrease of the effective relaxation time (and increase of the magnetic moment) was observed with increasing excitation field. This indicates that magnetically smaller structures fall in the MRX measurement window by increasing the excitation field. In good agreement with previous AC susceptibility measurements [2], a decreasing relaxation time (and magnetic moment) was observed with increasing DC bias field. Hence, we demonstrated the feasibility of MRX with high magnetic excitation fields and in the presence of a DC bias field. In the future, this MRX field dependency might allow to gain more specific information about the physiological or biological environment of MNP.

Acknowledgments

Financial support by the DFG priority program SPP1681 (WI4230/1-2) is gratefully acknowledged.

References

[1] V. Rusakov, Y. Raikher: Magnetorelaxometry in the Presence of a DC Bias Field of Ferromagnetic Nanoparticles Bearing a Viscoelastic Corona, Sensors **18**, 1661, 2018.

[2] J. Dieckhoff, D. Eberbeck, M. Schilling, F. Ludwig: "Magnetic-field dependence of Brownian and Néel relaxation times", J. Appl. Phys. **119**, 43903, 2016

Six-channel magnetorelaxometry device for characterization of magnetic nanoparticles in a laboratory environment

P. Radon, M. Liebl, D. Gutkelch, F. Wiekhorst

Physikalisch-Technische Bundesanstalt, Berlin, Germany

Introduction

Magnetic nanoparticles (MNP) are the major component in the development of many novel biomedical applications such as magnetic drug delivery, magnetic hyperthermia, bioanalytics, and diagnostic imaging. The efficiency of these applications vitally depends on the structural and magnetic MNP properties (e.g. magnetic moment distribution, colloidal stability, hydrodynamic size distribution, binding on biological targets).
This requires ongoing characterization of MNP, not only during their development but also afterwards to ensure quality and safety of these MNP based applications.
For this purpose, several highly sophisticated measurement techniques are available. One of them is Magnetorelaxometry (MRX) where the time dependent magnetic response of the MNP sample after switching-off a polarizing magnetic field is detected employing highly sensitive magnetic field sensors. MRX has been proven to be well suited for magnetic characterization of MNP and additionally, their specific quantification in biological systems with outstanding detection limits down to a few nanogram [1]. For measuring tiny MRX amplitudes down to 10^{-15} T, typically occurring for MNP concentrations in biomedical applications, the operation of superconducting quantum interference devices (SQUIDs) as magnetic sensors in a magnetically shielded environment is mandatory.
In this work, we enhanced an existing six-channel SQUID system (Figure 1) by a magnetizing unit and a dedicated sample support to enable high precision MRX measurements of small MNP samples in a conventional laboratory environment.

Setup of the laboratory MRX device

The system originally was developed for magnetically detecting heart signals (magnetocardiograms) in mice [2] and consists of a liquid helium Dewar vessel with a horizontal cylindrical warm bore of 700 mm length and 27 mm diameter. Six SQUID sensors circularly surrounding the center of the warm bore at a cold warm distance of 16 mm detect the magnetic fields perpendicular to the bore axis. Warm bore and SQUID sensors are enclosed by a superconducting niobium cylinder for shielding of magnetic interferences.

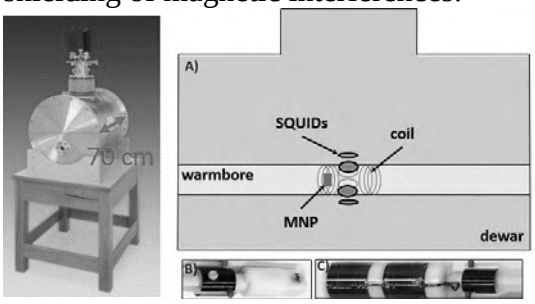

Figure 1: *Left: 6-channel SQUID measurement system with integrated superconducting shield for magnetocardiography on mice. Right: Scheme of system extension consisting of magnetizing unit (two coils left and right symmetrically to SQUIDs) and sample support to insert samples in one of the magnetizing coils at a defined and reproducible position.*

For MRX measurements we developed a magnetizing support which is inserted into the warm bore of the device. It consists of a magnetization coil (Figure 1C) to provide magnetic fields up to 4 mT (parallel to bore axis) that can precisely be adjusted to the SQUID sensors by a micrometer screw, so that the detection of magnetizing fields from the coil by the sensors is strongly suppressed. A second insert (Figure 1B)

was developed to accurately and reproducibly position MNP samples (volumes up to 150 µL) within the coil close with a defined distance to the SQUID sensors.

Characterization of the laboratory MRX device

Noise measurements without sample showed no distortions from power line or (electro-) magnetic interferences due to the outstanding performance of the integrated superconducting shied. The residual magnetic fields in the warm bore are below 100 nT, we measured a SQUID noise floor level of 5 fT/√Hz without sample. No mechanical vibrations in the noise spectra were visible proving the compact building design of about 50 kg weight.

After adjusting the magnetizing unit inside the warm bore to the optimum coil to sensor position by a micrometer screw a total gradiometric attenuation of the magnetizing field of about 80 dB at the sensors was achieved. Furthermore, the detection of MRX signals could start 200 µs after switching off the magnetizing field, already. This is the intrinsic switching time of the SQUID electronics; no ringing of the magnetizing coils was observed in this well-balanced arrangement.

We analyzed the performance of our device in a conventional laboratory environment by MRX measurements of the commonly used MNP system fluidMAG-D (chemicell GmbH, Germany). We measured samples of 60 µL volume at different concentrations in the fluid and immobilized state (Figure 2). The same samples were additionally measured with the PTB one-channel MRX system operated in the Berlin magnetically shielded room. The results showed that the shielding of the six-channel SQUID system is more robust against magnetically and electrically interferences. This leads to an improved signal to noise ratio of the relaxation curves and finally, a higher sensitivity for detection of MNP in our new system.

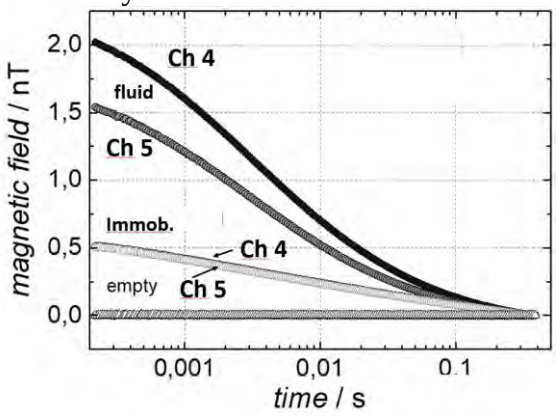

Figure 2: *Examples of measured relaxation curves of fluidMAG-D in a fluid and immobilized state together with the background signals for two selected SQUIDs (Ch 4 and Ch 5).*

Conclusions

Our transportable MRX device allows the comfortable and sensitive characterization of MNP in laboratory environment without need of an additional magnetically shielded room, but with at least the same sensitivity and performance as with the existing one-channel MRX system to be operated in the Berlin magnetically shielded room. By using faster SQUID electronics even shorter relaxation processes should become detectable increasing the range of applicability of MRX for MNP characterization.

Acknowledgments

This work was supported by Deutsche Forschungsgemeinschaft (DFG) in the framework of the priority program 1681 (WI4230/1-2) and within the PTB Core Facility for the Measurement of Ultra-Low Magnetic Fields.

References

[1] F. Wiekhorst et al., Pharm. Res., vol. 29, no. 5, pp.1189-1202, 2012.

[2] R. Ackermann et al., IEEE Trans. Magn., vol. 17, no. 2, pp.827-830, 2007.

Magnetic nanoparticle uptake by endothelial cells seen through the eyes of magnetic particle imaging (MPI)

H. Paysen[1], M. Schleicher[2], N. Loewa[1], A. Ludwig[2], F. Wiekhorst[1]

[1] *Physikalisch-Technische Bundesanstalt, Berlin, Germany*
[2] *Charité –Universitätsmedizin Berlin, Center for Cardiovascular Research, Berlin, Germany*

Magnetic nanoparticles (MNP) are a class of nanomaterials with great features for biomedical applications. Especially in cell-based diagnostics and therapies, the use of MNP showed promising results, e.g. for the visualization of atherosclerotic lesions [1]. For many of these applications, an effective imaging technique is needed, which is capable of determining the position and quantity of the MNP.

A possible candidate for this purpose is magnetic resonance imaging. This imaging technique relies on the measurement of the net magnetization generated by water protons, which precess in a homogenous magnetic field. The presence of MNP near these protons lead to a faster transversal signal decay. This can be observed as a negative contrast in the MR image. However high MNP concentrations might lead to imaging artifacts. Furthermore, a clear distinction of MNP in different biomedical environments (blood flow, extracellular/intracellular binding) is not possible. Moreover, imaging techniques allowing for distinction between healthy and pathological tissue would be highly desirable.

Magnetic particle imaging (MPI) is a rather young imaging modality based completely on the imaging and quantification of MNP. Combined static and dynamic magnetic fields are used, which generate a signal from the MNP based on their non-linear susceptibility. By solving an inverse problem, the MNP distribution can be calculated. The generated signal is highly specific and is dependent on the local environment of the particles (temperature, viscosity, binding state). Recently, it has been shown that this information can be included in the reconstruction algorithm, which makes MPI capable to discriminate between different particle types or different mobility states (fluid and immobilized) [2], a technique termed multi-color MPI.

Previously, we found that the dynamic magnetic MNP response changes depending on their biological environment [3], [4]. Here, we included this information in the reconstruction algorithm, similar to multi-color MPI. This allows us to generate multiple MPI images out of solely one measurement, weighted for MNP in different environments. To this end, we investigated the capability to distinguish free MNP in an aqueous solution and a cell-bound MNP after cellular contact. Two individual MPI system functions (SF) were acquired and combined for the image reconstructions. SFs are measured by placing a tiny MNP sample volume at multiple positions inside the field of view (FOV) to obtain reference signals. The first SF was acquired of a 2 µL fluidMAG CT50 (Chemicell GmbH, Germany) suspension at an iron concentration of 0.317 mol/L, while for the second SF a reference sample containing $1.5 \cdot 10^6$ endothelial cells (EA.hy926) loaded with CT50 (about 20 pg/cell) was used. A phantom consisting of a fluid CT50 sample placed next to a second cell sample (also about $1.5 \cdot 10^6$ cells) was then measured and used for the MPI image reconstruction (Fig 1a). The total data acquisition time was 2 s. Image reconstructions were performed with the regularized Kaczmarz algorithm using 2000 frequency components, 30 iterations and a relative regularization parameter of 0.1.

The reconstructions with the combined SF yield two images, which are sensitive for signals generated by free MNP and signals generated by cell-bound MNP, respectively. Therefore, the two samples can clearly be distinguished in both reconstructions based on the same, single measurement (Figure b, c). Only small residual signal intensities, of the other sample can be found in both reconstructions, which could be eliminated by optimizing the reconstruction parameters. In conclusion, this shows the high potential of MPI to map the biomedical environments of the MNP in vivo. We think, this technique can be used to image and quantify the cellular uptake of MNP into endothelial cells. This could be highly beneficial to gain additional information about the uptake mechanisms of cells and might be used to detect pathological changes in the target region. In general, this opens the way for functional MPI as a powerful diagnostic tool to detect changes on a (sub)cellular scale.

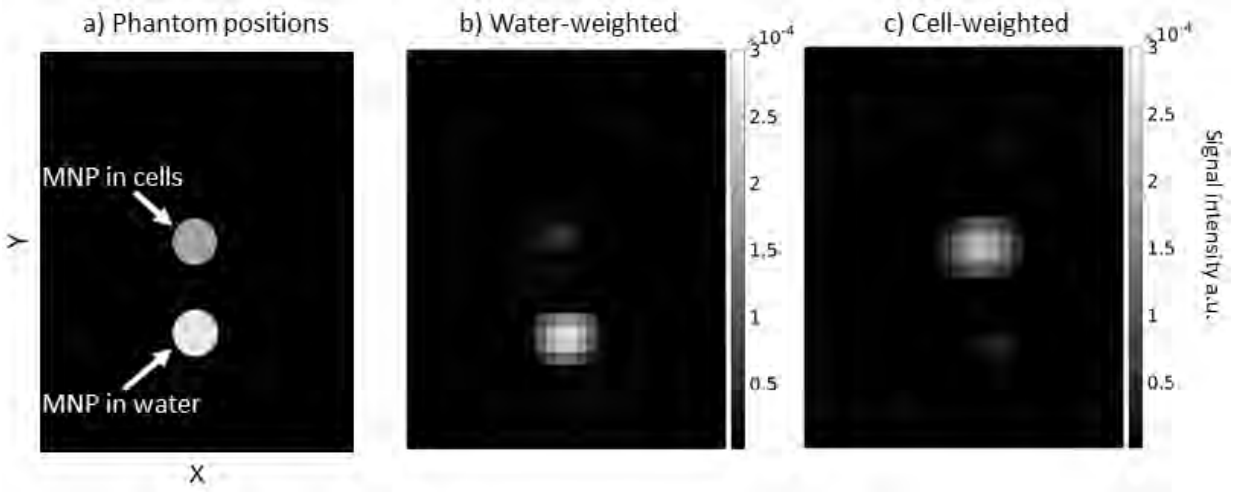

Figure: *a) Nominal phantom positions of the cell (dark grey) and the liquid sample (light greay) in the FOV. Maximum intensity projections along the z-axis of the reconstructed MPI images based on the same measurement, weighted for free MNP (b) and cell-bound MNP (c).*

Acknowledgments

This project was supported by the DFG research grants "AMPI: Magnetic particle imaging: Development and evaluation of novel methodology for the assessment of the aorta in vivo in a small animal model of aortic aneurysms" SHA 1506/2-1, "quantMPI: Establishment of quantitative Magnetic Particle Imaging (MPI) application oriented phantoms for preclinical investigations" 1 FKZ TR 408/9-1.

References

[1] W. C. Poller et al., Nano Res., vol. 9, no. 11, pp. 3437–3452, Nov. 2016.

[2] J. Rahmer et al., Phys. Med. Biol., vol. 60, no. 5, pp. 1775–1791, 2015.

[3] N. Loewa et al., IEEE Trans. Magn., vol. 49, no. 1, pp. 275–278, Jan. 2013.

[4] N. Löwa et al., J. Magn. Magn. Mater., vol. 427, pp. 133–138, Apr. 2017.

Magnetic Hyperthermia: A hands free option to trigger phase transitions in thermoresponsive matrices

N. Lucht[1], C. Pelz[1], B. Fischer[1]

[1] *University of Hamburg, Department of Physical Chemistry, Grindelallee 117, 20146 Hamburg*

Hyperthermia is a term that describes a locally elevated temperature in the body of mammals due to an external influence. In magnetic particle science the term was borrowed to describe the excitation of particles utilizing an alternating current magnetic field. In this work we present first results of introducing our system into a high frequency coil setup to examine the response of the system.

The transfer efficiency of the field energy to heat is generally described as the specific absorption rate (SAR) which can be described using the following formula:

$$\mathrm{SAR} = P = \frac{\mathrm{c}}{\mathrm{m}} \cdot \frac{\Delta T}{\Delta t}$$

With the heat capacity of the container *c*, *i.e.* water, the mass of the magnetic material *m* and the time dependent temperature slope of the AC-field heating. The temperature is measured directly in solution with an infrared camera mounted on top of the samples. The concentration dependent SAR can be derived from Figure 1 and follows a nearly linear trend, as expected. A quick comparison with recent literature shows that our particle system has comparably high absorption rates even in a very weak magnetic field of 1.93 $\mathrm{kA \cdot m^{-1}}$ and a for cobalt ferrite ineffective field frequency of 243 kHz.[1] While cobalt ferrite itself, even when not encapsulated, is only moderately cytotoxic it is imperative for possible future applications in the medical sector for the particle concentration to be as low as possible as nanoparticles in general tend to accumulate in organs.[2] In our standard procedure – as presented prior – we coat our particles with a stabilizing silica shell and coat them with a hydrogel consisting of crosslinked *N*-isopropylacrylamide (pNIPAM).

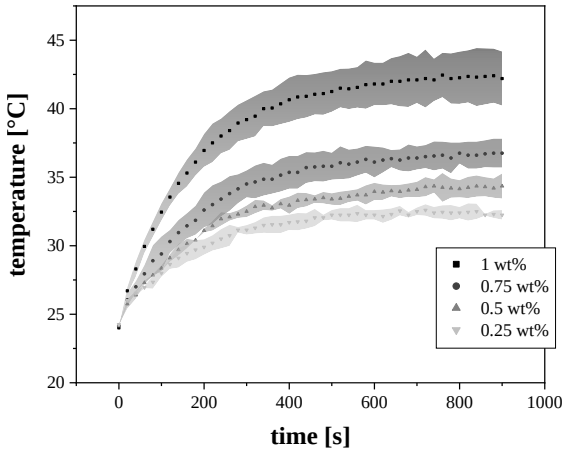

Figure 1: Time dependent heating curves of different particle concentrations of Cobaltferrite in a weak high frequency magnetic field with 1.93 kA · m^{-1} at 243 kHz. The uncertainty is depicted as colored clouds around the mean value.

In low concentrations pNIPAM shows little to no cytotoxicity.[3] Paired with the thermoresponsive behavior it is a preferential material to be used in biological applications. While we have by no means the ability to assess the actual biocompatibility of our system we can at least roughly estimate a sufficient tolerance of our particle system in low concentrations.

pNIPAM is a thermoresponsive material which can swell with water and above its lower critical solution temperature (around 34°C) it undergoes a coil-to-globule transition and expels the water. In combination with the magnetic response of the incorporated ferrite particles this transition can be triggered by applying an ac-field.

In the next steps we want to increase the particle to gel ratio to increase the effectiveness of heating while keeping the gel concentration stable.

Acknowledgments

The author thanks Hilke Remmer and Sebastian Draack for magnetic measurements and field simulations. The authors acknowledge the Deutsche Forschungsgemeinschaft (DFG) via the priority program SPP 1681 "Feldgesteuerte Partikel-Matrix-Wechselwirkungen" Grand Nr. Fi 1235/2-2.

References

[1] E. Garaio, Nanotechnology. 26 **(2015)** 1-18.
[2] K. Laznev, IEEE Transactions on magnetics. 49 **(2013)** 425-428.
[3] M. A. Cooperstein, Biointerphases. 8 **(2013)** 1-12.

Development of Hybrid Stents for Hyperthermic Ablation of Endoluminal Tumors

B. Mues*[1], U. Engelmann*[1], K.-M. Kossel[2], F. Jiang[1], T. Schmitz-Rode[1], I. Slabu[1]

[1] *Applied Medical Engineering, Helmholtz Institute, RWTH Aachen University, Germany*
[2] *Institut für Textiltechnik, RWTH Aachen University, Germany*
** These authors contributed equally to this work.*

Introduction

The life quality of patients with endoluminal tumours (e. g. trachea carcinoma, esophagus adenocarcinoma or bile duct Klatskin tumours) which cannot be removed with surgery is increased in medical practice by implanting a metallic stent. This widens the occluded endoluminal site. However, after a while tumor tissue ingrowth takes place causing a re-closure, so-called restenosis, of the hollow organs. In order to avoid this restenosis, the application of a hybrid stent made of fibers with incorporated magnetic nanoparticles (MNP) is envisaged. This is meant to permit local hyperthermia treatment destroying the tumour tissue in close vicinity to the stent. Removal of tumor tissue causing restenosis, so called ablation, is reliably achieved for temperatures about 49 °C [1].
Usually, solutions containing freely dispersed MNP easily develop such high temperatures when they are exposed to an alternating magnetic field (AMF). In this case, both Néel and Brownian relaxation mechanisms contribute to the overall heating of the MNP solution. A specified temperature is achieved by matching AMF parameters (amplitude, frequency) to MNP characteristics (size, magnetization) and to the MNP concentration in the solution. For MNP immobilized inside the hybrid stent, the Brownian relaxation is partially or fully blocked causing a change of the heating characteristics. Consequently, for the development of hybrid stents with specified heating values, the effect of MNP immobilization on the heating behavior must be quantified.
In this study, the heating behavior of both polylactic-co-glycolic acid (PLGA) fibers and agarose gels, either with incorporated MNP are investigated. The fibers are used for realization of the hybrid stent. The agarose gels have different mesh sizes and mimic the different immobilization states of MNP inside the fibers.

Materials and Methods

The fibers were produced by melt spinning of PLGA pellets mixed with 2 wt% freeze-dried MNP. The MNP had a core diameter of (10.2 ± 4.0) nm and a saturation magnetization of (98.9 ± 0.7) emu/g.
Using MNP with similar size (8.9 ± 1.2) nm and magnetization values (119.1 ± 0.6) emu/g various agarose gels with up to 10 wt% low melting agarose content were prepared. Higher content of agarose leads to the realization of smaller mesh sizes of the gels [2]. Each agarose gel sample had an iron concentration of 300 µg/ml.
These gels as well as 1 cm of a 0.3 mm thick fiber with incorporated MNP and a reference fiber without MNP were exposed to an AMF at 40 kA/m and 270 kHz for 30 min. The measurements were carried out with a custom-built hyperthermia setup (Trumpf Hüttinger, Freiburg, Germany). The specific loss power (*SLP*) value was calculated according to:

$$SLP = c/\rho \cdot [(dT/dt)]_{(t \to 0)} \quad (1)$$

with c = 4.187 J/g/K the specific heat capacity of water, ρ the MNP weight fraction,

T the temperature and *t* the measurement time [3].

Results and Discussion

Figure 1 shows the evolution of temperature difference ΔT between the fiber with incorporated MNP and the reference fiber measured at the surface of the fibers. ΔT converges to about 2.9 °C, while the absolute saturation temperature value of the fiber with incorporated MNP is about 40 °C (not shown in Figure 1). Using the heat capacity of PLGA (c = 1.5 J/g/K), an *SLP* value of (0.89 ± 0.03) W/g was calculated.

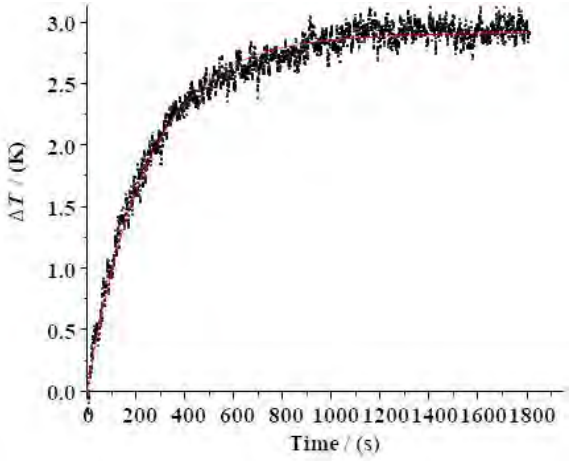

Figure 1: Temperature difference ΔT (including exponential fit / red line) between the fiber with incorporated MNP and the reference fiber without MNP.

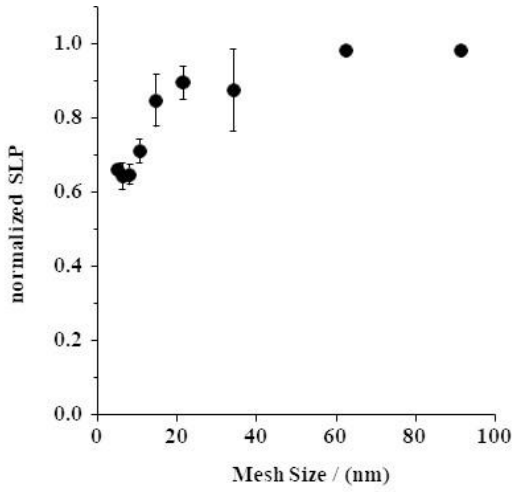

Figure 2: Normalized *SLP* values for agarose gels with incorporated MNP for different mesh sizes of the gels. The gels had a fixed iron concentration of 300 µg/ml.

The *SLP* value decreases with decreasing mesh sizes of the agarose gels by up to 40 % compared to the *SLP* value of MNP dispersed in water (normalization value in Figure 2). The drop in the *SLP* value starts at mesh sizes of ca. 20 nm which is in the order of the hydrodynamic diameter of the MNP of 20.6 nm. This demonstrates the strong influence of MNP immobilization on the heating characteristics. In strong alternating magnetic fields - such as the one employed here - the contribution of both relaxation mechanisms is significant [4]. We expect that the Néel relaxation is dominant, so that even for fully immobilized MNP heating could be achieved.

Conclusions

The slight temperature increase of the PLGA fibers with incorporated MNP and the decrease of the SLP value for immobilized MNP show that further optimization of AMF parameters as well as MNP properties has to be performed in order to reach the necessary temperature for tumor ablation.

Acknowledgements

The research project is funded as part of the program “Joint Industrial Research (IGF)” by the German Federal Ministry of Economics (contract number: 19735 N).

References

[1] Chu, K. F. and Dupuy, D. E. (2014). *Nature Reviews Cancer*, *14*(3), 199.

[2] Narayanan, J., Xiong, J. Y. and Liu, X. Y. (2006). *Journal of Physics: Conference Series*, *28*(1), 83.

[3] Wildeboer, R. R., Southern, P. and Pankhurst, Q. A. (2014). *Journal of Physics D: Applied Physics*, *47*(49), 495003.

[4] Dieckhoff, J., Eberbeck, D., Schilling, M. and Ludwig, F. (2016). *Journal of Applied Physics*, *119*(4), 043903.

Interaction of biological systems with serum protein coated magnetic nanoparticles

A. Weidner[1], C. Gräfe[2], P. Warncke[3], M. von der Lühe[4], D. Fischer[3], J.H. Clement[2], F.H. Schacher[4], S. Dutz[1]

[1] *Institute of Biomedical Engineering and Informatics, Technische Universität Ilmenau, Germany*
[2] *Abteilung Hämatologie und Internistische Onkologie, Universitätsklinikum Jena, Jena, Germany*
[3] *Institut für Pharmazie, Lehrstuhl für Pharmazeutische Technologie und Biopharmazie, Friedrich-Schiller-Universität Jena, Jena, Germany*
[4] *Institut für Organische und Makromolekulare Chemie (IOMC) and Jena Center for Soft Matter (JCSM), Friedrich-Schiller-Universität Jena, Jena, Germany*

Introduction

Hybrid magnetic nanoparticles are very promising materials for different medical applications. Before a potential application in animals or humans, cytotoxicity issues as well as interactions with the human body have to be investigated. One of the key factors influencing particle-tissue interaction is the evolving so-called protein corona which is formed immediately on the surface of magnetic nanoparticles (MNP), if they are exposed to the blood stream or any other protein source [1].

Methods

To investigate the influence of protein corona on interaction of MNP with biological systems, protein-coated MNP were prepared by *in vitro* serum incubation by using iron oxide MNP with various shells and defined mixtures of cell culture medium (RPMI) and fetal calf serum (FCS) serving as protein source as described before [2]. After incubation, the particles were magnetically washed to remove unbound FCS components and to access the *hard* protein corona for further investigation.
Before and after the incubation, the physical properties of the MNP with the evolving corona were analyzed by means of vibrating sample magnetometry (VSM), thermogravimetric analysis (TGA), transmission electron microscopy (TEM), sodium dodecyl sulfate polyacrylamide gel electrophoresis (SDS-PAGE) and zeta potential measurements.
To investigate the interactions of the bare as well as protein coated hybrid MNP with biological systems, the effect of the protein coating on cell viability was investigated for living human brain microvascular endothelial cells (HBMEC) by Presto Blue™ assay and real time cell analysis (RTCA). By means of flow cytometry and confocal laser scanning microscopy (CLSM) with fluorochrome-labelled particles, the precise particle-cell interactions with HBMEC were studied. To assess toxicity *in vivo*, a hen's egg test on the chick area vasculosa (HET-CAV) was performed by injecting the MNP intravenously into the vitelline vein.

Results

Zeta potential measurements, SDS-PAGE and TGA clearly demonstrate an influence of FCS concentration in incubation media on the manifestation of the protein corona. The higher the FCS content, the higher the protein amount in the *hard* protein corona and the lower the surface charge of the protein coated MNP.
For *in vitro* toxicity studies it was found that, initially toxic MNP show a much less or no toxicity after protein coating which means a toxicity masking effect of the protein corona. Furthermore, flow cytometry and CLSM investigations indicated, that

the protein coating reduces the velocity of the particle-cell interactions (see figure 1).

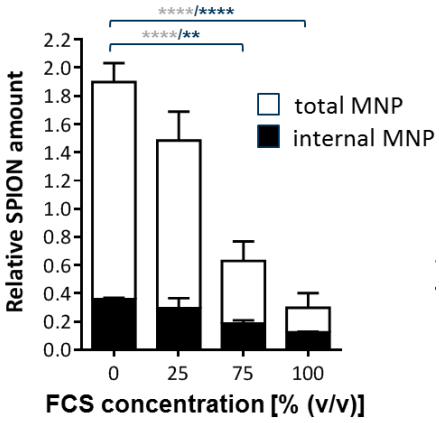

Figure 1: Quantitative analysis of CLSM images confirms a pronounced influence of the amount of protein coating on MNP / cell interaction after short time incubation (30 minutes).

The HET-CAV *in vivo* studies revealed, that protein coating of MNP with a positively charged shell (DEAE dextran) reduces the tendency to form agglomerates (thrombosis) in the blood stream after systemic injection. This can also be taken as an indication for the masking effect and thus the slower interaction with the biological system described before. For protein coated MNP with a neutrally or negatively charged shell (PEG, PDha, or CM dextran) no cytotoxic effects were found.

Conclusions

It was demonstrated that the amount and composition of the protein coating on the surface of MNP can be tuned by the composition of the incubation media serving as protein source. By variation of the protein amount on the MNP, the interaction of MNP and biological systems can be controlled. A more pronounced protein coating reduces the velocity of particles-cell interactions, can mask a cytotoxic effect and reduces the probability of thrombosis after injection of such particles into biological systems.

Resulting from these investigations it can be concluded that protein coatings reduce the interactions between MNP and biological systems which might result in a longer blood half-life which would be interesting for the preparation of longer circulating magnetic markers for MPI and MRI investigations.
In an additional study it was shown already, that protein coated MNP can be sterilized by UV irradiation and made storable by lyophilization with no alteration of protein coating [3] which is an additional prerequirement for medical application of such particle systems.

Acknowledgments

This work is supported by Deutsche Forschungsgemeinschaft (DFG) in frame of priority program 1681 (FKZ: CL202/3-2, DU1293/4-2, SCHA1640/7-1).

References

[1] A. Weidner, C. Gräfe, M. v.d. Lühe, H. Remmer, J.H. Clement, D. Eberbeck, F. Ludwig, R. Müller, F.H. Schacher, S. Dutz. Preparation of Core-Shell Hybrid Materials by Producing a Protein Corona around Magnetic Nanoparticles. Nanoscale Res. Lett. 10: 282 (2015).

[2] C. Gräfe, A. Weidner, M. v.d. Lühe, C. Bergemann, F.H. Schacher, J.H. Clement, S. Dutz. Intentional formation of a protein corona on nanoparticles - Serum concentration affects protein corona mass, surface charge, and nanoparticle-cell interaction. Int. J. Biochem. Cell Biol. 75: 196–202 (2016).

[3] S. Dutz, S. Wojahn, C. Gräfe, A. Weidner, J.H. Clement. Influence of Sterilization and Preservation Procedures on the Integrity of Serum Protein Coated Magnetic Nanoparticles. Nanomaterials 7: 453 (2017).

An extended study on the effect of SPIONs on the expression of inflammation-associated genes

M. Haist[1], J. Demut[1], C. Grüttner[2], R. Quaas[3], F. Müller[4], A. Hochhaus[1], J. H. Clement[1]

[1] *Klinik für Innere Medizin II, Abt. Hämatologie & Internistische Onkologie, Universitätsklinikum Jena, Am Klinikum 1, D-07747 Jena, Germany; mail to: johanna.demut@med.uni-jena.de*
[2] *Micromod Partikeltechnologie GmbH, Friedrich-Barnewitz-Straße 4, D-18119 Rostock, Germany*
[3] *Chemicell GmbH, Eresburgstraße 22-23, D-12103 Berlin, Germany*
[4] *Otto-Schott-Institut für Materialforschung, Professur für Oberflächen- und Grenzflächentechnologie, Löbdergraben 32, D-07743 Jena, Germany*

Introduction

Superparamagnetic iron oxide nanoparticles (SPIONs) have become important for the field of biomedicine due to their magnetic properties and their biological performance [1]. The nanoparticles interact with the biological system, e.g. gain a protein corona which can proceed to inflammation and toxicity [2]. Not only the protein corona affects the cells but also the characteristics of the nanoparticles namely their size, shell and the similarity to biomolecules can interfere with cellular functions [3, 4]. To obtain a further understanding of the cell-cell interaction, 3-dimensional multicellular models (spheroids) were used. The metabolism and the expression of genes differ from those of 2D-cell cultures [5].
The aim of this study is to investigate the influence of SPIONs on cells by analyzing the interactions in a more complex biological system. For this purpose, 2D-cell cultures and 3D-spheroids were used to analyze the expression of inflammation-associated genes after nanoparticle exposure.

Materials and Methods

Cell culture: FaDu cells (hypopharyngeal squamous cell carcinoma cells) were cultured in DMEM + 10% FCS at 37 °C in a humidified atmosphere with 5% CO_2.

Nanoparticle-incubation: FaDu cells were incubated in 2D culture for 3h and 24h. Spheroids were incubated for 24h with different SPIONs (cationic polyethyleneimine - coated PEI-M, anionic silica-iron oxide composite SiliFe41, neutral glucuronic acid-coated fluidMAG-ARA). The cells were exposed to 100 µg/mL of SPIONs.
The spheroids were analyzed via quantitative real-time PCR, the 2D-cell cultures were studied via real-time PCR and Western-Blot.

qRT-PCR: For analyzing the gene expression incubated 2D FaDu cell cultures were prepared with the RNeasy kit (Analytik Jena) and mRNA was transcribed into cDNA. The incubated spheroids were prepared for qRT via Cells-to-C^t kit (Invitrogen) and the expression levels of selected inflammation-associated genes (*C-FOS, ICAM, PDGFB, VEGFA, FTH*) were evaluated according to Pfaffl [6] with the housekeeping gene *EEF1A1*.

Western-Blot: Proteins were isolated from spheroids and 2D-cell cultures. The protein concentration was determined with Bradford reagent at 595 nm. 20 µg total protein per line was loaded on BisTris polyacrylamide gels. Blotting of proteins onto a PVDF membrane was performed with the Trans-Blot® Turbo Blotting System (Bio-Rad). The membrane was submersed for 1h in 4% BSA blocking buffer and afterwards incubated with antibodies for selected intracellular signaling proteins (pp38, p38, pAKT, AKT, pp44/42, p44/42). The detection was performed using chemilumines-

cence and the quantification via imageJ with the housekeeping protein GAPDH.

Results and Discussion

For the spheroids it was shown that the expression of inflammation-associated genes increased after 24h of nanoparticle-incubation. Especially after application of the cationic PEI-M all studied genes were up-regulated. Both, SiliFe41 and fluidMAG-ARA exhibited comparable expression levels for the analyzed genes of interest.
In 2D-cell cultures each gene responded with characteristic expression levels. The expression of *C-FOS* and *ICAM* increased after 3h and showed a decrease of *PDGFB*, *VEGFA* and *FTH* after incubation with cationic particle PEI-M. Regarding 24h incubation, only *C-FOS* was down-regulated. *ICAM* exhibited a high increase of expression, *FTH*, *PDGFB* and *VEGFA* showed a minor increase.
After 3h of incubation with the anionic particle SiliFe41 all genes were down-regulated, especially *VEGFA* and *PDGFB*. Furthermore, after 24h *ICAM*, *PDGFB* and *FTH* are up-regulated whereas *C-FOS* and *VEGFA* were down-regulated.
The neutral charged fluidMAG-ARA particles induced a slight increase in the expression after a 3h incubation period except for the gene *FTH*. After 24h *FTH*, *C-FOS* and *ICAM* mRNA levels increased, nevertheless *PDGFB* and *VEGFA* decreased.
On the protein level the phosphorylation status of important signaling molecules was quantified and levelled to GAPDH. The protein AKT showed no increase in phosphorylation except after 3h incubation with fluidMAG-ARA; an increase of 9% is documented. In contrast, p38 showed a high increase after PEI-M and SiliFe41 addition after 3h and 24h. For the protein p42, PEI-M induced a 100% increase after 3h and 24h incubation. P42 phosphorylation was only increased after 24h after application of SiliFe41 and fluidMAG-ARA. PEI-M showed the most dramatic effects on p44 activation: After 3h an increase of 900% and after 24h of 400%.

Conclusion

Comparison of spheroids to 2D-cell cultures reveals a difference in the cellular response to SPION application. The characteristics like the size, shell and charge of the nanoparticles has an impact on the reactions in the biological system. PEI-M is already known to be cytotoxic which approves the referred results [7].
Future studies will cover a broader spectrum of affected genes and proteins using microarray HTS technologies.

Acknowledgement

We thank Cornelia Jörke for excellent technical assistance. This work was supported by the BMBF joint project NanoBEL (grant 03XP0003).

References

[1] M. Mohammadi, A. Malkovskiy, P. Jothimuthu, et al., *Scientific Reports.* **2018**, *8, 1-11*
[2] D. Westmeier, R. Stauber, D. Docter, *Toxicology and Applied Pharmacology.* **2016**, *15, 53-57*
[3] M. Mahmoudi, S. Sant, B. Wang, et al., *Advanced Drug Delivery Reviews.* **2011**, *63, 24-46*
[4] P. Tran, T. Tran, T. Vo, B. Lee, *Archives of Pharmacal Research.* **2012**, *35, 2045-2061*
[5] E.-T. Verjans, J. Doijen, W. Luyten, et al., *Journal of Cellular Physiology.* **2017**, *233, 2993-3003*
[6] M. Pfaffl, *Nucleic Acid Research.* **2001**, *29, 2001-2007*
[7] L. Chou, K. Ming, W. Chan, *Chemical Society Reviews.* **2011**, *40, 233-245*

The tyrosine kinase inhibitor Imatinib alters the interaction of magnetic nanoparticles with a cellular barrier

A. Stelz, N. Schwarze, J. Demut, A. Hochhaus, J. H. Clement, C. Gräfe

Klinik für Innere Medizin II, Abt. Hämatologie & Internistische Onkologie, Universitätsklinikum Jena, Am Klinikum 1, D-07747 Jena, Germany; mail to: joachim.clement@med.uni-jena.de

Introduction

The diverse biomedical applications of nanomaterials such as superparamagnetic iron-oxide nanoparticles (SPIONs) including anti-tumor therapy, targeted drug delivery systems and application as contrast agents during magnetic resonance imaging are a considerably promising area of research [1,2]. During pregnancy, SPIONs might offer the opportunity to selectively target either the pregnant woman, or the fetus or the placenta for treatment of various diseases, thereby reducing side effects. Before administration of any active agent, the substance's impact onto the human body especially the biodistribution, tissue penetration and other interactions need to be investigated. For this purpose, an *in vitro* model of the blood-placenta barrier (BPB) was used to study the interaction and passage of SPIONs coated with neutral starch (D) with the biological barrier. Additionally, this system was exploited in order to test a potential harm of tyrosine kinase inhibitor (TKI) Imatinib used in the treatment of chronic myeloid leukemia. Therefore, processes involved in cellular binding, uptake and passage through cell layers were studied.

Materials and Methods

For the co-culture *in vitro* BPB model, the human choriocarcinoma trophoblastic cell line BeWo was seeded on the apical side and primary placental pericytes on the basolateral side of a Transwell insert for six days [3]. As reporter cell line Imatinib-sensitive leukemia cells (K562) were present in the lower compartment. All cells were cultivated in DMEM +15 % FCS +1 % Pen/Strep. This cell layer was incubated with 100 µg/cm^2 neutral starch coated fluidMAG-D particles (chemicell, Berlin) for 24h starting at day 5 and with 20µM Imatinib for 48h starting at day 4. The interactions and cytotoxicity of the SPIONs and the TKI with the cells was determined by MTT cytotoxicity assay using the reporter cell line K562, as well as diverse microscopic analyses and immunohistochemical staining of tight junction protein *zonula occludens-1* (ZO-1) and ß-Catenin of the BeWo layer. Cell barrier integrity was verified by trans-endothelial electrical resistance (TEER) measurements (days 3-6) and molecular permeability assays using 10 minute incubation with sodium fluorescein. Furthermore, the cell layer containing membranes were embedded into agarose, sectioned into histological slices (10-20µm), and stained using Nuclear Fast Red and Prussian Blue.

Results and Discussion

TEER measurements showed minor reduced barrier integrity upon Imatinib application (Figure 1). Moreover, the immunohistochemistry revealed a decreased expression of both the tight junction protein ZO-1 and β- catenin upon Imatinib incubation while nanoparticle administration did not exhibit any effect. This supports the TEER results showing reduced barrier integrity after 48h TKI incubation by reducing the cell-cell contacts. Regarding the molecular permeability of the cellular barrier, neither Imatinib nor fluidMAG-D had an impact on the paracellular transport of the fluorescent dye through the membrane (Figure 2).

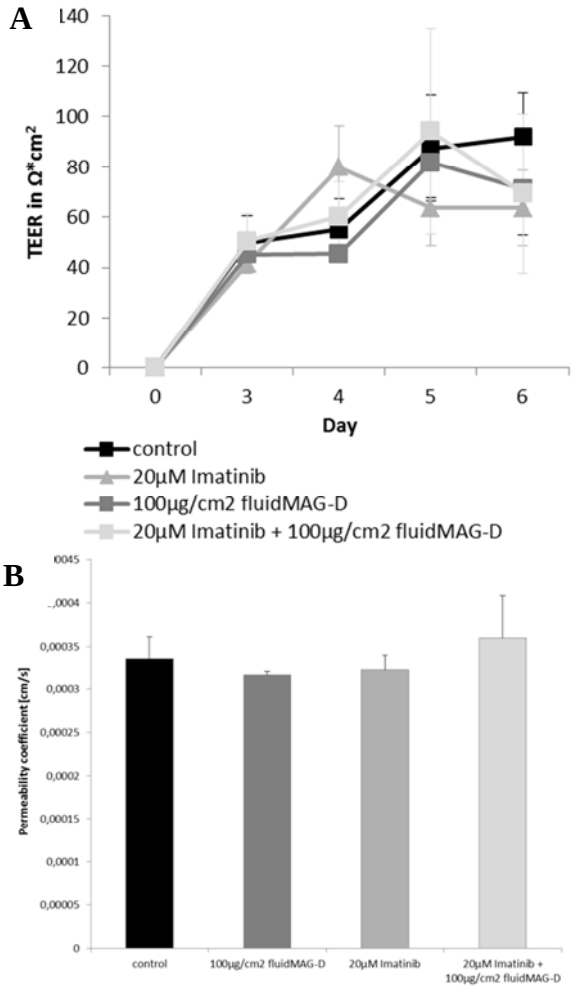

Figure 1: Barrier function is not impaired by Imatinib and SPIONs

A Transendothelial electrical resistance.
The cellular barrier model was cultivated for 6 days with incubation of 20µM Imatinib after day 4 and 100µg/cm² fluidMAG-D particles after day 5. TEER was measured every day as indicated.

B Sodium fluorescein permeability.
After 6 days of cultivation, the sodium fluorescein dye was administered to the cellular barrier model for 10 minutes.

The interaction and internalization of SPIONs was confirmed by confocal LSM and Prussian Blue staining. In order to analyze the passage of Imatinib through the cellular barrier, the viability of reporter cells in the lower compartment was determined using an MTT assay. The tyrosine kinase inhibitor decreases the viability of K562 cells by 53% whereas nanoparticle incubation alone does not reduce their viability (Figure 2).

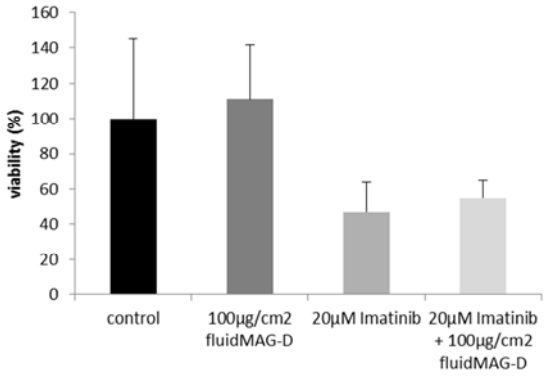

Figure 2: Viability of K562 after Imatinib administration
After 6 days of cultivation, the tetrazolium dye MTT was administered directly to the reporter cells K562 in the lower compartment for 90 minutes.

Conclusion

The tyrosine kinase inhibitor Imatinib has a negative impact on the barrier integrity and the viability of reporter cells. For administration during pregnancy, a targeted drug delivery system which prevents the passage through the blood-placenta barrier is needed. Moreover, administration of neutral starch coated SPIONs does not influence the integrity of the *in vitro* cellular blood-placenta barrier model and shows no toxic effects on reporter cells in this system. These findings indicate that those particles might be candidates for targeted drug delivery systems.

Acknowledgements

This work was supported by Deutsche Forschungsgemeinschaft (DFG) in the framework of the priority program 1681 (CL202/3-2).

References

[1] R.A. Revia, M. Zhang. **2016,** Materials Today, *19*: 157-168
[2] S. Dutz, J. H. Clement, et al. 2009. Journal of Magnetism and Magnetic Materials, 321: 1501-1504
[3] E. K. Müller et al. 2018, Nanomaterials, 8(2), 108

Chemotherapeutics affect the interaction of SPIONs with an *in vitro* blood-placenta barrier

N. Schwarze, A. Stelz, J. Demut, A. Hochhaus, J. H. Clement, C. Gräfe

Klinik für Innere Medizin II, Abt. Hämatologie & Internistische Onkologie, Universitätsklinikum Jena, Am Klinikum 1, D-07747 Jena, Germany; mail to: christine.graefe@med.uni-jena.de

Introduction

The incidence of cancer during pregnancy is increasing due to the fact that women delay pregnancy to older ages, where the overall risk of cancer occurrence is elevated [1].
But the treatment of cancer during pregnancy is still a challenging task and therefore advanced research is necessary.
Superparamagnetic iron oxide nanoparticles (SPIONs) can serve as essential imaging contrast agent for magnetic resonance imaging (MRI) for early detection in pregnant woman due to their physiochemical and magnetic properties. No harmful potential for the developing fetus is expected [2, 3].
The aim of our study is to investigate the effects of selected chemotherapeutic agents on the interaction of neutrally charged SPIONs with an established cell culture-based *in vitro* barrier model (blood-placenta barrier) [4]. This includes the analysis of the viability and integrity of the cell layers as well as the passage of the SPIONs through the cell layers.

Materials and Methods

To investigate interactions between biological barriers and nanoparticles in the presence of therapeutic substances, a tri-culture model of human trophoblast representing placenta cells (BeWo), pericytes (hPC-PL) and breast cancer cells (MCF-7) (all cultivated in DMEM +15 % FCS +1 % Pen-Strep for 7 days) were used. Cells were exposed to 0.002 mg/ml doxorubicin (D) and 0.006 mg/ml paclitaxel (P) on day 4 for 48 hours. At day 5 co-cultures were incubated with 100 µg/cm^2 fluidMAG-D (chemicell, Berlin) for 24 hours. To investigate the influence of these chemotherapeutic substances and SPIONs on the cell barrier integrity was verified by trans-endothelial electrical resistance (TEER) measurements and molecular permeability assay using sodium fluorescein as well as the immunofluorescence staining of the tight junction-associated protein ZO-1.
Additionally the passage of chemotherapeutic agents through the barrier was evaluated via determination of the viability of MCF-7 cells (in the lower compartment) by flow cytometry (Annexin V APC/PI).

Results and Discussion

Both, TEER measurements and molecular permeability assay showed a negative influence of doxorubicin and paclitaxel on the blood-placenta barrier integrity (Figure 1) with little potential of regeneration over time. Furthermore the presence of neutral charged SPIONs showed no additional effects on barrier formation and persistence.
This also could be confirmed by the visualization of tight junction-associated protein ZO-1 (Figure 2). Doxorubicin treatment led to a marked reduction of cell-cell contacts, whereas paclitaxel had no significant effect. The addition of fluidMAG-D bears no further impact on tight junctions.
Confocal microscopy further confirmed the interaction and internalization of SPIONs at least in the apical BeWo cell layer.

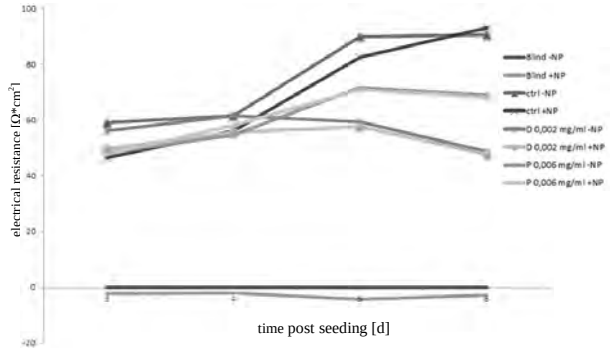

Figure 1: Barrier integrity estimated by TEER. Tri-cultures were incubated with 0.002 mg/ml doxorubicin (D) and 0.006 mg/ml paclitaxel (P) as well as 100 µg/cm^2 fluidMAG-D.

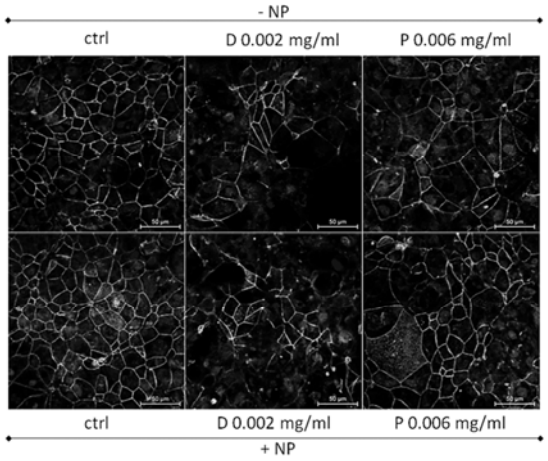

Figure 2: Immunofluorescence staining of tight junction-associated protein ZO-1. Tri-cultures were incubated with indicated concentrations of doxorubicin (D) and paclitaxel (P). Cell borders are clearly visible in control as well as in paclitaxel-treated cultures.

In order to determinate the passage of chemotherapeutic substances into the lower compartment MCF-7 cells were analysed by Annexin V APC and propidium iodide staining (Figure 3). Both substances caused a reduction of living cell percentage, whereby the effect was slightly stronger under doxorubicin treatment. Likewise other results the application of neutral charged SPIONs had no appreciable influence on cell viability.

Conclusion

Doxorubicin clearly affected the blood-placenta barrier to a greater extent than paclitaxel demonstrated by electrical resistance, the molecular retention of sodium fluorescein and cell contact integrity. The addition of neutral charged SPIONs did not enhance this virtue.

After passing the blood-placenta barrier cell layer the chemotherapeutic substances still had negative effects on sensitive breast cancer cell line cells. Consistent with the previously presented data the application of fluidMAG-D showed no further impact.

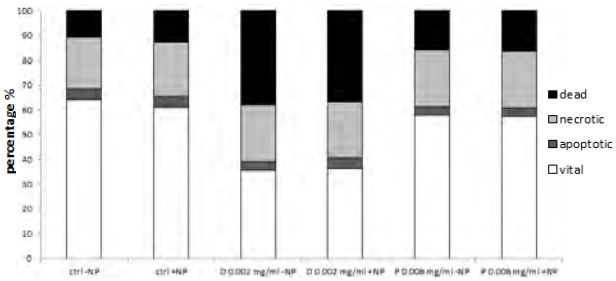

Figure 3: Analysis of vitality (Annexin V APC/PI double staining). Tri-cultures were incubated with indicated concentrations of doxorubicin (D) and paclitaxel (P). MCF-7 cells were stained with Annexin V APC/PI and measured via flow cytometry.

Actually, we quantify the iron content of the different compartments using atomic absorption spectroscopy (AAS). Future work will focus on the determination of altered levels of Reactive Oxygen Species (ROS) and putative changes in the production of pro- and anti-inflammatory cytokines.

Acknowledgement

We thank Cornelia Jörke for excellent technical assistance. This work was supported by Deutsche Forschungsgemeinschaft (DFG) in the framework of the priority program 1681 (CL202/3-3).

References

[1] F. Rovera et al., *Int J Surg.* **2013**, *11(s1), 64*

[2] S. Dutz, J. H. Clement, D. Eberbeck, et al., *J Magn Magn Mater*. **2009**, *321, 1501*

[3] Y. Javed, et al., *J Nanopart Res.* **2017**, *19, 366*

[4] E. K. Müller et al., *Nanomaterials* **2018**, *8, 108*